5. Production of high P_T jets

5.1 Introduction

5.2 Reminder: the structure of QCD, calculation of matrix elements

5.3 Jet production at hadron colliders

5.4 Impact on parton distribution functions

5.5 Direct photon production

5.6 Measurements of α_s

5.1 Introduction

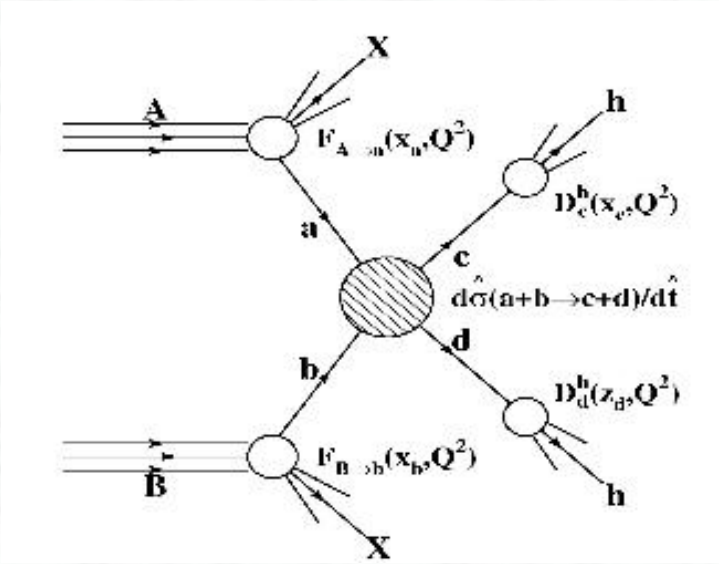

Leading order

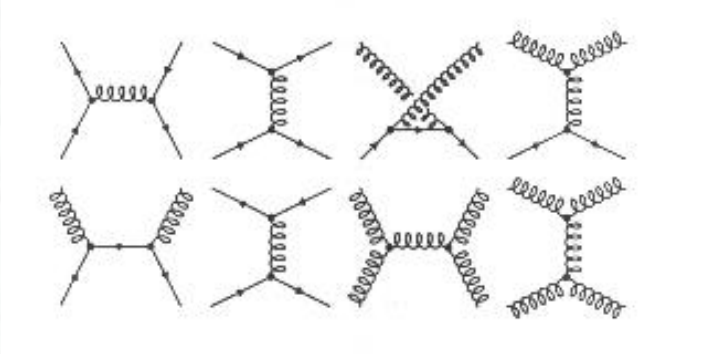

…some NLO contributions

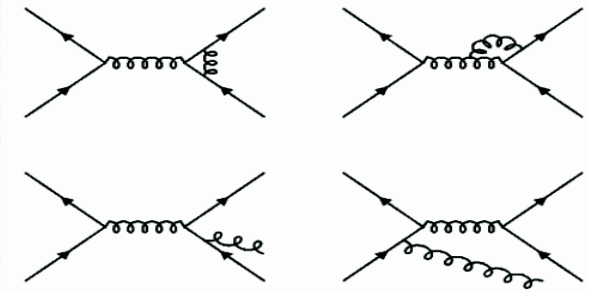

- Hard scattering processes at hadron colliders are dominated by jet production
- QCD process, originating from qq, qg and gg scattering
- Cross sections can be calculated in QCD (perturbation theory)

Comparison between experimental data and theoretical predictions constitutes an important test of the theory.

Deviations?

→ Problem in the experiment ?
Problem in the theory (QCD) ?
New Physics, e.g. quark substructure ?

- Large cross sections….
- Fast rising with √s

Leading order

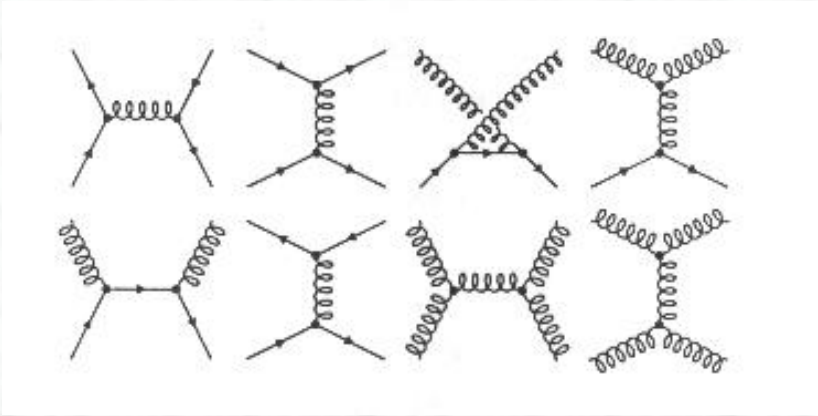

…some NLO contributions

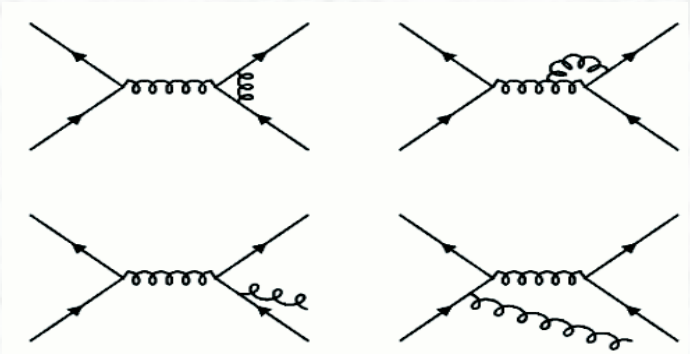

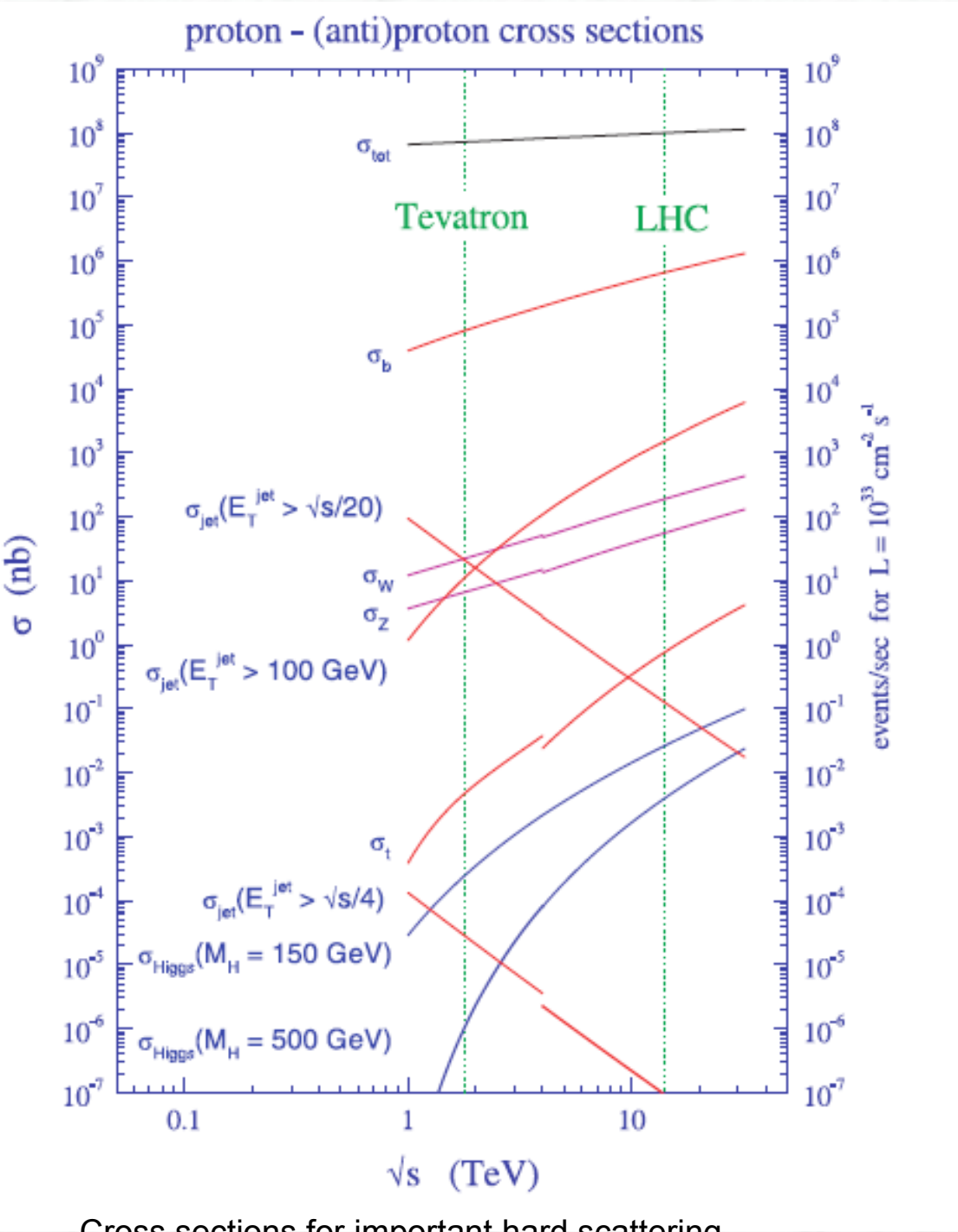

Cross sections for important hard scattering Standard Model processes at the Tevatron and the LHC colliders

Jets from QCD production: Tevatron vs LHC

- Rapidly probe perturbative QCD in a new energy regime (at a scale above the Tevatron, large cross sections)

- Experimental challenge: understanding of the detector
  - main focus on jet energy scale
  - resolution

- Theory challenge:
  - improved calculations…
    (renormalization and factorization scale uncertainties)
  - pdf uncertainties

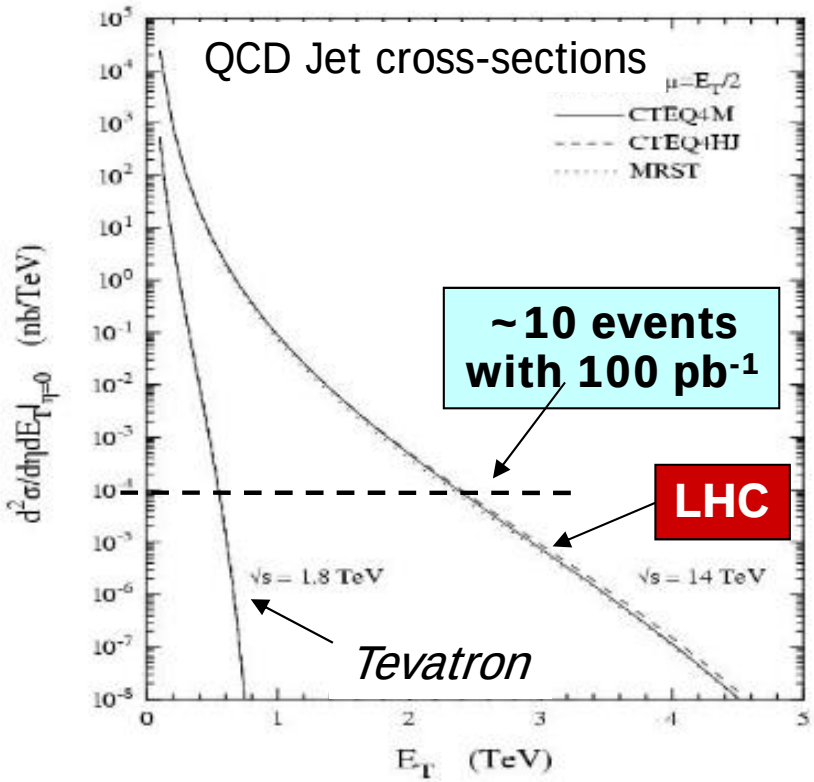

5.2 Reminder: structure of QCD, matrix element calculation

Theory	Interaction	charge	Gauge boson(s)
QED	electromagnetic	electric charge	Photon
QCD	strong	colour charge	Gluons

Coupling constants

$g_e = \sqrt{4\pi\alpha}$ QED

$g_s = \sqrt{4\pi\alpha_s}$ QCD

Gluon Colour states

$$c = \begin{pmatrix} 1 \\ 0 \\ 0 \end{pmatrix}$$ red

$$c = \begin{pmatrix} 0 \\ 1 \\ 0 \end{pmatrix}$$ blue

$$c = \begin{pmatrix} 0 \\ 0 \\ 1 \end{pmatrix}$$ green

SU3:

Color Octet

$$|1\rangle = (r\bar{b} + b\bar{r})/\sqrt{2}$$
$$|2\rangle = -i(r\bar{b} - b\bar{r})/\sqrt{2}$$
$$|3\rangle = (r\bar{r} - b\bar{b})/\sqrt{2}$$
$$|4\rangle = (r\bar{g} + g\bar{r})/\sqrt{2}$$
$$|5\rangle = -i(r\bar{g} - g\bar{r})/\sqrt{2}$$
$$|6\rangle = (b\bar{g} + g\bar{b})/\sqrt{2}$$
$$|7\rangle = -i(b\bar{g} - g\bar{b})/\sqrt{2}$$
$$|8\rangle = (r\bar{r} + b\bar{b} + 2g\bar{g})/\sqrt{6}$$

Color Singlet

$$|9\rangle = -i(r\bar{r} + b\bar{b} + g\bar{g})/\sqrt{3}$$

Color Singlet gluons do not exist. Since the gluons have m=0, this would give a strong gravity force.

Quark and gluon states:

a quark is characterized by
- momentum p
- spin state s
- color state c

$$u^{(s)}(p)c$$

a gluon is characterized by
- momentum p
- polarisation ε
- color state a^α

$$\epsilon_\mu(p)a^\alpha$$

Color states of the gluon

$$a^1 = \begin{pmatrix} 1 \\ 0 \\ 0 \\ 0 \\ 0 \\ 0 \\ 0 \\ 0 \end{pmatrix}, \quad a^2 = \begin{pmatrix} 0 \\ 1 \\ 0 \\ 0 \\ 0 \\ 0 \\ 0 \\ 0 \end{pmatrix}, \quad \dots$$

Gluons carry color charge, therefore they can couple to each other.
This is not possible for photons.

The Gell-Mann λ-matrices are the generators of SU3, equivalent to the Pauli matrices for SU2.

$$\lambda^1 = \begin{pmatrix} 0 & 1 & 0 \\ 1 & 0 & 0 \\ 0 & 0 & 0 \end{pmatrix} \quad \lambda^2 = \begin{pmatrix} 0 & -i & 0 \\ i & 0 & 0 \\ 0 & 0 & 0 \end{pmatrix} \quad \lambda^3 = \begin{pmatrix} 1 & 0 & 0 \\ 0 & -1 & 0 \\ 0 & 0 & 0 \end{pmatrix} \quad \lambda^4 = \begin{pmatrix} 0 & 0 & 1 \\ 0 & 0 & 0 \\ 1 & 0 & 0 \end{pmatrix}$$

$$\lambda^5 = \begin{pmatrix} 0 & 0 & -i \\ 0 & 0 & 0 \\ i & 0 & 0 \end{pmatrix} \quad \lambda^6 = \begin{pmatrix} 0 & 0 & 0 \\ 0 & 0 & 1 \\ 0 & 1 & 0 \end{pmatrix} \quad \lambda^7 = \begin{pmatrix} 0 & 0 & 0 \\ 0 & 0 & -i \\ 0 & i & 0 \end{pmatrix} \quad \lambda^8 = \frac{1}{\sqrt{3}} \begin{pmatrix} 1 & 0 & 0 \\ 0 & 1 & 0 \\ 0 & 0 & -2 \end{pmatrix}$$

The commutators of the λ-matrices define the structure constants of SU3.

$$\left[\lambda^\alpha,\ \lambda^\beta\right] = 2if^{\alpha\beta\gamma}\lambda^\gamma$$

with $f^{\beta\alpha\gamma} = f^{\alpha\gamma\beta} = -f^{\alpha\beta\gamma}$

completely antisymmetric

There are 8x8x8=512 structure constants.
Most are zero, except for the following and their antisymmetric permutations.

$$f^{123} = 1$$
$$f^{147} = f^{246} = f^{257} = f^{345} = f^{516} = f^{637} = \frac{1}{2}$$
$$f^{458} = f^{678} = \sqrt{\frac{3}{2}}$$

Feynman rules for QCD:

1. External Lines

Quark	incoming	$u^{(s)}(p)c$
	outgoing	$\bar{u}^{(s)}(p)c^{+}$
Antiquark	incoming	$\bar{v}^{(s)}(p)c^{+}$
	outgoing	$v^{(s)}(p)c$
Gluon	incoming	$\epsilon_{\mu}(p)a^{\alpha}$
	outgoing	$\epsilon^{*}_{\mu}(p)\,(a^{\alpha})^{*}$

2. Propagators

$q, \bar{q}$	$\frac{i(\gamma^{\mu}q_{\mu}+mc)}{q^2-m^2c^2}$
g	$\frac{-ig_{\mu\nu}\delta^{\alpha\beta}}{q^2}$

3. Vertices

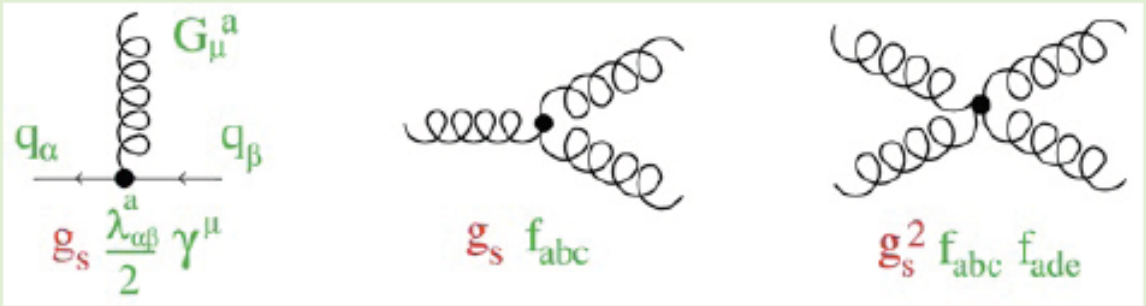

4. Internal Loop Diagrams
   More complicated than in QED.
   Not treated here.

5. δ-function for momentum conservation

Example: invariant amplitude for u dbar → u dbar scattering

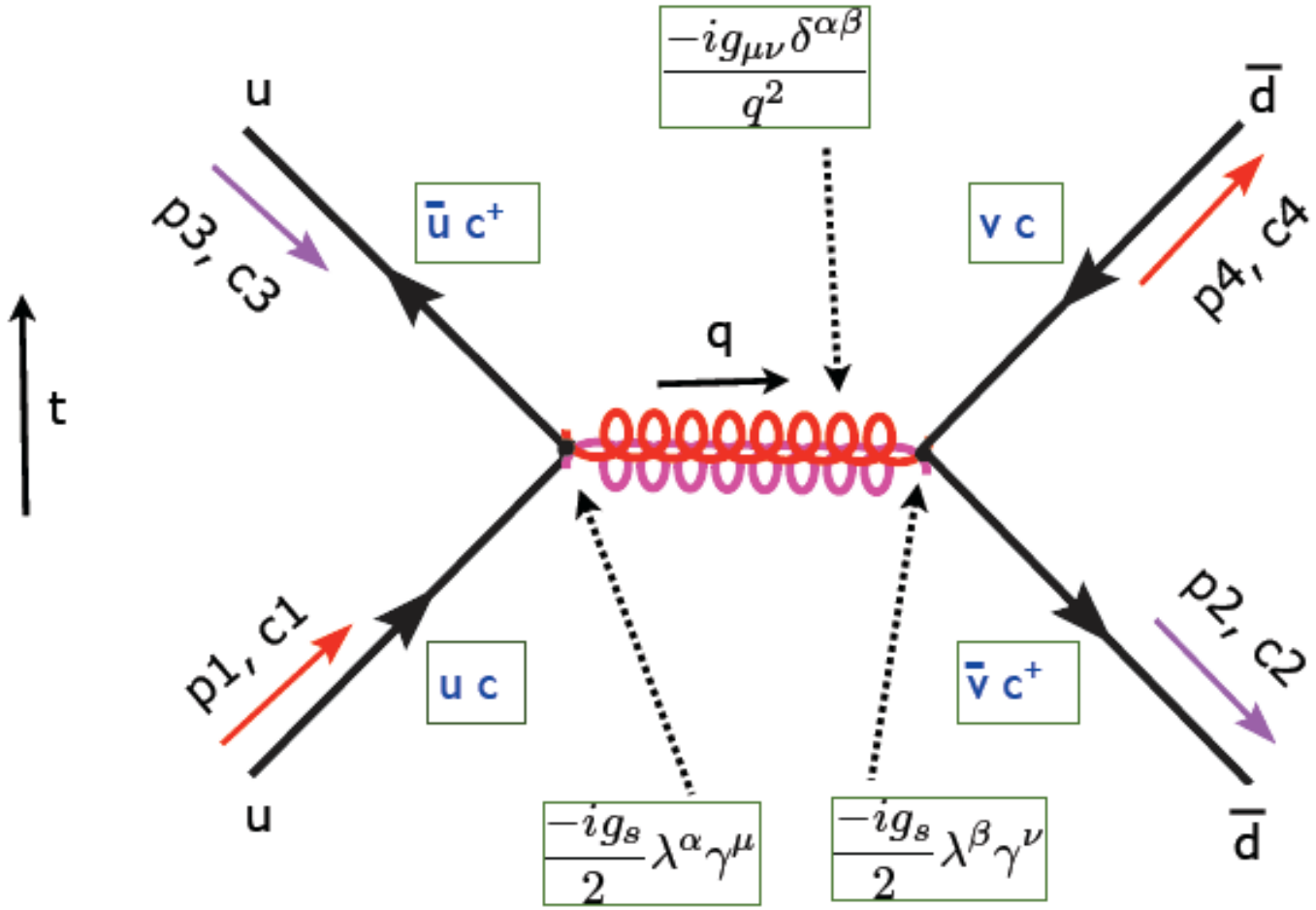

Like in QED also in QCD the charge is conserved.

Thus diagrams have continuous flow of color.

Matrix elements are like in QED, but they contain a color factor.

$$-i\mathcal{M} = \bar{u}(3)c_3^+\left[-i\frac{g_s}{2}\lambda^\alpha\gamma^\mu\right]u(1)c_1\frac{-ig_{\mu\nu}\delta^{\alpha\beta}}{q^2}\bar{v}(2)c_2^+\left[-i\frac{g_s}{2}\lambda^\beta\gamma^\nu\right]v(4)c_4$$

$$\mathcal{M} = \frac{-g_s^2}{4q^2}\left[\bar{u}(3)\gamma^\mu u(1)\right]\left[\bar{v}(2)\gamma_\mu v(4)\right]\left[c_3^+\lambda^\alpha c_1\right]\left[c_2^+\lambda^\alpha c_4\right]$$

Example (ii): u ubar → gg

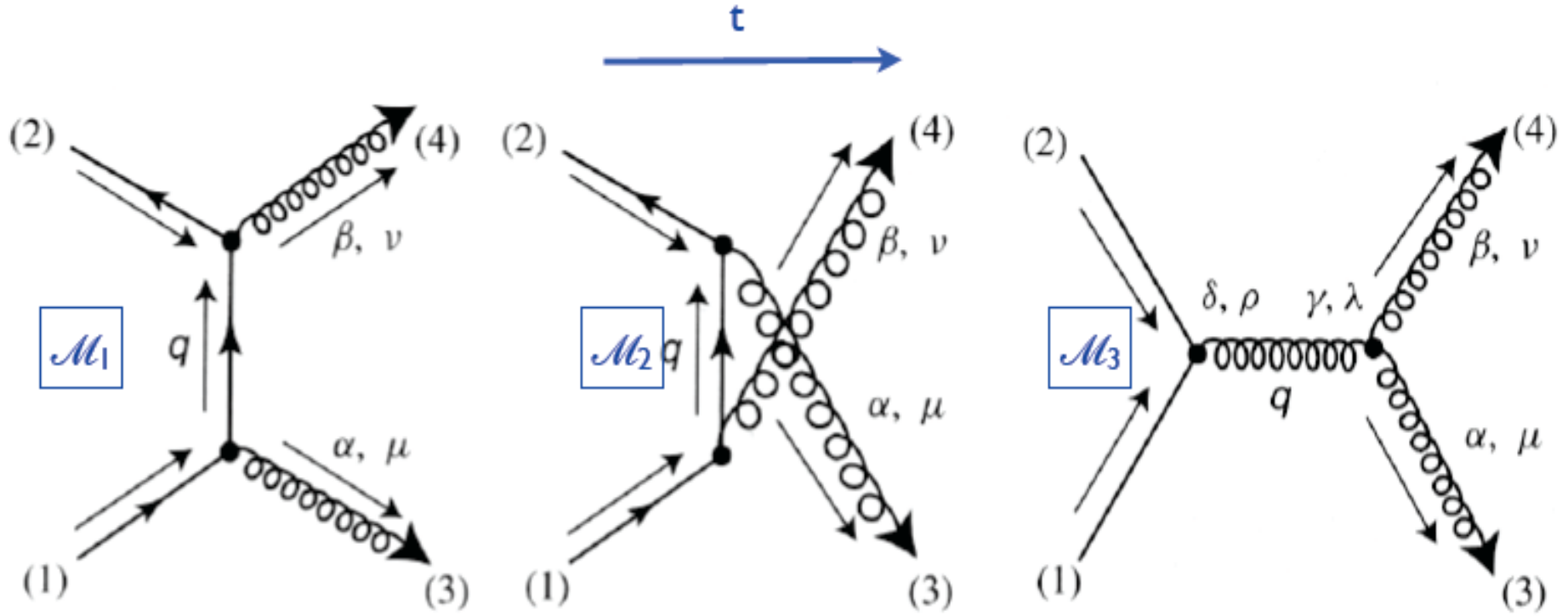

$$\mathcal{M}_1 = i\bar{v}(2)c_2^\dagger\left[-i\frac{g_s}{2}\lambda^\beta\gamma^\nu\right][\epsilon^*_{4\nu}a_4^{\beta*}]\left[\frac{i(\not{q}+mc)}{q^2-m^2c^2}\right]$$
$$\times\left[-i\frac{g_s}{2}\lambda^\alpha\gamma^\mu\right][\epsilon^*_{3\mu}a_3^{\alpha*}]u(1)c_1$$

$$\mathcal{M}_3 = i\bar{v}(2)c_2^\dagger\left[-i\frac{g_s}{2}\lambda^\delta\gamma_\sigma\right]u(1)c_1\left[-i\frac{g^{\sigma\lambda}\delta^{\delta\gamma}}{q^2}\right]\{-g_sf^{\alpha\beta\gamma}[g_{\mu\nu}(-p_3+p_4)_\lambda$$
$$+g_{\nu\lambda}(-p_4-q)_\mu+g_{\lambda\mu}(q+p_3)_\nu]\}[\epsilon_3^\mu a_3^\alpha][\epsilon_4^\nu a_4^\beta]$$

$$\mathcal{M}_2 = \frac{-g_s^2}{8}\frac{1}{p_1\cdot p_4}\left\{\bar{v}(2)[\not{\epsilon}_3(\not{p}_1-\not{p}_4+mc)\not{\epsilon}_4]u(1)\right\}a_3^\alpha a_4^\beta(c_2^\dagger\lambda^\alpha\lambda^\beta c_1)$$

colour flow in hard processes:

One Feynman graph can correspond to several possible colour flows, e.g. for $qg \to qg$:

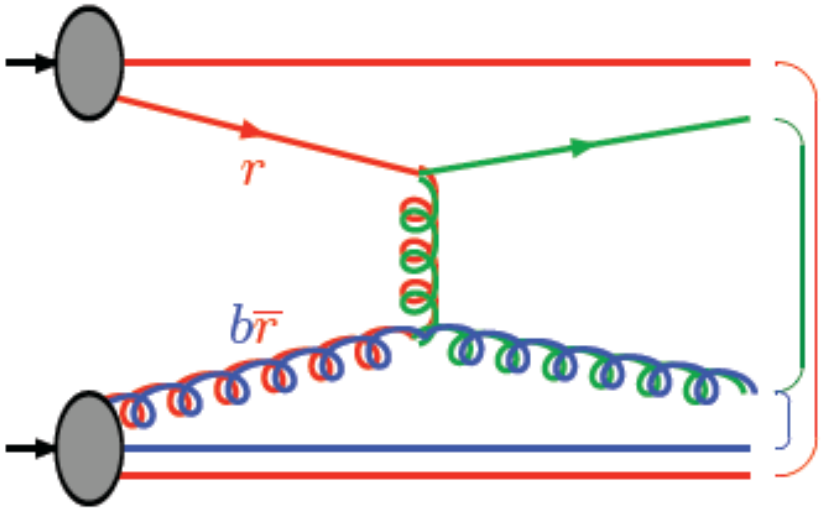

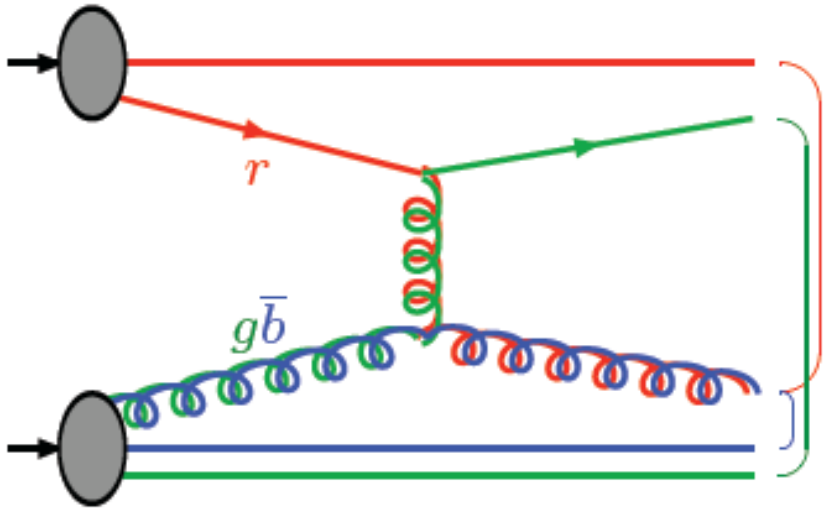

while other $qg \to qg$ graphs only admit one colour flow:

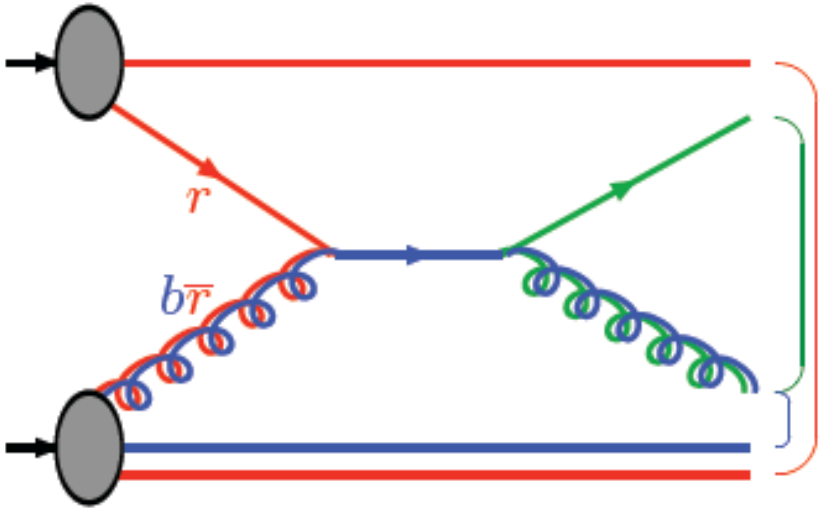

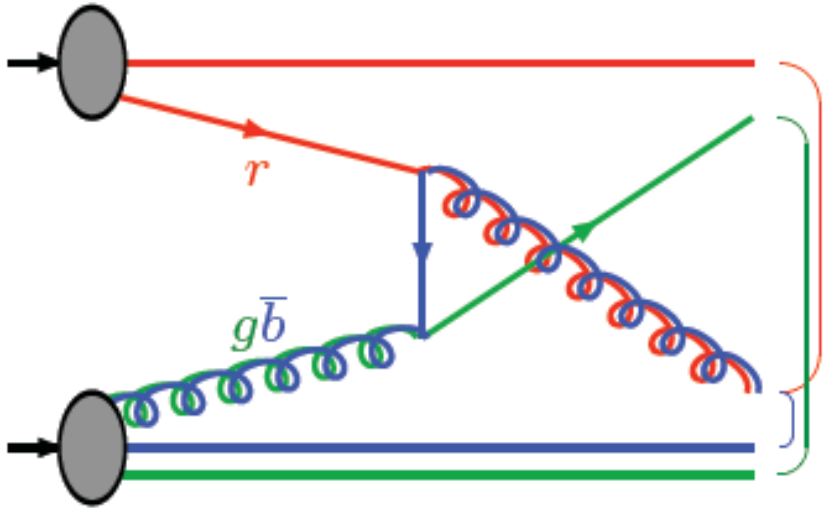

Quarks and gluon loops, running of α_s:

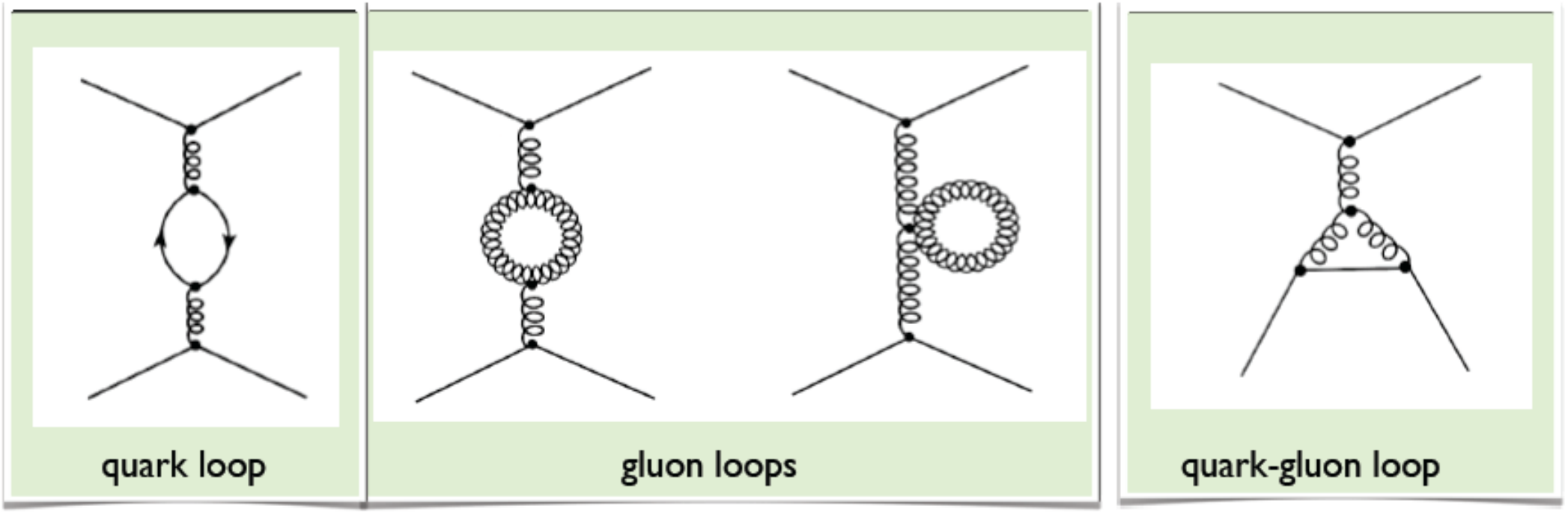

Quark loops: increase $\alpha_s(|q^2|)$ with $|q^2|$

Gluon loops: decrease $\alpha_s(|q^2|)$ with $|q^2|$

$$\alpha_s(|q^2|) = \frac{\alpha_s(\mu^2)}{1 + [\alpha_s(\mu^2)/12\pi](11n - 2f)\ln(|q^2|/\mu^2)} \qquad (|q^2| \gg \mu^2)$$

n: # of colors(=3)
f : # of flavors, which are open at $|q^2|$

Leading log approximation. This formula gives the running of $\alpha_s(|q^2|)$. If we know it at $|q^2|=\mu$, we can calculate in for every $|q^2|$.

Running of α_s:

$$\alpha_s(|q^2|) = \frac{\alpha_s(\mu^2)}{1 + [\alpha_s(\mu^2)/12\pi](11n - 2f)\ln(|q^2|/\mu^2)} \qquad (|q^2| \gg \mu^2)$$

The energy scale μ must be chosen such that $\alpha_s(|q^2|) < 1$, otherwise the power expansion does not converge and perturbation theory is not valid.

One can define the Λ - Parameter:

$$\ln \Lambda^2 = \ln \mu^2 - 12\pi/[(11n - 2f)\alpha_s(\mu^2)]$$

Then the single parameter Λ determines the running of α

$$\alpha_s(|q^2|) = \frac{12\pi}{(11n - 2f)\ln(|q^2|/\Lambda^2)} \qquad (|q^2| \gg \Lambda^2)$$

From experimental measurements on finds: 100 MeV < Λ < 350 MeV

One usually choses $\mu = m_Z$ as a reference scale, since $\alpha_s(m_z^2)$ has been measured very precisely at LEP. With the formula above, values measured at other energies can be extrapolated to m_Z.

Experimental measurements of α_s:

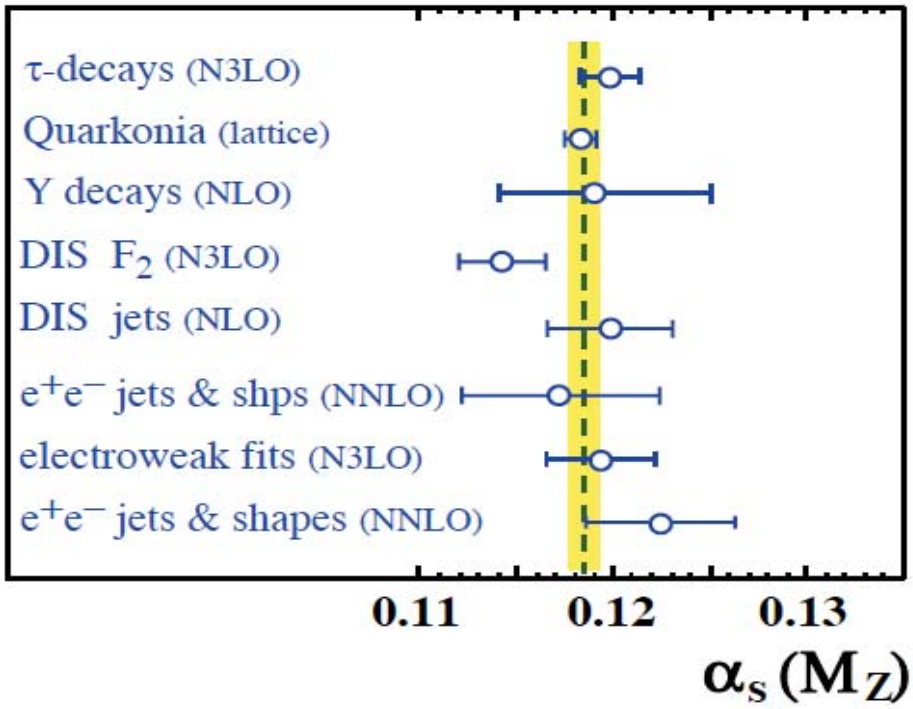

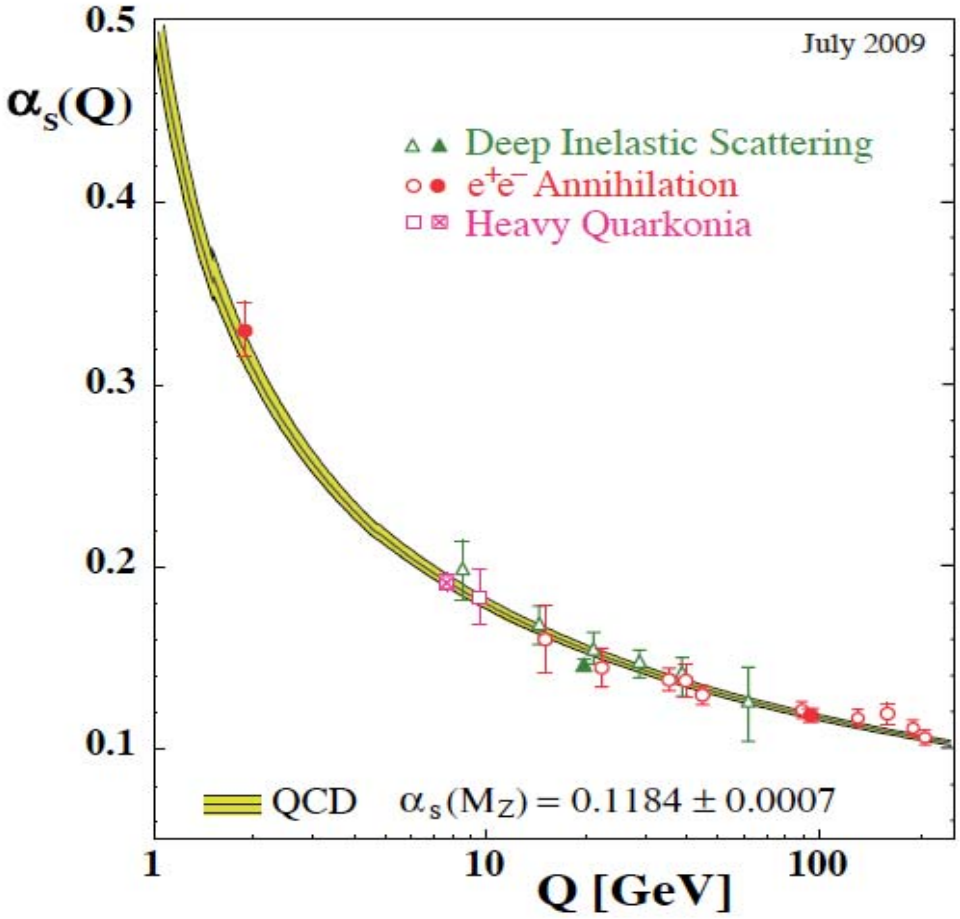

Summary of measurements of α_s (m_Z^2), used as input for the world average value (from Particle Data Group).

Summary of measurements of α_s as a function of the respective energy scale Q (from Particle Data Group).

5.3 Jet production at hadron colliders

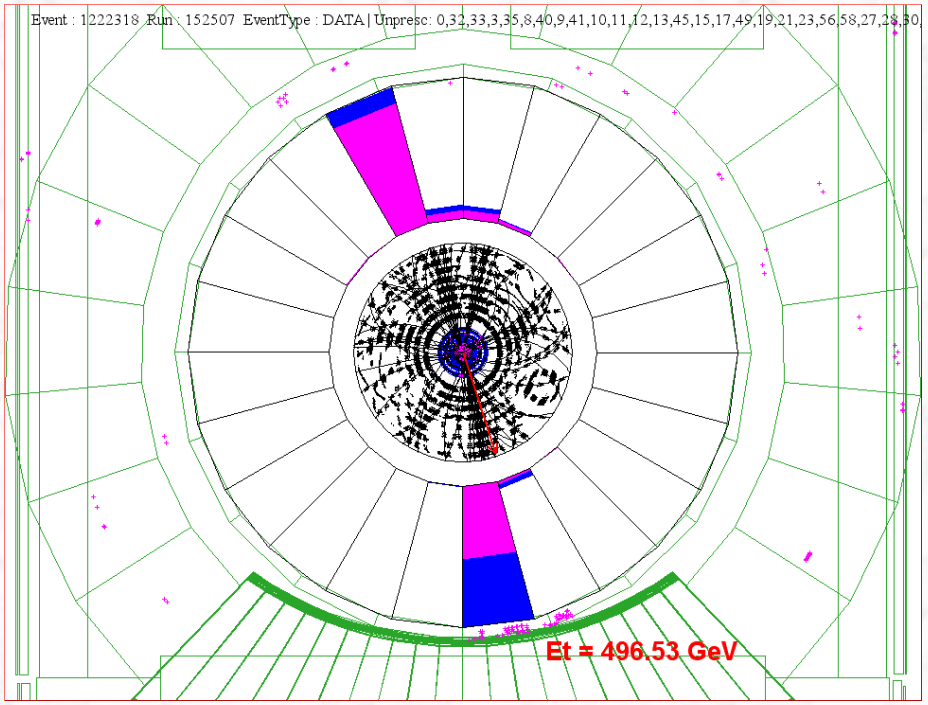

CDF (ϕ-r view)

Dijet mass = 1364 GeV/c^2

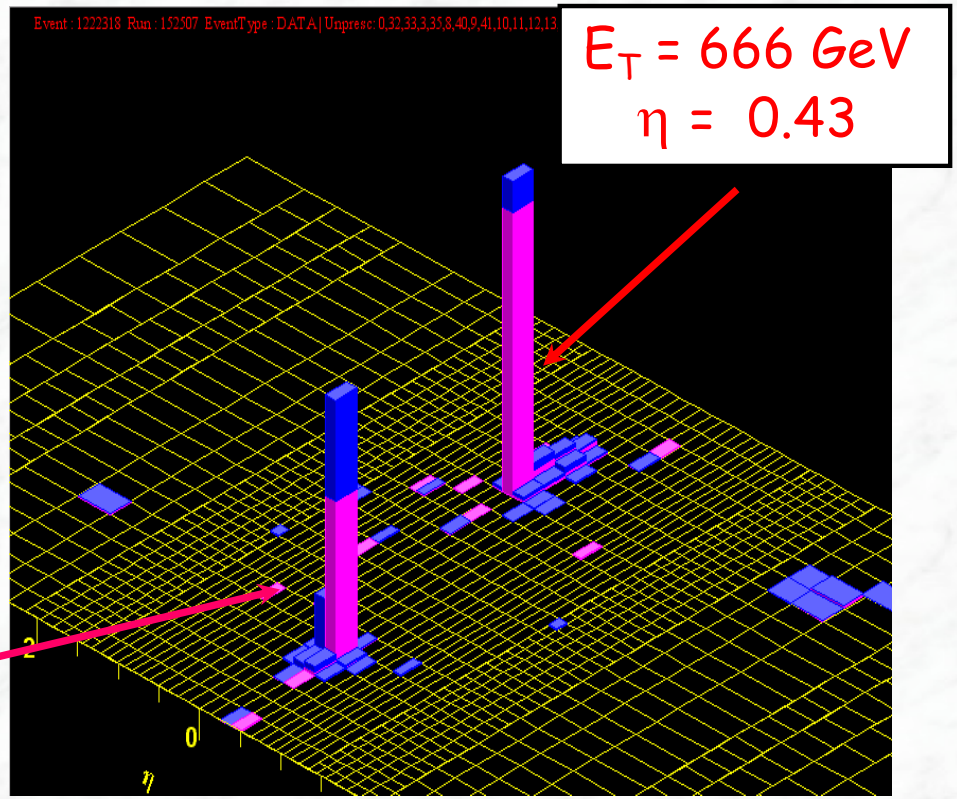

A two jet event at the Tevatron (CDF)

5.3.1 Theoretical calculations

Leading order

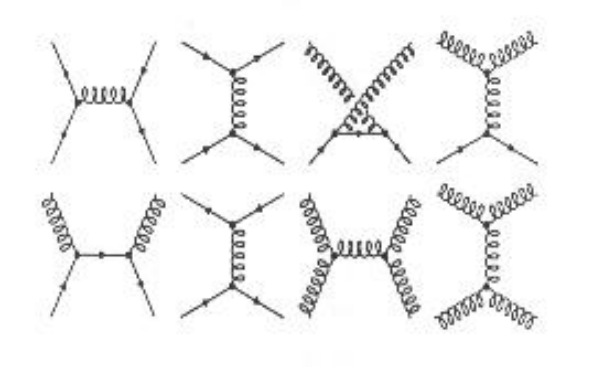

…some NLO contributions

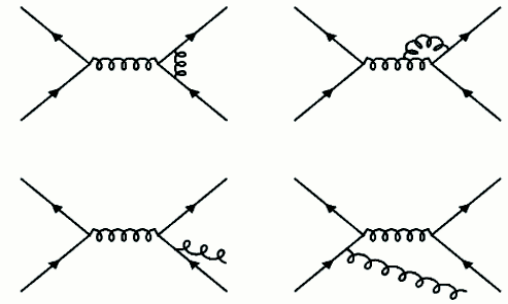

$$\frac{d\hat{\sigma}}{d\hat{t}}(ab \to cd) = \frac{|\,M\,|^2}{(16\pi\hat{s}^2)}$$

Subprocess	$\lvert\mathcal{M}\rvert^2/g_s^4$	$\lvert\mathcal{M}(90°)\rvert^2/g_s^4$
$qq' \to qq'$ $q\bar{q}' \to q\bar{q}'$	$\frac{4}{9}\frac{\hat{s}^2+\hat{u}^2}{\hat{t}^2}$	2.2
$qq \to qq$	$\frac{4}{9}\left(\frac{\hat{s}^2+\hat{u}^2}{\hat{t}^2}+\frac{\hat{s}^2+\hat{t}^2}{\hat{u}^2}\right)-\frac{8}{27}\frac{\hat{s}^2}{\hat{u}\hat{t}}$	3.3
$q\bar{q} \to q'\bar{q}'$	$\frac{4}{9}\frac{\hat{t}^2+\hat{u}^2}{\hat{s}^2}$	0.2
$q\bar{q} \to q\bar{q}$	$\frac{4}{9}\left(\frac{\hat{s}^2+\hat{u}^2}{\hat{t}^2}+\frac{\hat{t}^2+\hat{u}^2}{\hat{s}^2}\right)-\frac{8}{27}\frac{\hat{u}^2}{\hat{s}\hat{t}}$	2.6
$q\bar{q} \to gg$	$\frac{32}{27}\frac{\hat{u}^2+\hat{t}^2}{\hat{u}\hat{t}}-\frac{8}{3}\frac{\hat{u}^2+\hat{t}^2}{\hat{s}^2}$	1.0
$gg \to q\bar{q}$	$\frac{1}{6}\frac{\hat{u}^2+\hat{t}^2}{\hat{u}\hat{t}}-\frac{3}{8}\frac{\hat{u}^2+\hat{t}^2}{\hat{s}^2}$	0.1
$qg \to qg$	$\frac{\hat{s}^2+\hat{u}^2}{\hat{t}^2}-\frac{4}{9}\frac{\hat{s}^2+\hat{u}^2}{\hat{u}\hat{s}}$	6.1
$gg \to gg$	$\frac{9}{4}\left(\frac{\hat{s}^2+\hat{u}^2}{\hat{t}^2}+\frac{\hat{s}^2+\hat{t}^2}{\hat{u}^2}+\frac{\hat{u}^2+\hat{t}^2}{\hat{s}^2}+3\right)$	30.4

- Right: Results of the LO matrix elements for the various scattering processes, expressed in terms of the Mandelstam variables s, t and u. (Kripfganz et al, 1974);
- gg scattering is the dominant contribution at $\eta = 0$;
  (sensitivity to gluons, sensitivity to gluon self-coupling, as predicted by QCD)
- NLO predictions have meanwhile been calculated (2002).

The composition of the partons involved as function of the p_T of the jet at the Tevatron:

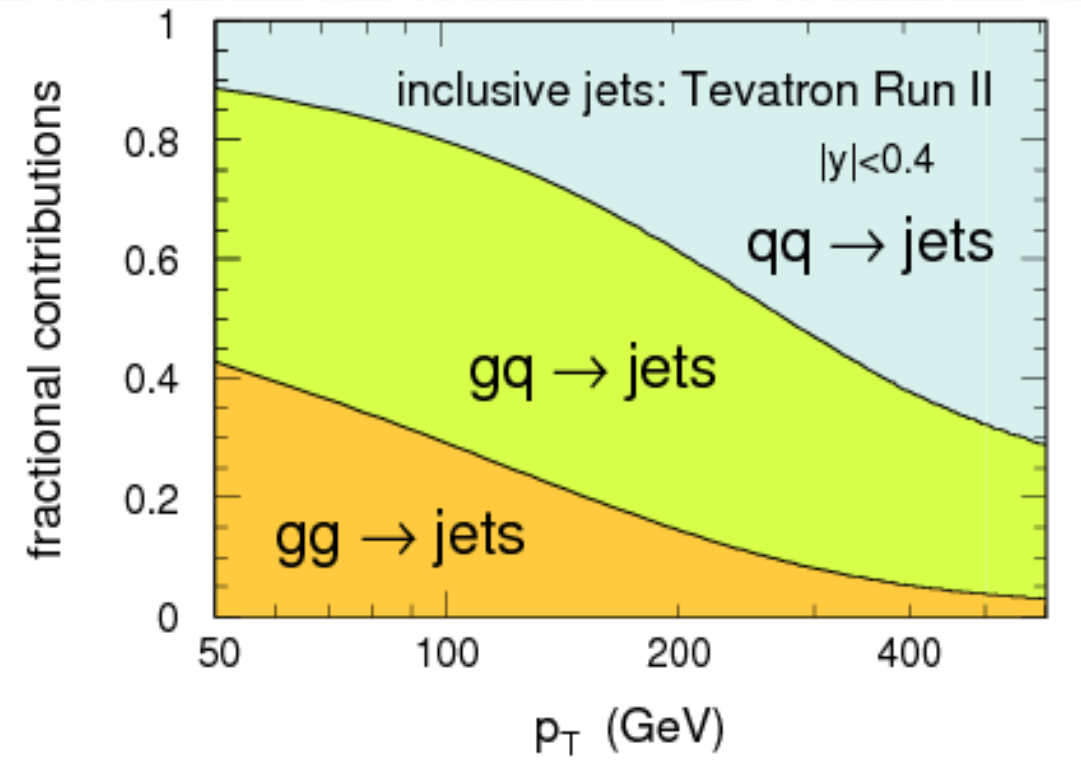

Tevatron,
ppbar, $\sqrt{s}$ = 1.96 TeV,
central region $|\eta| < 0.4$

- qq scattering dominates at high p_T
- However, gluons contribute over the full range

5.3.2 Experimental issues

$$d^2\sigma / dp_T\, d\eta = N / (\varepsilon \cdot L \cdot \Delta p_T \cdot \Delta\eta)$$

- In principle a simple counting experiment
- However, steeply falling p_T spectra are sensitive to jet energy scale uncertainties and resolution effects (migration between bins)
  → corrections (unfolding) to be applied
- Sensitivity to jet energy scale uncertainty:
  DØ: 1% energy scale error
  → 10% cross section uncert. at $|\eta|<0.4$

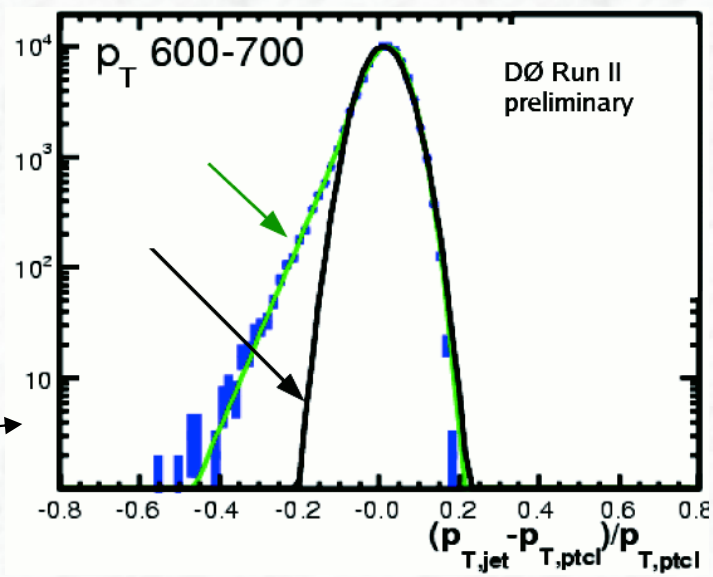

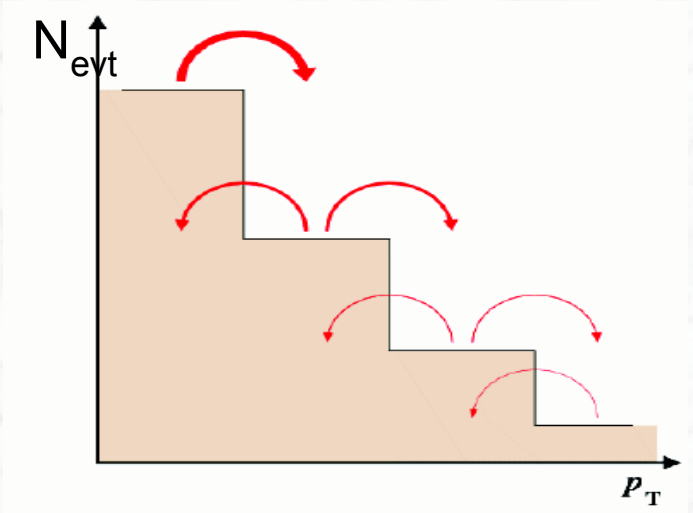

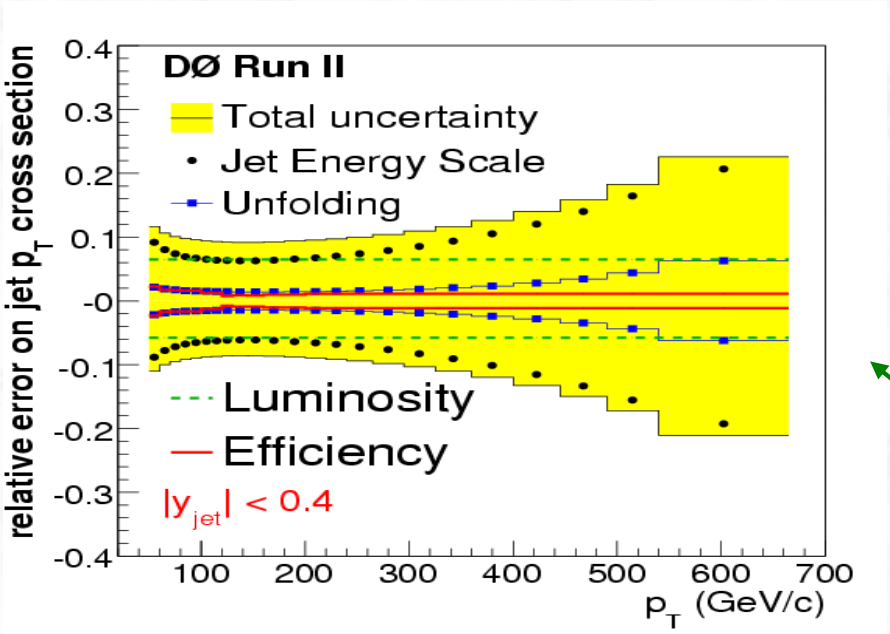

Major exp. errors:
energy scale, luminosity (6%),…

Jet reconstruction and energy measurement

- A jet is NOT a well defined object
  (fragmentation, gluon radiation, detector response)

- The detector response is different for particles interacting electromagnetically (e,γ) and for hadrons
  → for comparisons with theory, one needs to correct back the calorimeter energies to the „particle level“ (particle jet)
  Common ground between theory and experiment

- One needs an algorithm to define a jet and to measure its energy
  conflicting requirements between experiment and theory (exp. simple, e.g. cone algorithm, vs. theoretically sound (no infrared divergencies))

- Energy corrections for losses of fragmentation products outside jet definition and underlying event or pileup energy inside

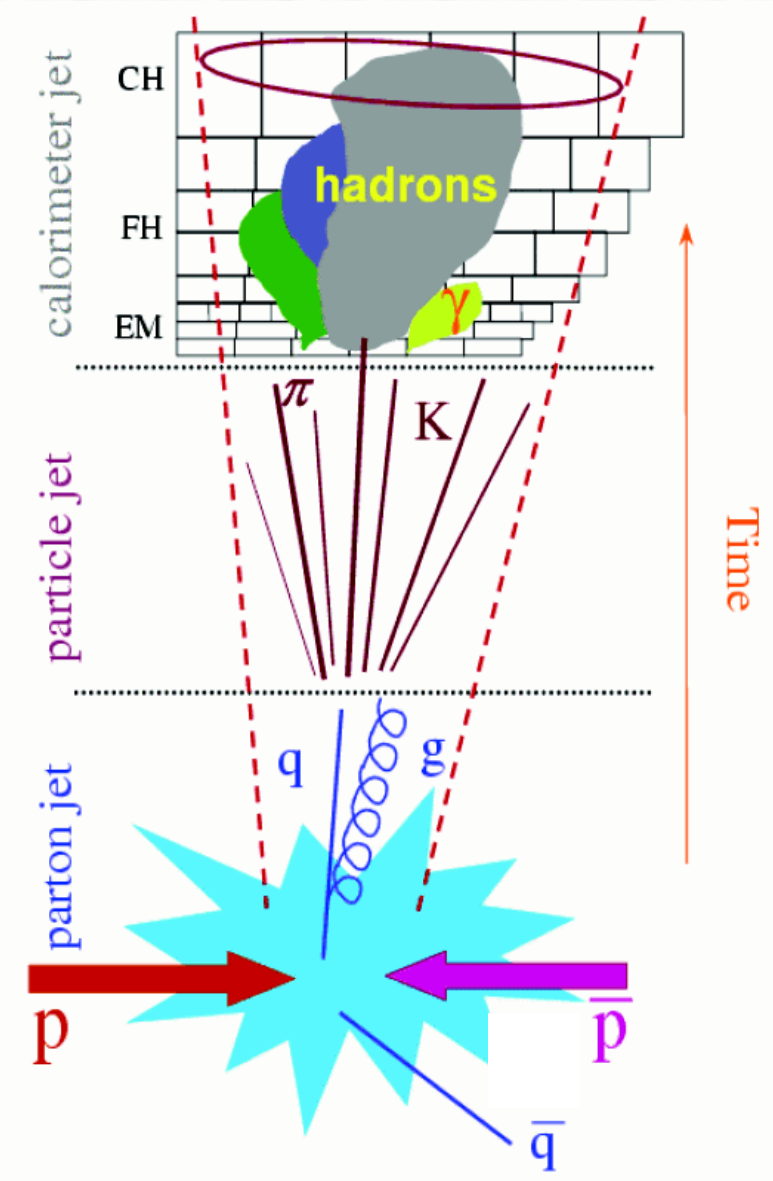

Infrared and collinear safeness

- To compare an experimental result with theory, often jet counting is involved (for example, inclusive jet cross section
- Need to have a jet reconstruction algorithm which is “collinear” and “infrared” safe

- Collinear safe: jet definition independent on the presence of partons radiated collinear to the quark

- Infrared safe: jet definition independent on the presence of soft radiation

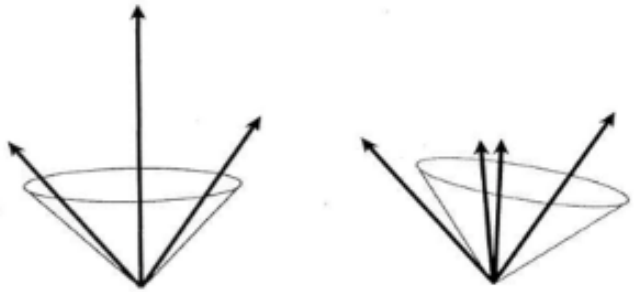

Figure 4.3: *Collinear safety violation. The splitting of one tower into two can change the jet properties.*

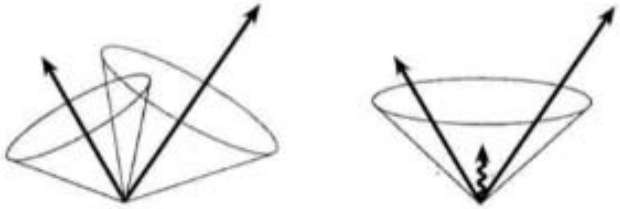

Figure 4.2: *Infrared safety violation: the radiation of a soft gluon can change the jet properties.*

A family of “safe” algorithms

- The k_T family algorithms are the most used nowadays
- For every pair of particles i,j compute d_{ij}

$$d_{ij} = min(E_{Ti}^{a}, E_{Tj}^{a}) \frac{\Delta\eta^2 + \Delta\varphi^2}{R^2} \qquad \text{i != j}$$

$$d_{ij} = E_T^2 \qquad \text{i = j}$$

- If a = -1, one has the Anti-k_t algorithm

Find $d_{min} = \min(d_i, d_{ij})$.

If $d_{min} = d_{ij}$ for some j, merge tower i and j to a new tower k with momentum $p_k^\mu = p_j^\mu + p_j^\mu$.

If $d_{min} = d_i$ then a jet is found.

Iterate until the list of tower is empty.

Main corrections:

- In general, calorimeters show different response to electrons/photons and hadrons

- Subtraction of offset energy not originating from the hard scattering
  (inside the same collision or pile-up contributions, use minimum bias data to extract this)

- Correction for jet energy out of cone
  (corrected with jet data + Monte Carlo simulation)

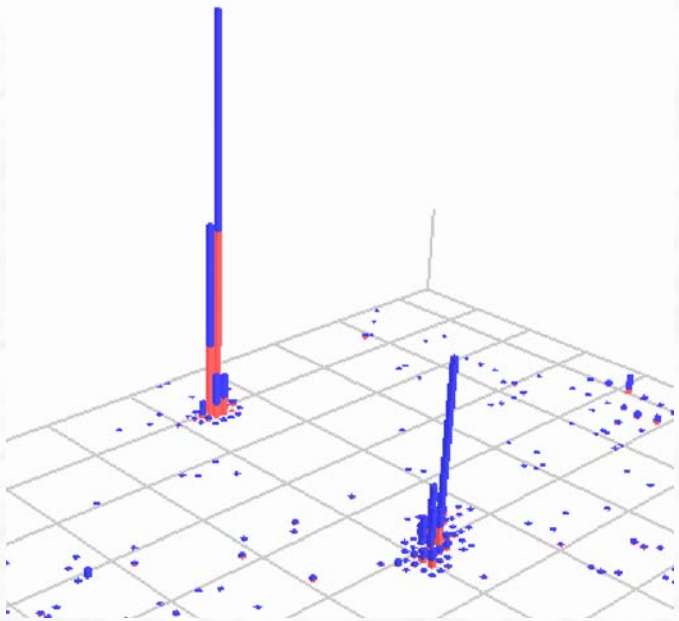

Jet Energy Scale

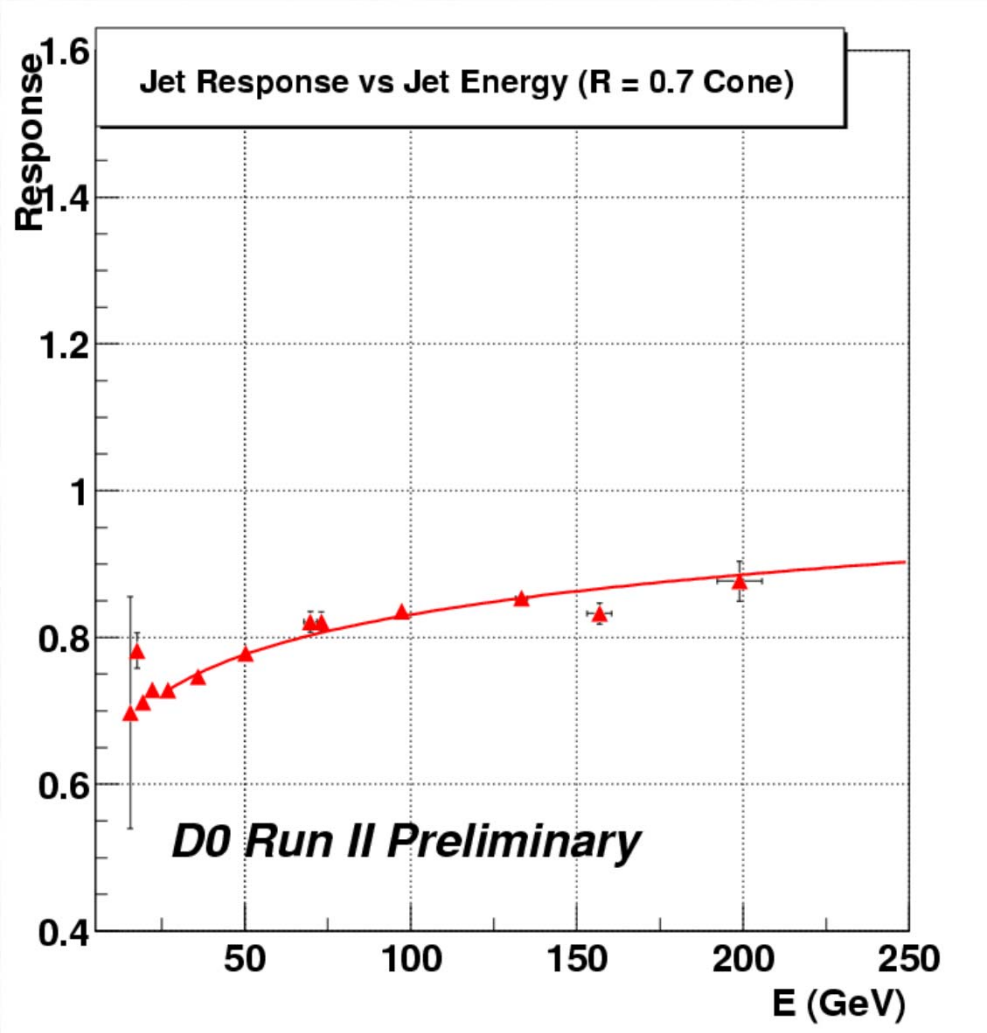

Jet response correction in DØ:

- Measure response of particles making up the jet
- Use photon + jet data - calibrate jets against the better calibrated photon energy

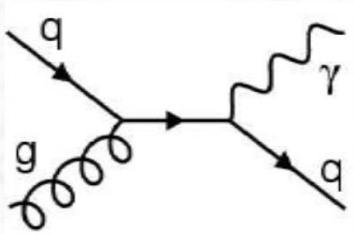

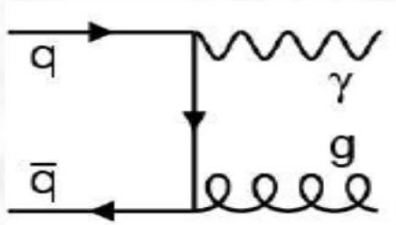

- Achieved jet energy scale uncertainty:

DØ: $\Delta E / E$ ~1-2%
(excellent result, a huge effort)

Jet energy scale at the LHC

- A good jet-energy scale determination is essential for many QCD measurements
  (arguments similar to Tevatron, but kinematic range (jet p_T) is larger, ~20 GeV – ~3 TeV)

- Propagate knowledge of the em scale to the hadronic scale, but several processes are needed to cover the large p_T range

Measurement process	**Jet p_T range**
Z + jet balance	$20 < p_T < 100 – 200$ GeV
γ + jet balance	$50 < p_T < 500$ GeV (trigger, QCD background)
Multijet balance	500 GeV $< p_T$

Reasonable goal: 5-10% in first runs (1 fb^{-1})
1- 2% long term

Example: Z + jet balance

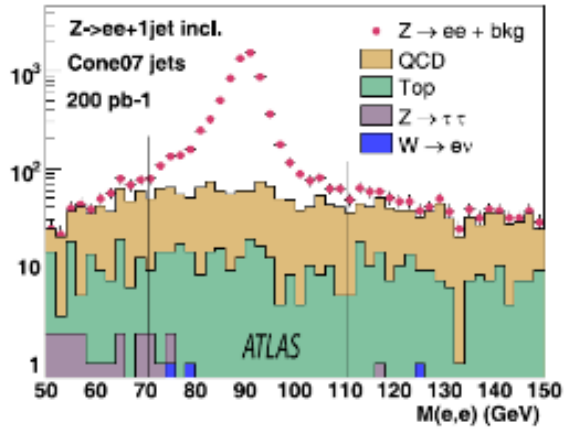

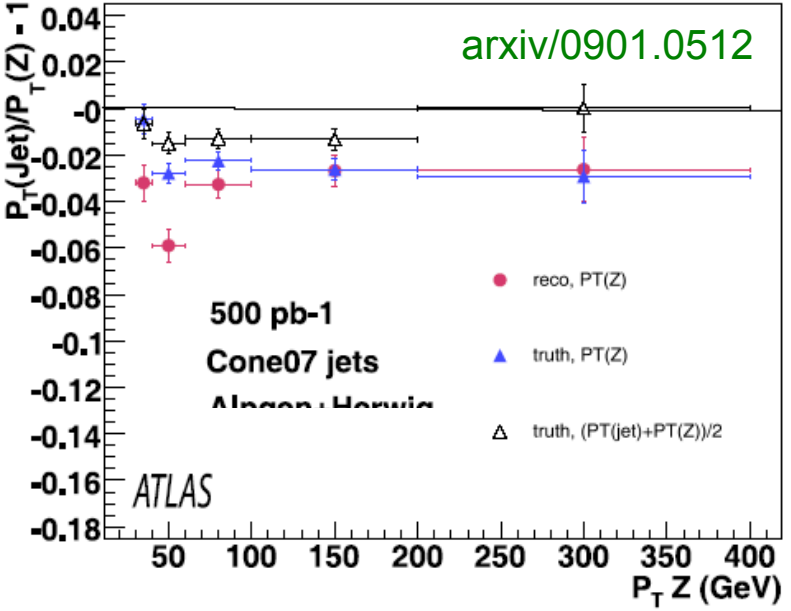

Stat. precision (500 pb^{-1}): 0.8%
Systematics: 5-10% at low p_T, 1% at high p_T

Test of QCD Jet production

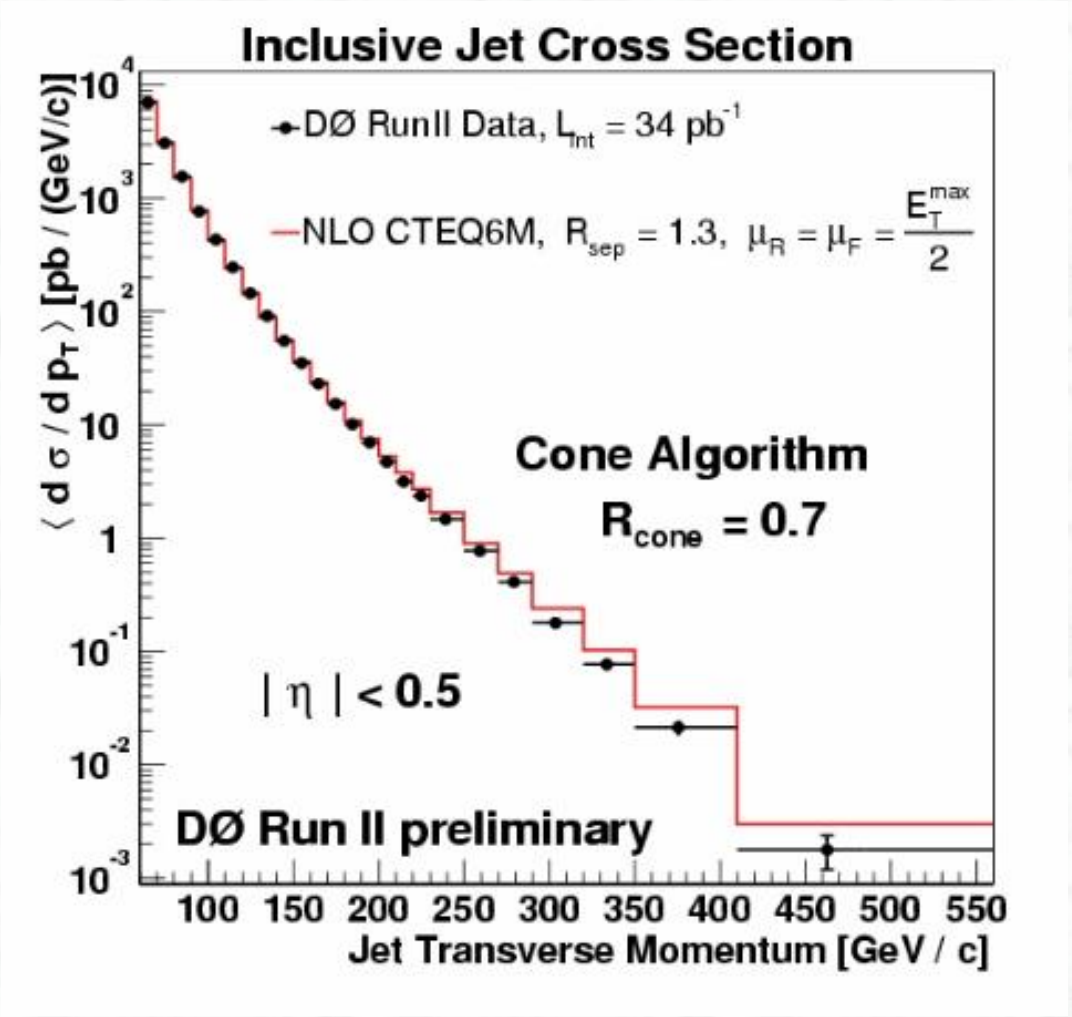

An **"early"** result from the DØ experiment (34 pb^{-1})

Inclusive Jet spectrum as a function of Jet-p_T

Very good agreement with NLO pQCD calculations over many orders of magnitude !

within the large theoretical and experimental uncertainties

Double differential distributions in p_T and η

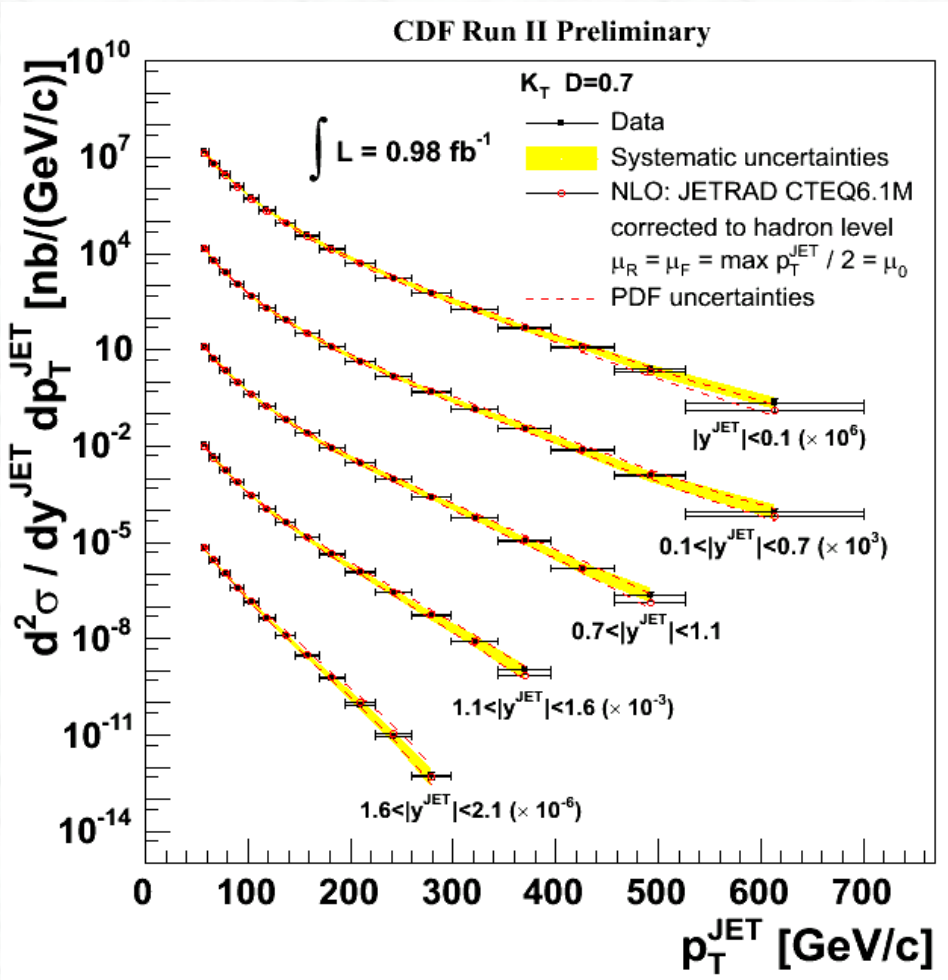

PRD 78 052006 ('08)

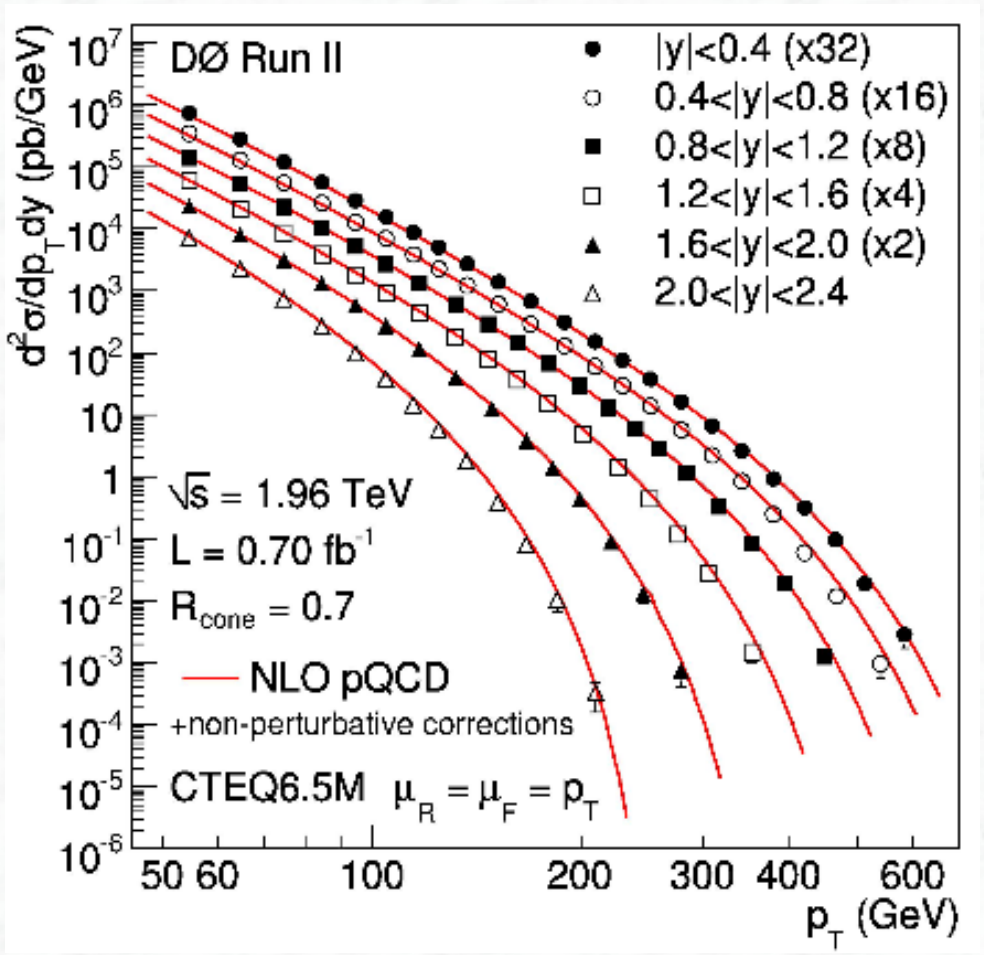

PRL 101 062001 ('08)

- Measurement in 5-6 different rapidity bins, over 9 orders of magnitude, up to p_T ~650 GeV
- Data corresponding to ~ 1 fb^{-1} (CDF) and 0.7 fb^{-1} (DØ)

Comparison between data and theory

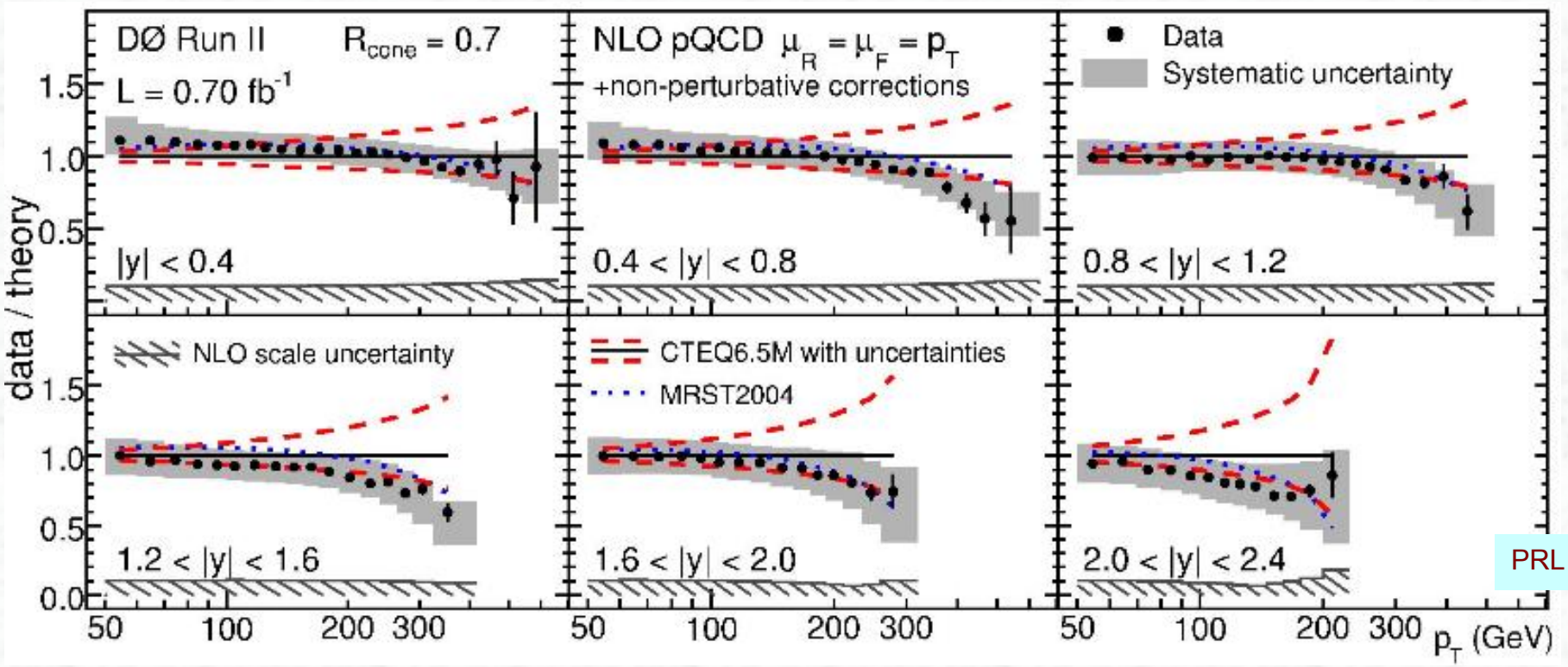

PRL 101 062001 ('08)

- CDF and DØ agree within uncertainties

- Experimental uncertainties are smaller than the pdf uncertainties

(in particular large for large x, gluon distribution)

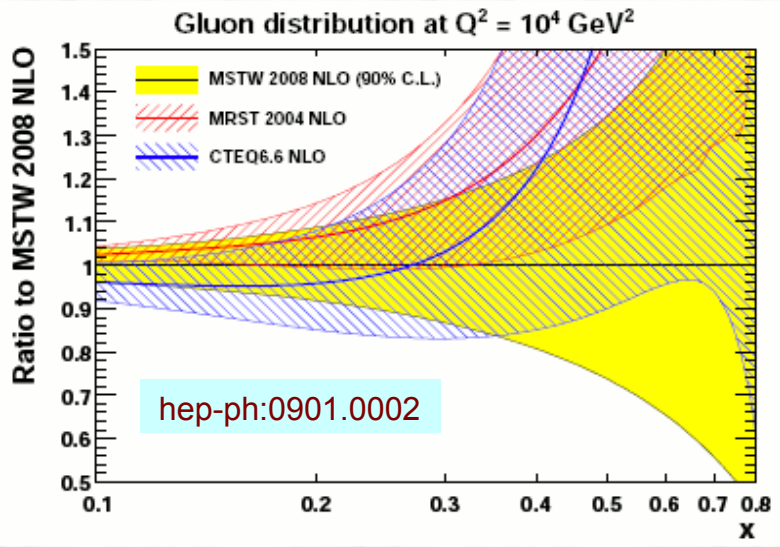

Di-jet angular distributions

- *Reduced sensitivity to jet energy scale*
- *Sensitivity to higher order QCD corrections preserved*

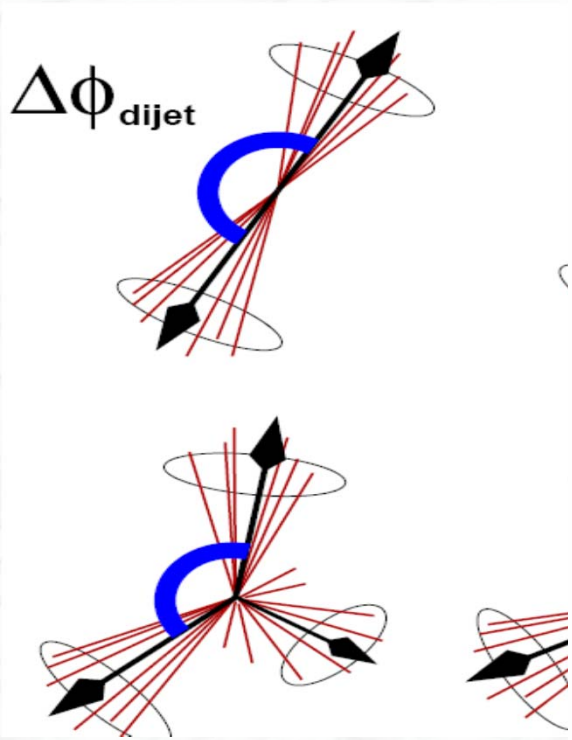

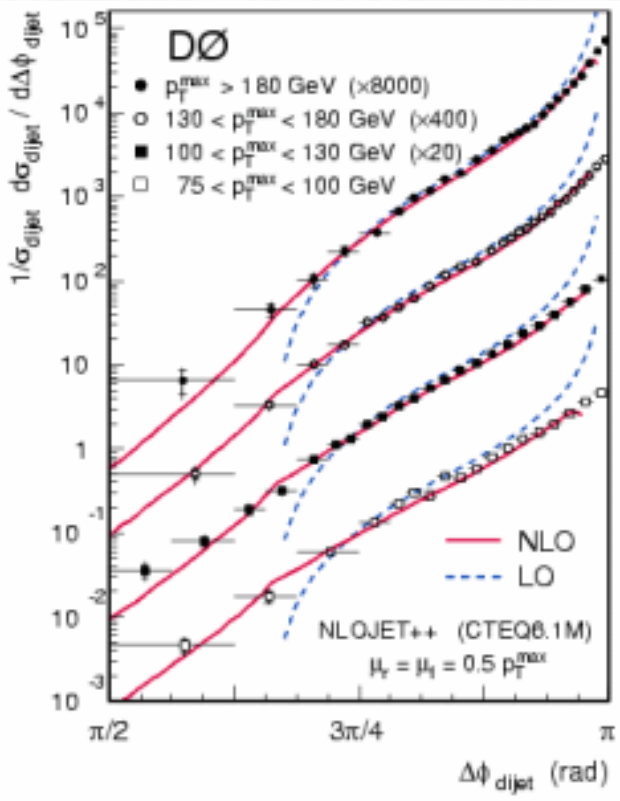

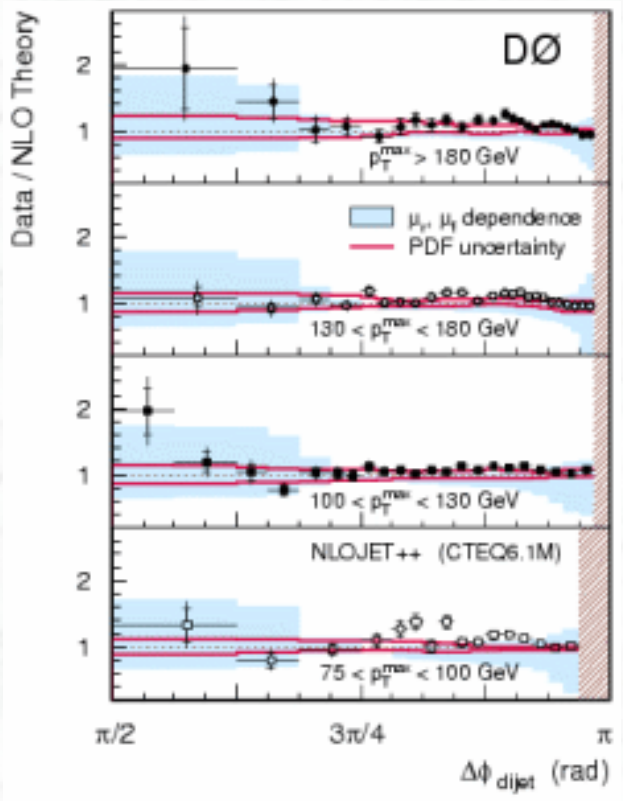

Good agreement with
next-to-leading order QCD predictions

High p_T jet events at the LHC

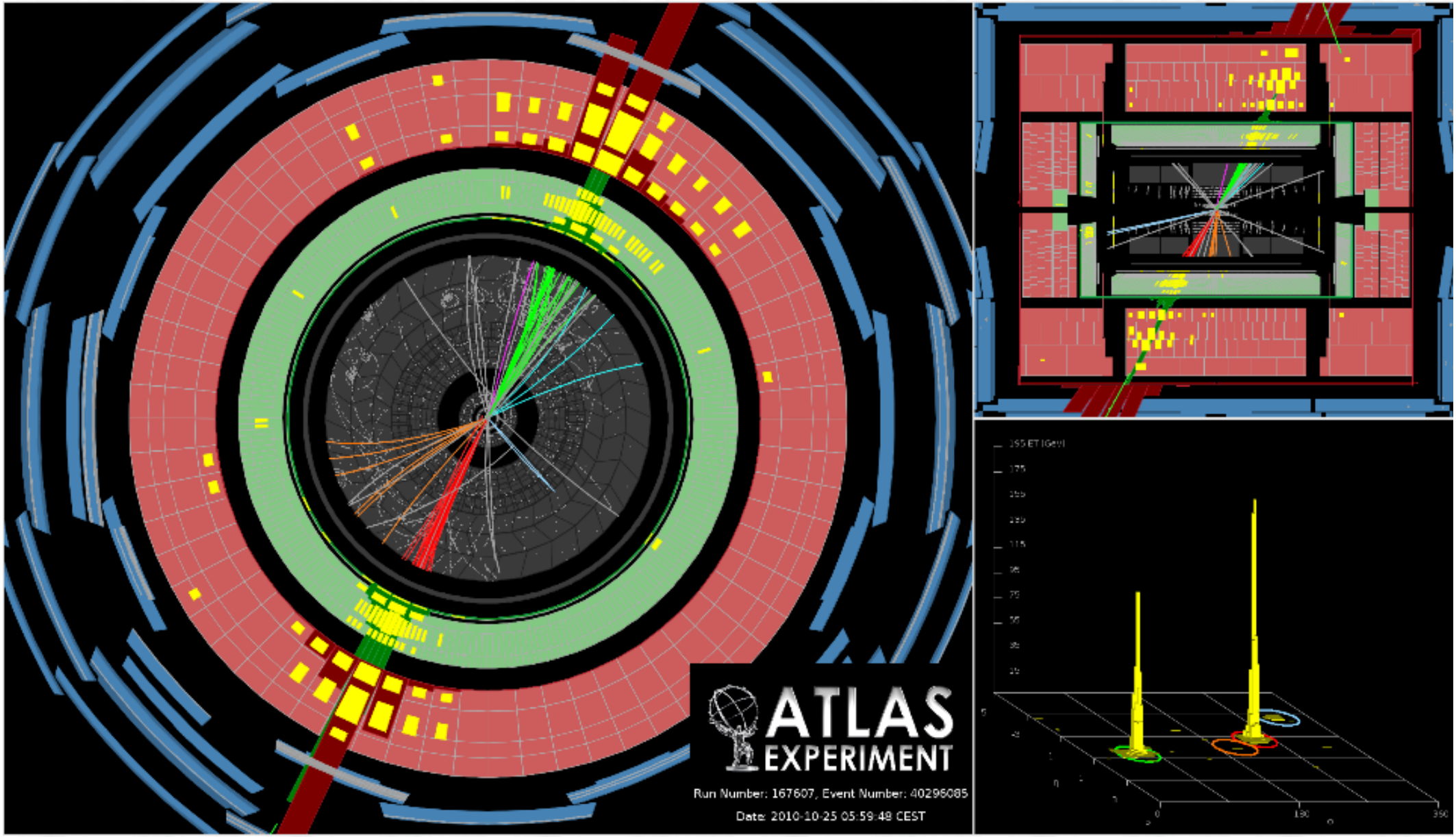

Event display that shows the highest-mass central dijet event collected during 2010, where the two leading jets have an invariant mass of 3.1 TeV. The two leading jets have (p_T, y) of (1.3 TeV, -0.68) and (1.2 TeV, 0.64), respectively. The missing E_T in the event is 46 GeV. From ATLAS-CONF-2011-047.

An event with a high jet multiplicity at the LHC

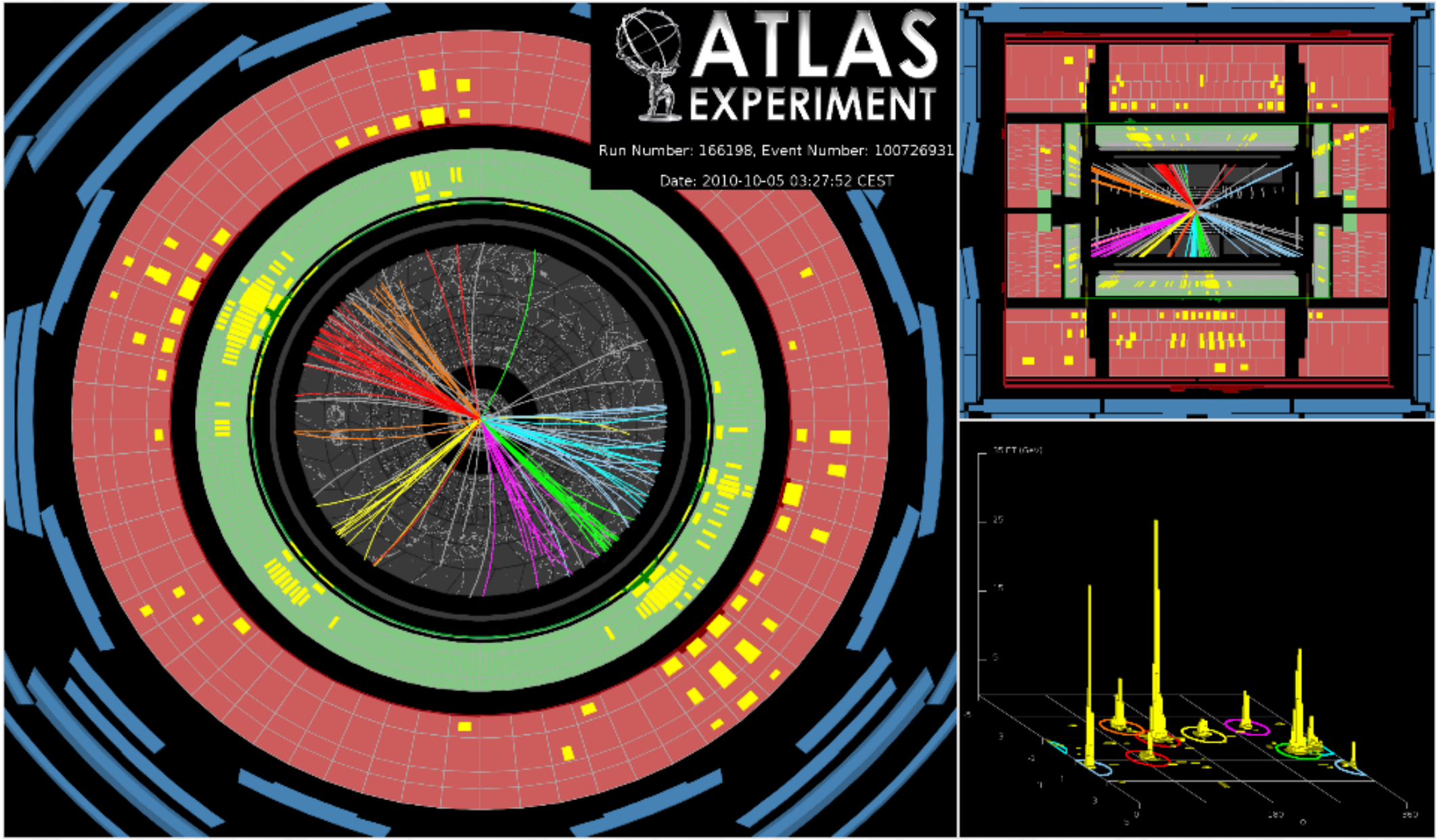

The highest jet multiplicity event collected by the end of October 2010, counting jets with p_T greater than 60 GeV: this event has eight. 1st jet (ordered by p_T): p_T = 290 GeV, η = -0.9, Φ = 2.7; 2nd jet: p_T = 220 GeV, η = 0.3, Φ = -0.7 Missing E_T = 21 GeV, Φ = -1.9, Sum E_T = 890 GeV. The event was collected on 5 October 2010.

Initial jet energy scale calibration:

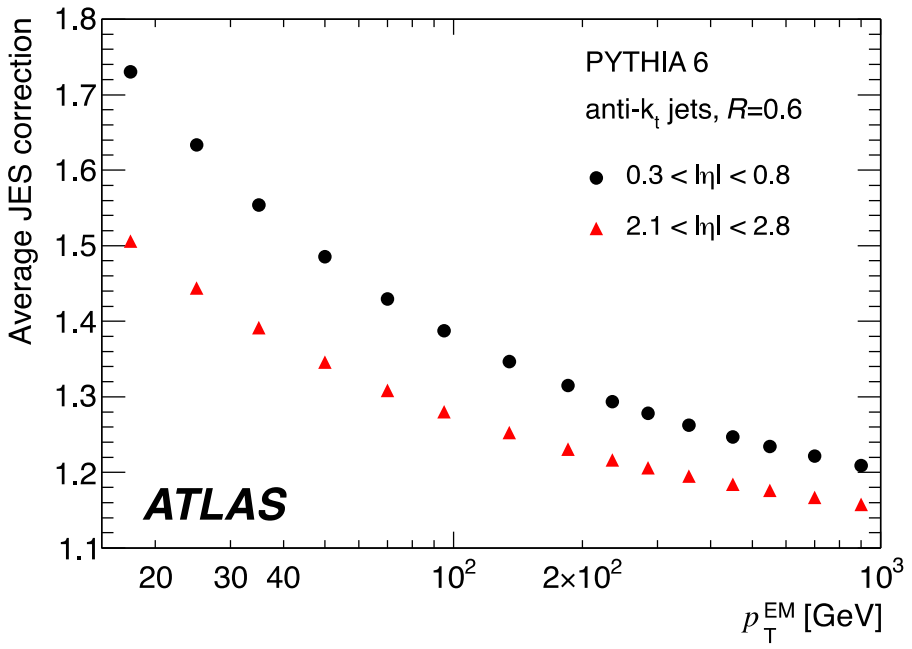

Average jet energy scale correction, evaluated using PYTHIA 6, as a function of jet transverse momentum at the EM scale for jets in the central barrel (black circles) and endcap (red triangles) regions, shown in EM scale p_T bins and η regions.

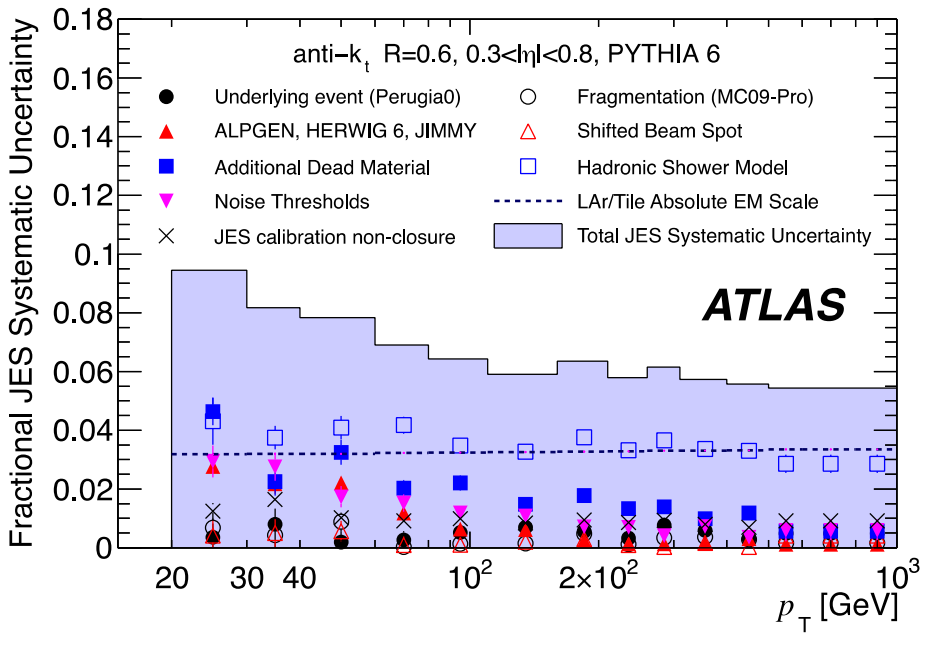

Fractional jet energy scale systematic uncertainty as a function of p_T for jets in the pseudorapidity region $0.3 < |\eta| < 0.8$ in the barrel calorimeter. The total systematic uncertainty is shown as the solid light blue area. The individual sources are also shown, with statistical errors if applicable.

Further improvements

Several in-situ techniques have reduced the jet energy scale uncertainty significantly:

- Single particle response (E(calorimeter) / p(tracking detector) measurements)

- Di-jet balance

And, more recently:

– γ + jet balance
- Z + jet balance

Strong impact on all measurements involving jets

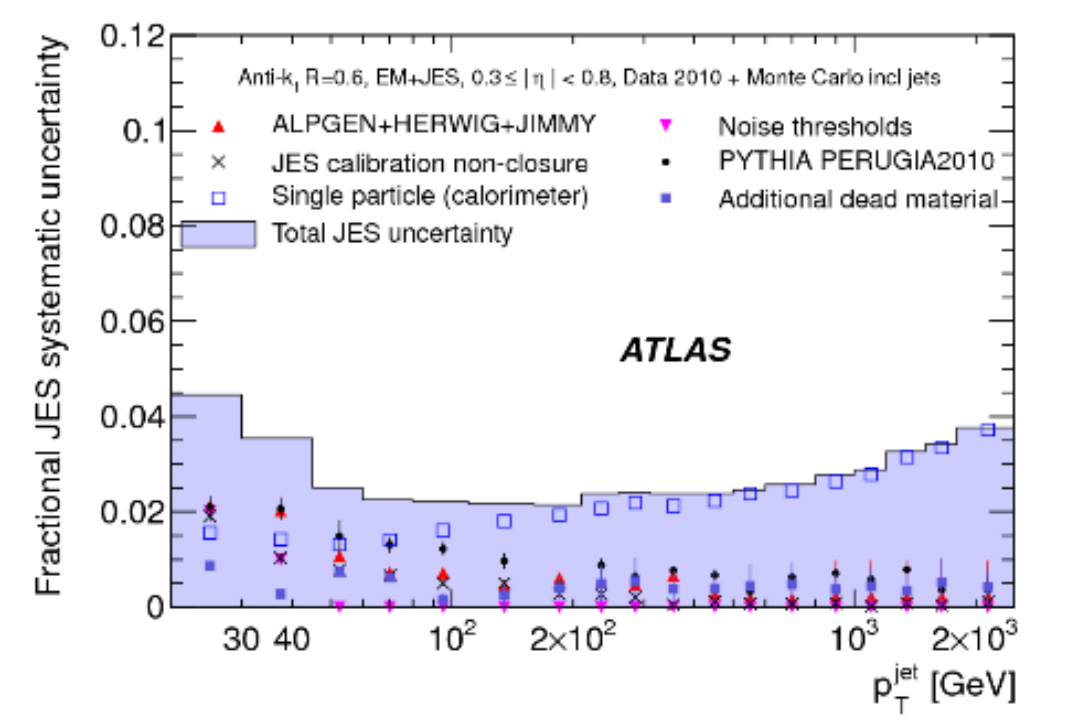

Final uncertainty in 2011 data

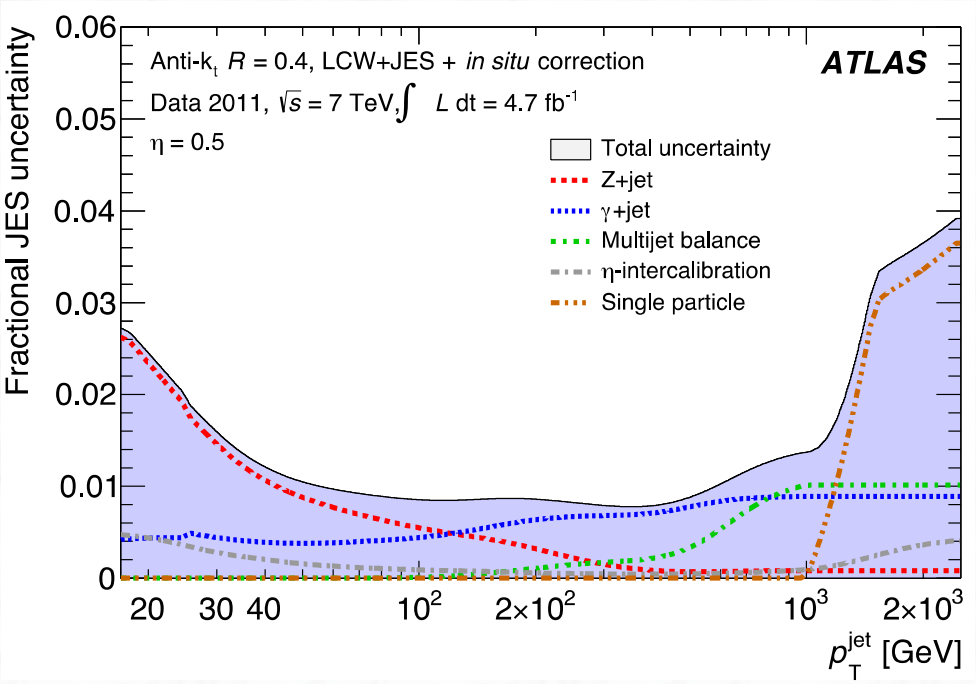

< 2 % for central jets with
p_T in 25 GeV < p_T < 1000 GeV

increase of uncertainty
for larger pseudorapidities

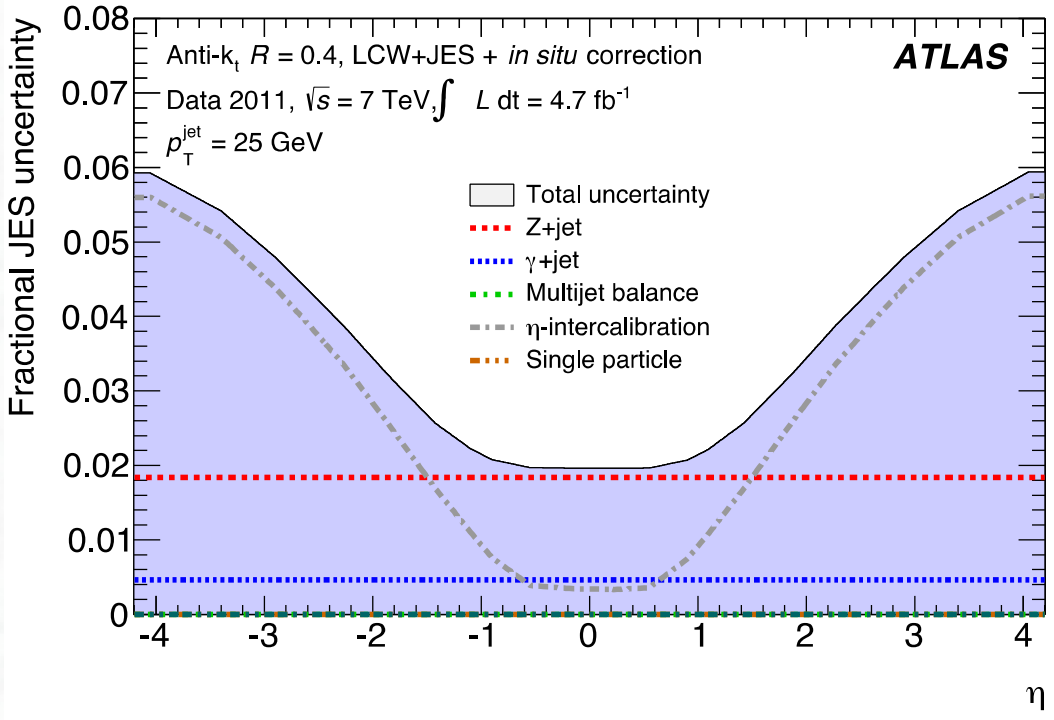

Jet energy resolution

Select di-jet events in back-to-back-topology in transverse plane
(additional activity is corrected for in complicated procedure)

Consider asymmetry in p_T balance

$$A(p_{T,1}, p_{T,2}) \equiv \frac{p_{T,1} - p_{T,2}}{p_{T,1} + p_{T,2}}$$

$$\sigma(A) = \frac{\sqrt{\sigma^2(p_{T,1}) + \sigma^2(p_{T,2})}}{\langle p_{T,1} + p_{T,2} \rangle} \simeq \frac{1}{\sqrt{2}} \frac{\sigma(p_T)}{p_T}$$

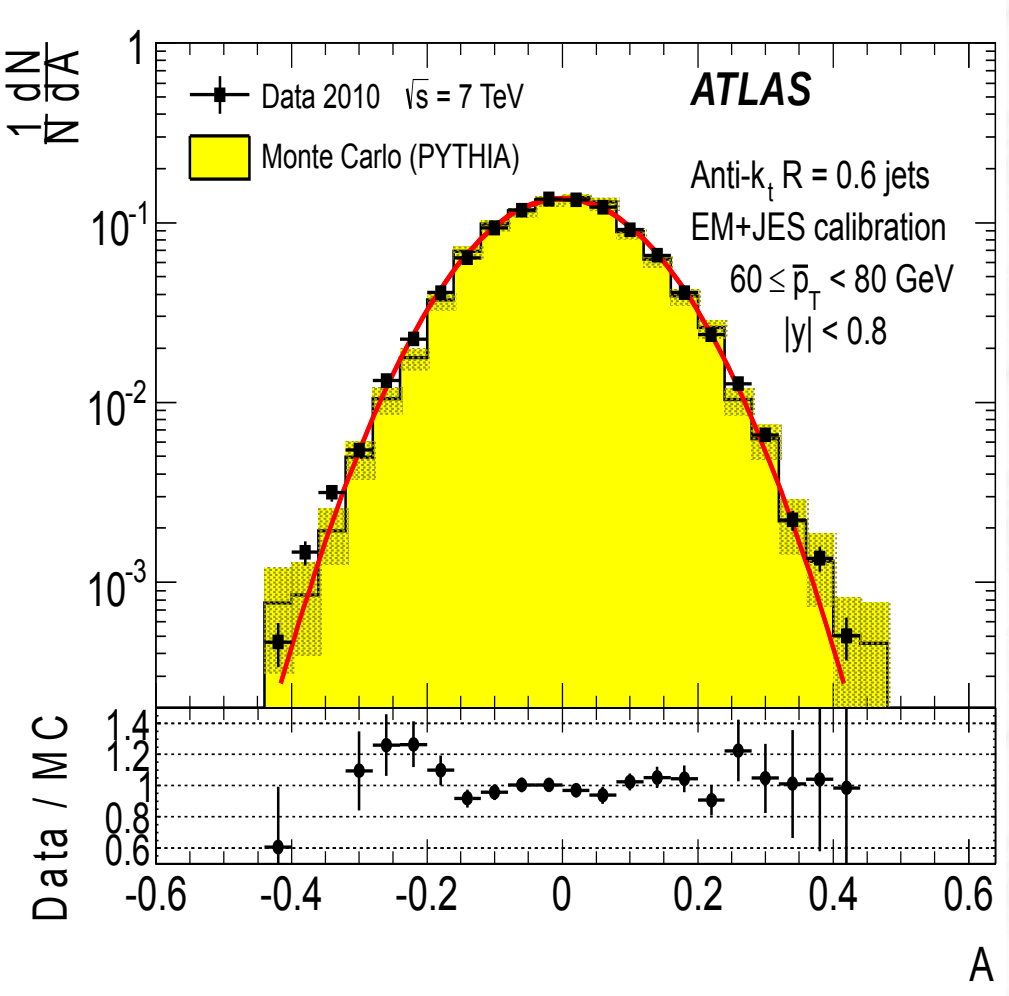

First measurements of jet p_T spectra:

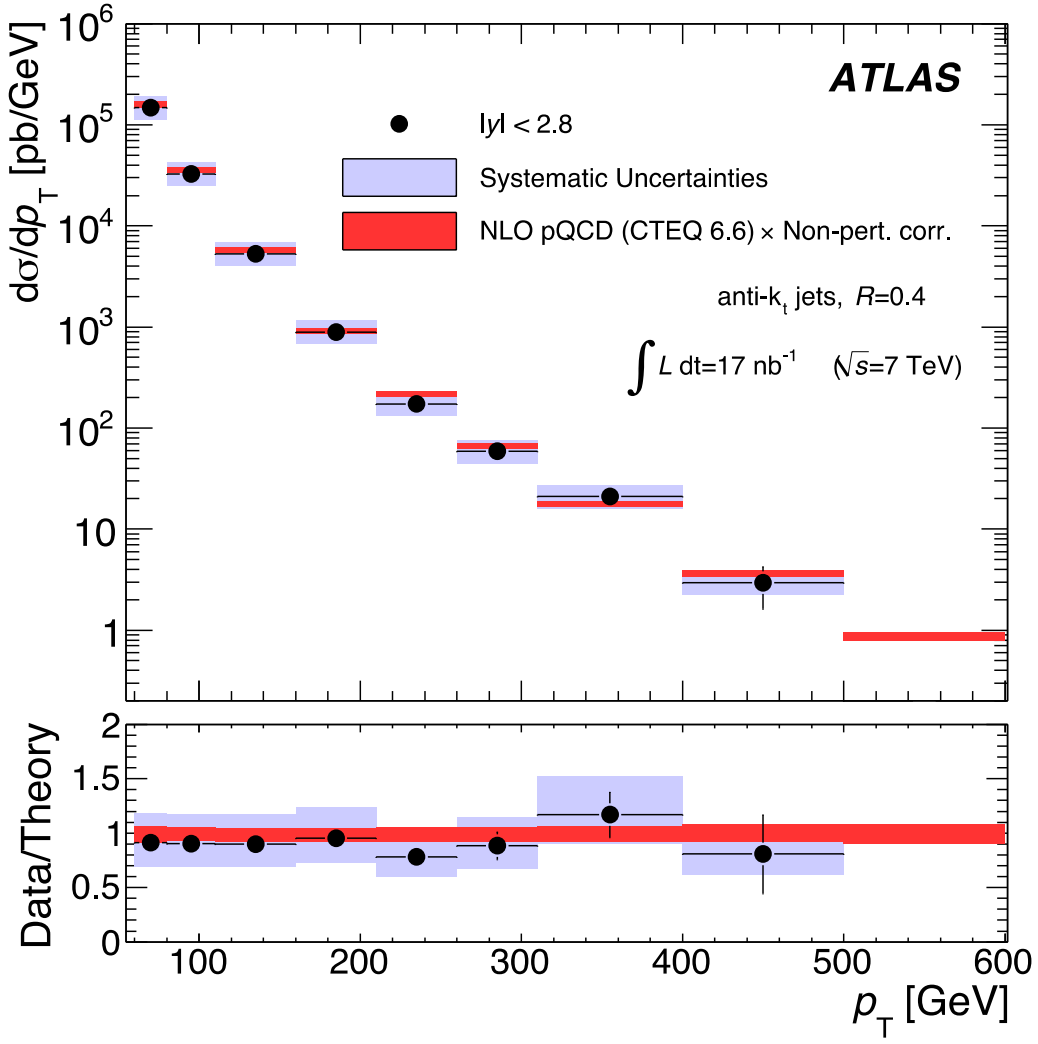

Inclusive jet differential cross section as a function of jet p_T integrated over the full region |y| < 2.8 for jets identified using the anti-kt algorithm with R = 0.4. The data are compared to NLO pQCD calculations to which soft QCD corrections (e.g. underlying event) have been applied. The error bars indicate the statistical uncertainty on the measurement, and the grey shaded bands indicate the quadratic sum of the systematic uncertainties, dominated by the jet energy scale uncertainty. The theory uncertainty shown in red is the quadratic sum of uncertainties from the choice of renormalisation and factorisation scales, parton distribution functions, $\alpha_s(m_Z)$, and the modelling of soft QCD effects.

From 2010 to 2011 data

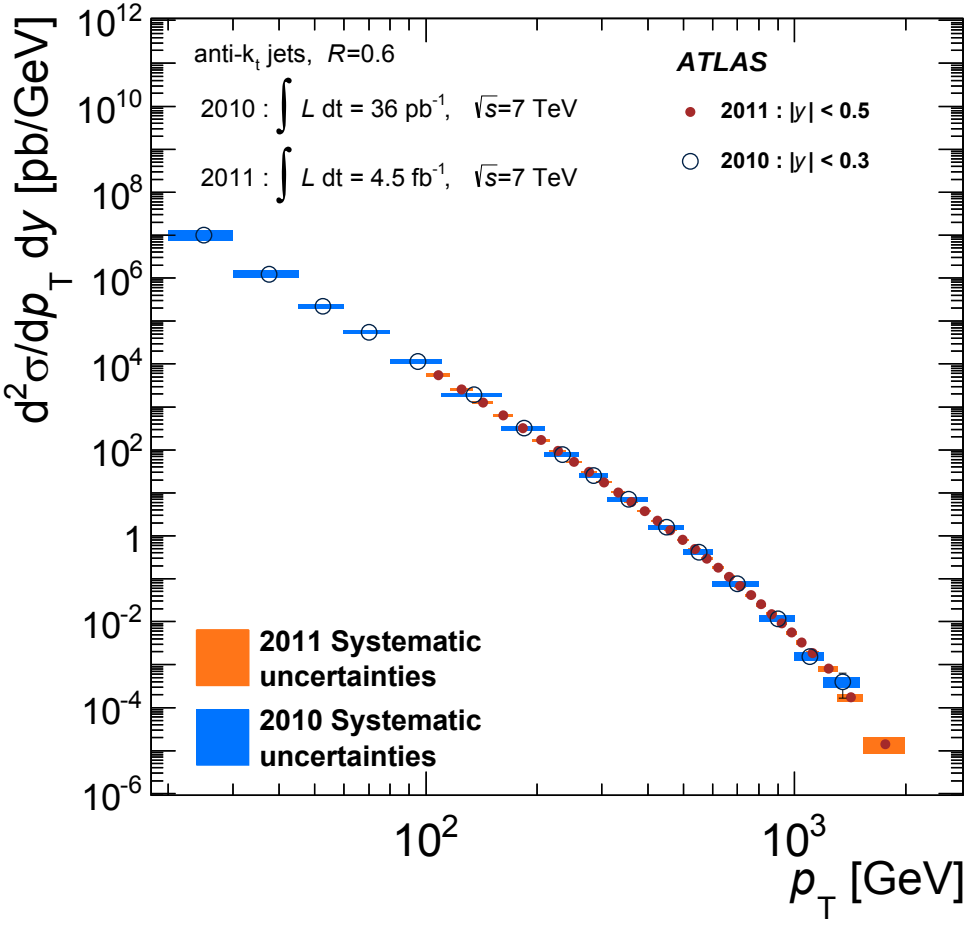

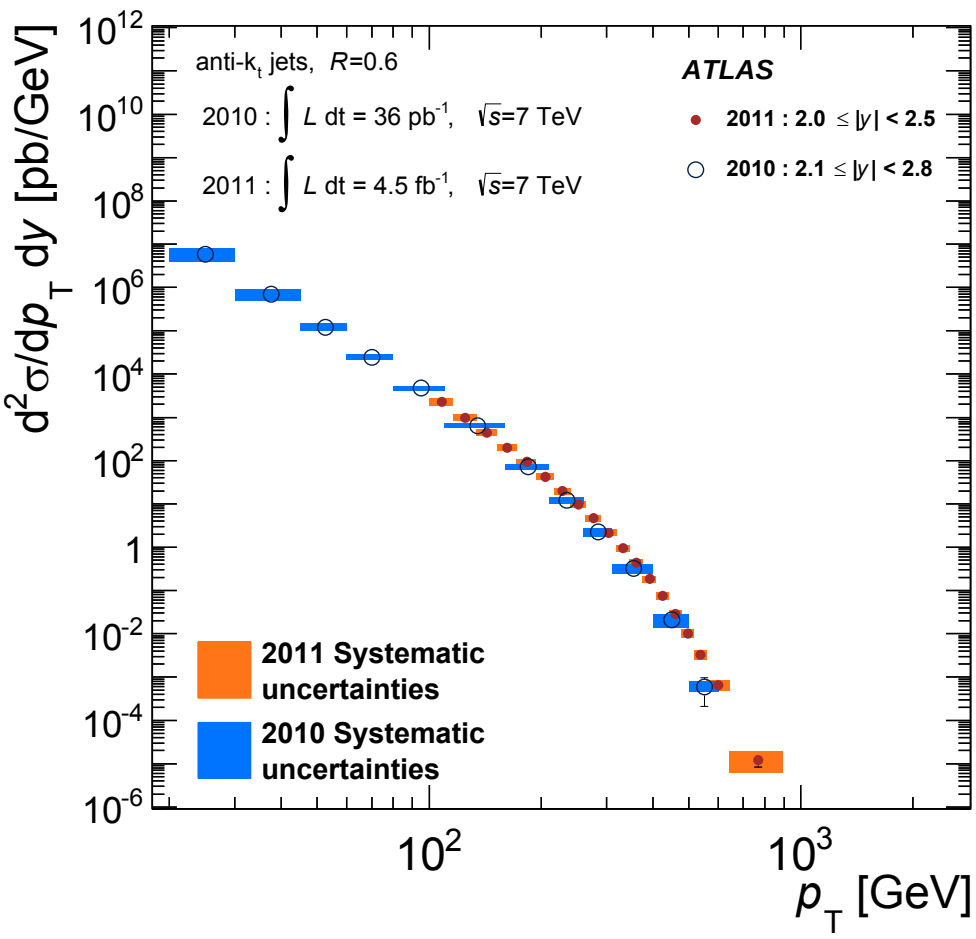

Recent LHC measurement

(full ATLAS dataset at 7 TeV)

JHEP 02 (2015) 153

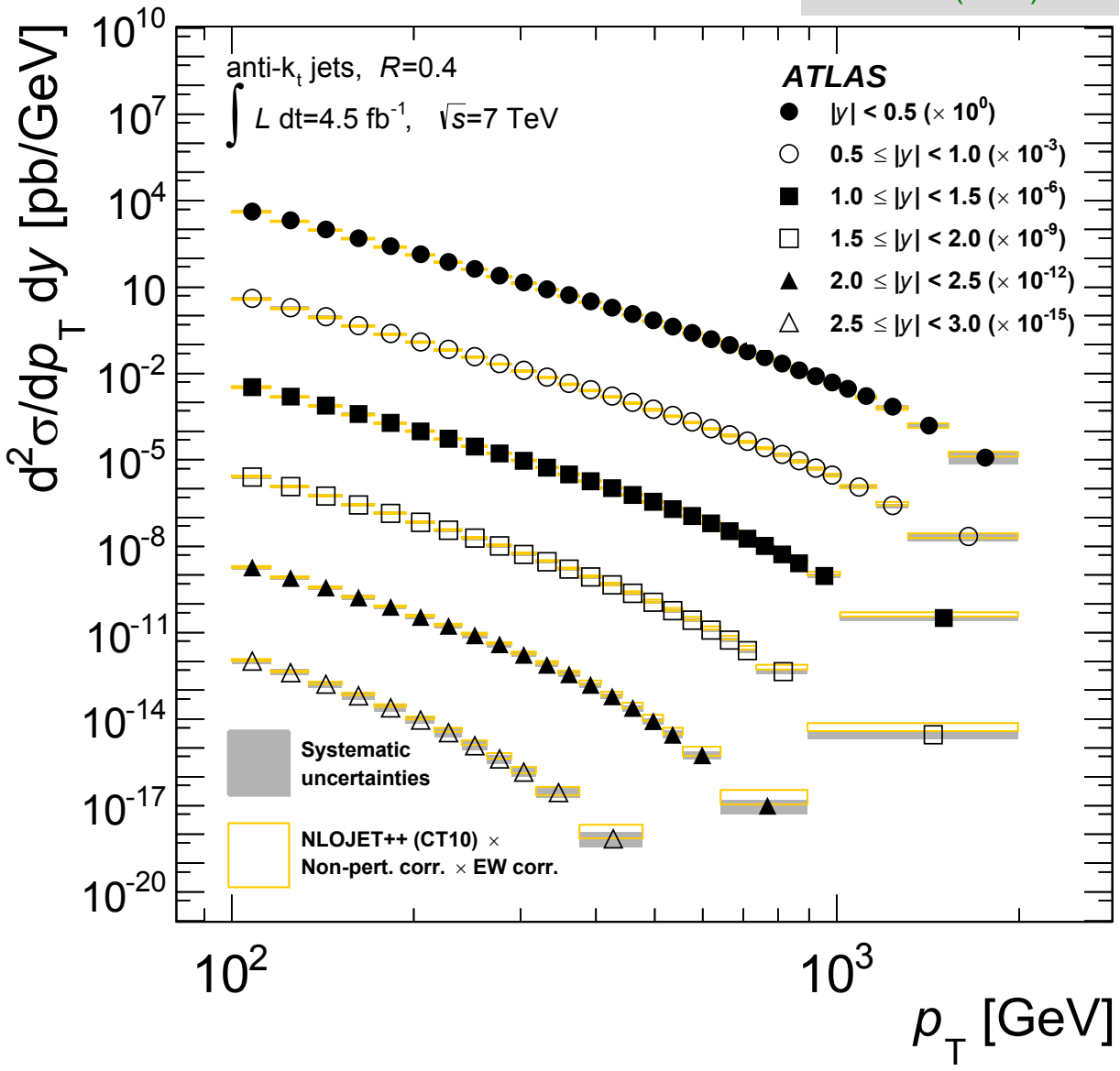

Data are well described by NLO perturbative QCD calculations (NLOJet++), within the experimental and theoretical uncertainties

Theoretical uncertainties on the NLO prediction

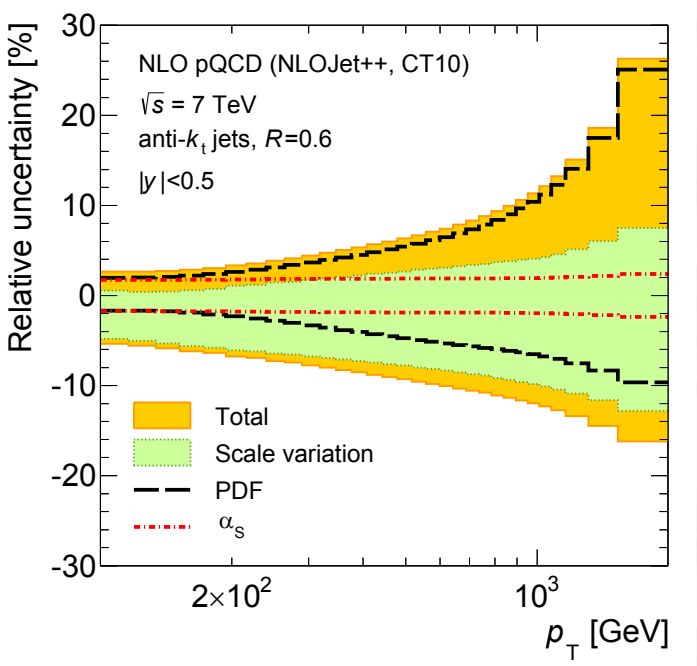

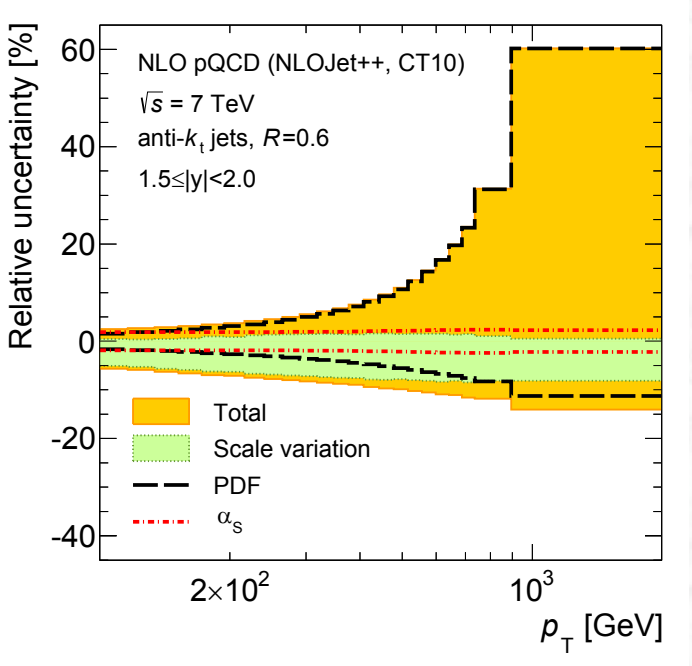

JHEP 02 (2015) 153

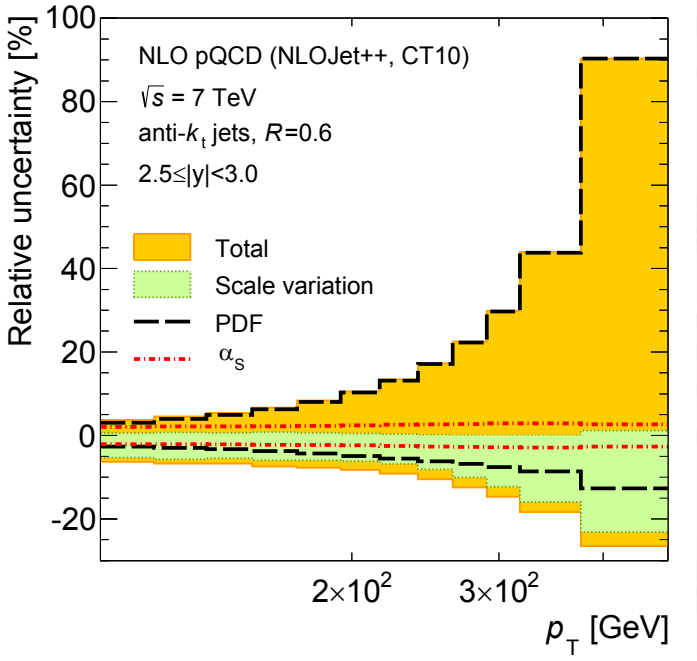

- PDFs result in a significant uncertainty in the theoretical prediction at large p_T and at large rapidities

- Scale uncertainties at the level of ±5% at low p_T, growing to ±10-20% at high p_T

Experimental uncertainties

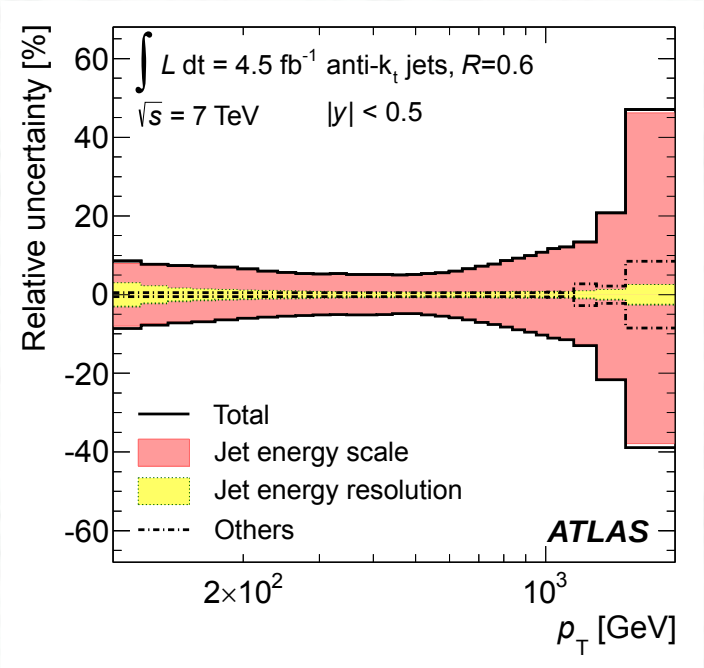

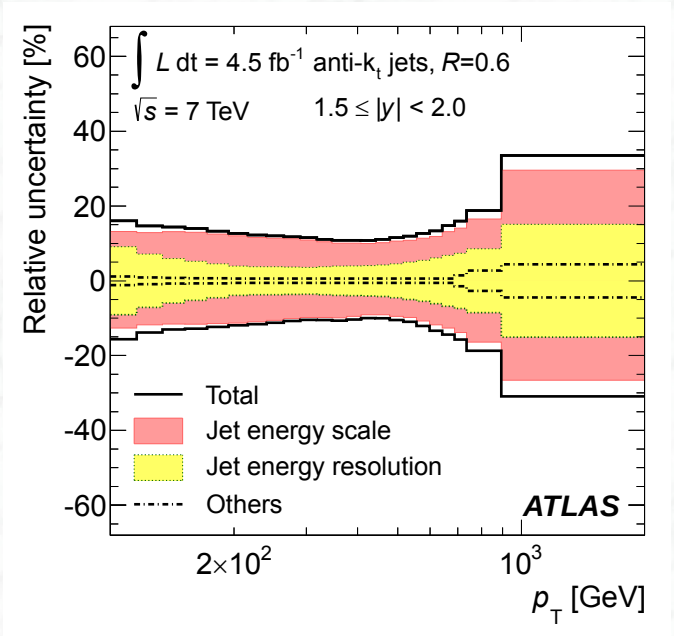

JHEP 02 (2015) 153

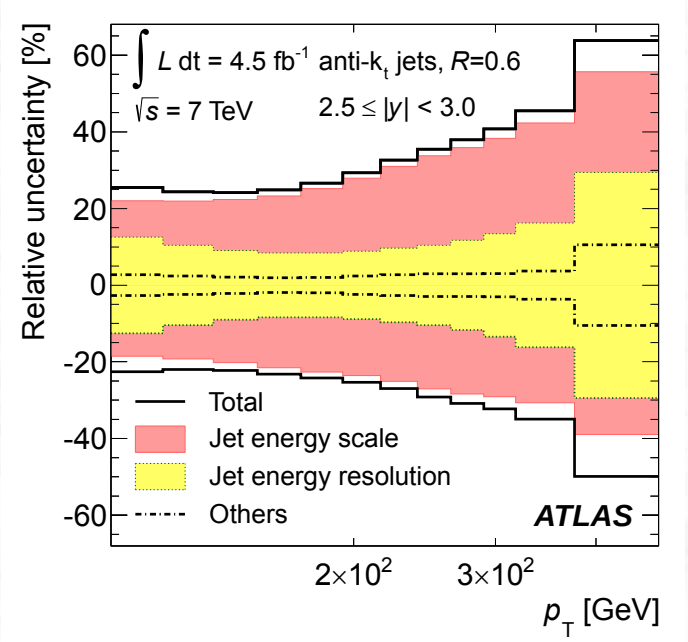

- Experimental uncertainties are dominated by uncertainties on the Jet Energy Scale (largest at high p_T)

Detailed Comparison between data and theory

JHEP 02 (2015) 153

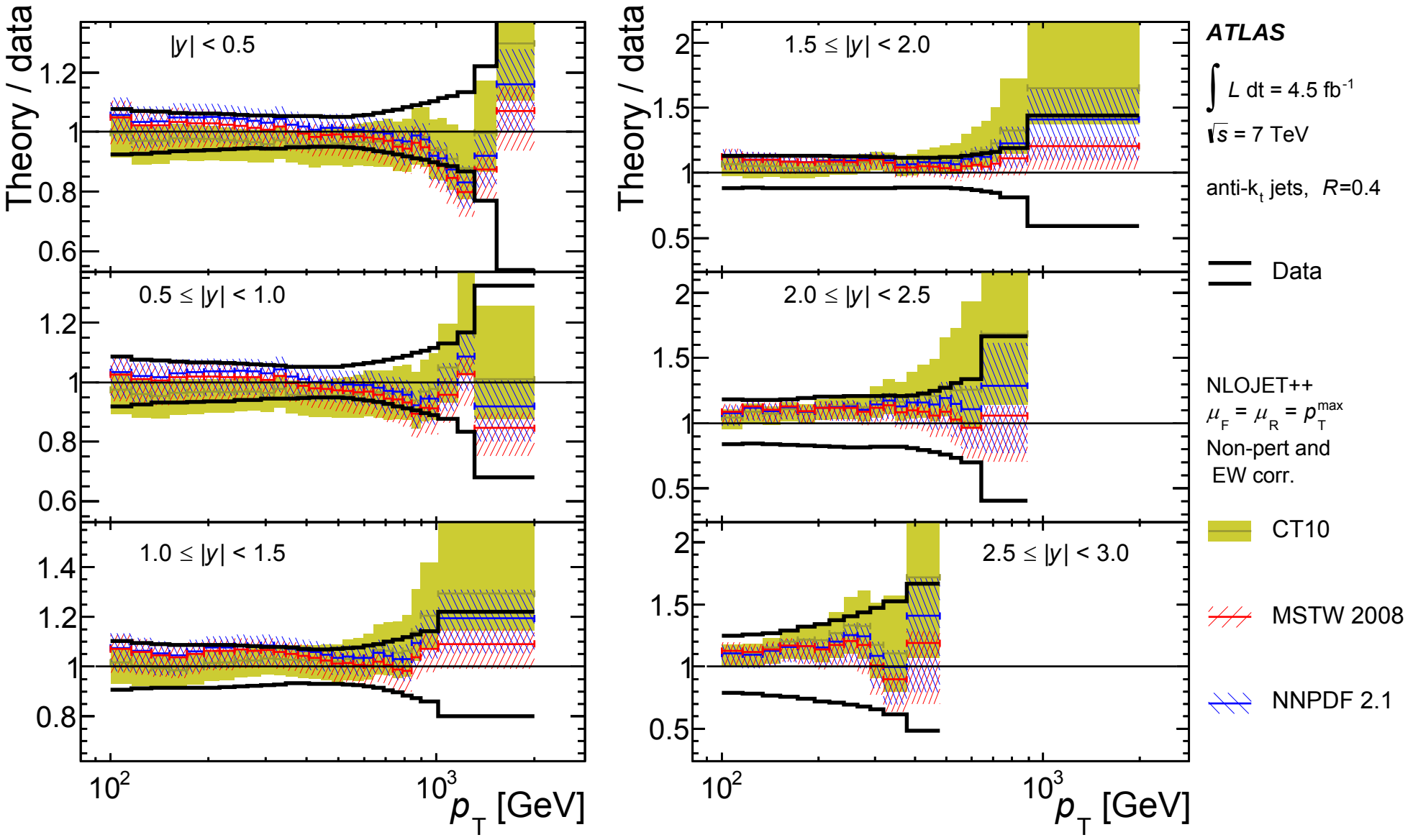

Good agreement over the full p_T and η range within uncertainties

Study of Compatibility

JHEP 02 (2015) 153

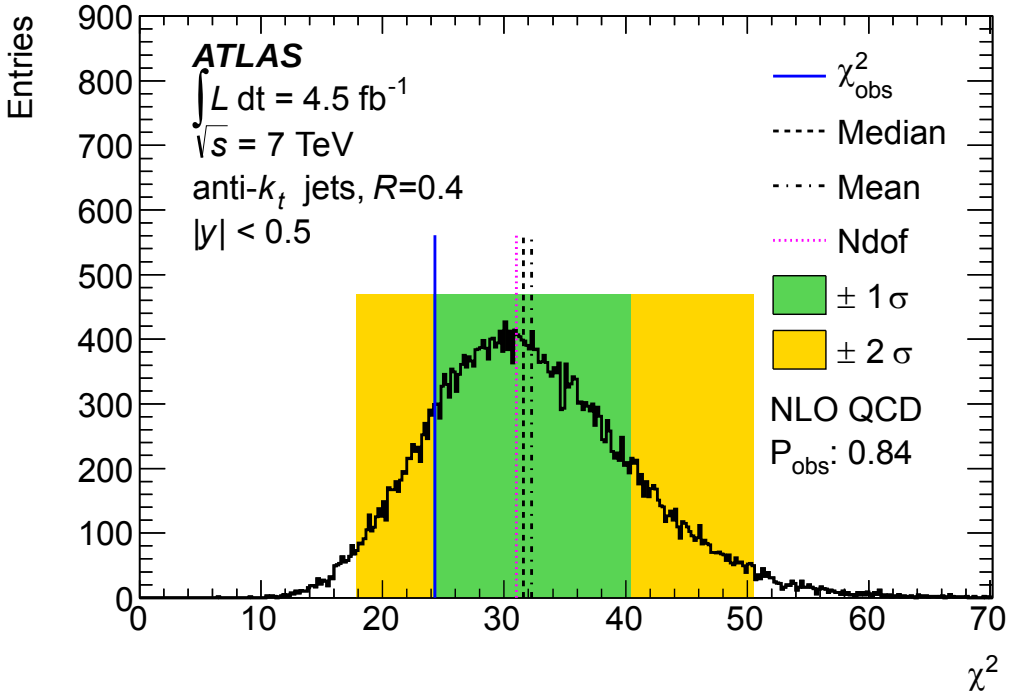

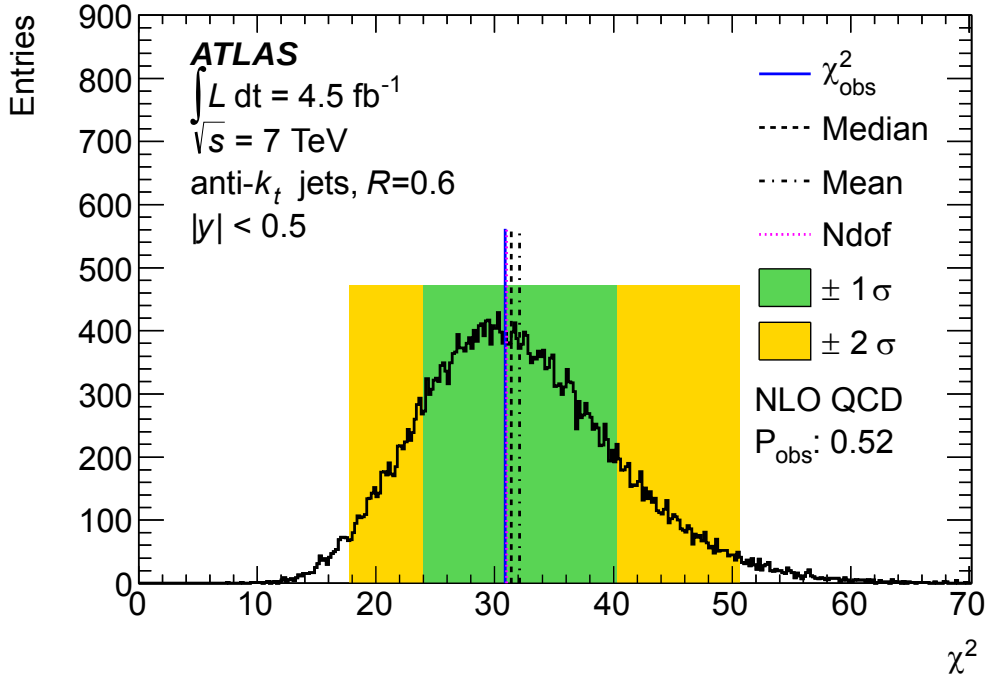

The χ2 distribution of pseudo-experiments (black histogram) for NLO pQCD prediction using the CT10 PDF set for jets with R=0.4. The full information on the uncertainties, including their asymmetries and correlations is used. The black vertical dashed (solid) line indicates the median (mean) of the distribution, while the green (yellow) band indicates the ±1σ (±2σ) region. The blue dot-dashed vertical lines indicate the observed χ2obs with the corresponding observed p-value, Pobs, given in the legend. The pink dotted lines show the number of degrees of freedom.

Angular correlations:

The differential cross section (1/sigma)(d sigma/d delta phi) binned in nine p_T^{max} regions. Overlaid on the data (points) are results from the NLO pQCD calculation. The error bars on the data points indicate the statistical (inner error bar) and systematic uncertainties added in quadrature in this and subsequent figures. The theory uncertainties are indicated by the hatched regions. Different bins in pTmax are scaled by multiplicative factors of ten for display purposes. The region near the divergence at delta phi --> pi is excluded from the calculation.

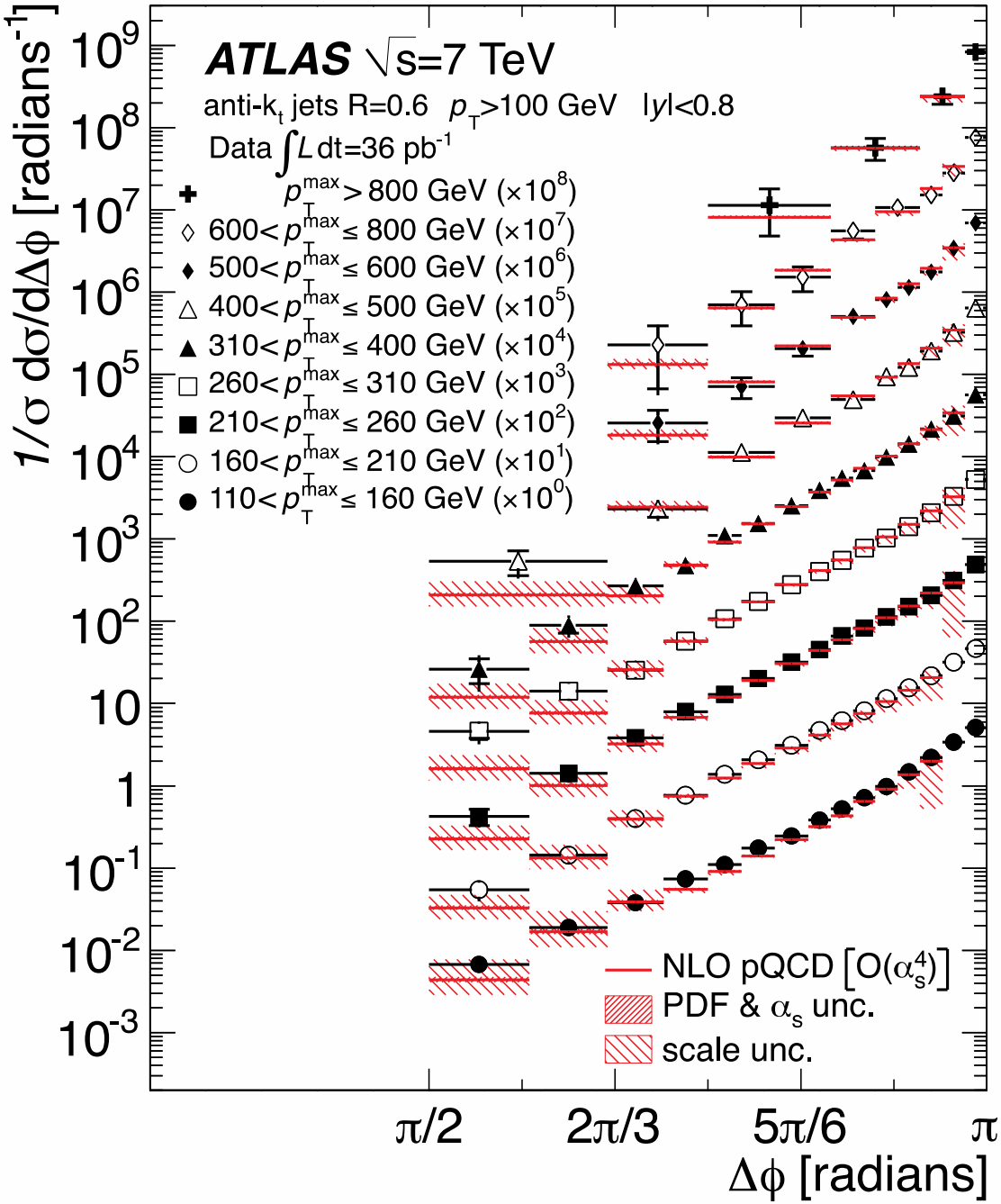

Ratio between data and NLO calculations:

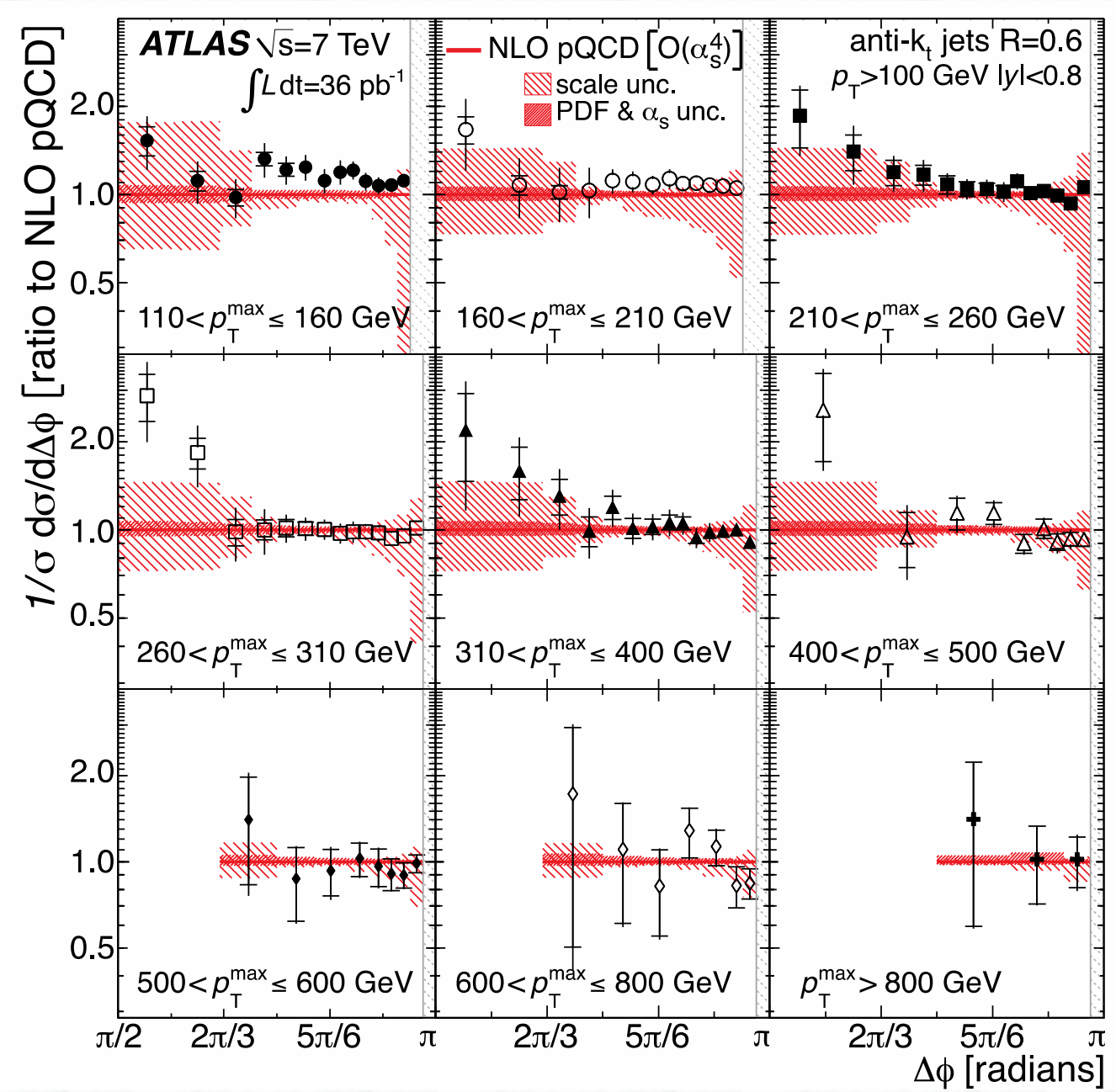

Ratio of the differential cross section (1/sigma)(d sigma/d delta phi) measured in data with respect to expectations from NLO pQCD (points). The theory uncertainties are indicated by the hatched regions. The region near the divergence at delta phi --> pi is excluded from the comparison.

Invariant di-jet mass spectra, ratio data/theory:

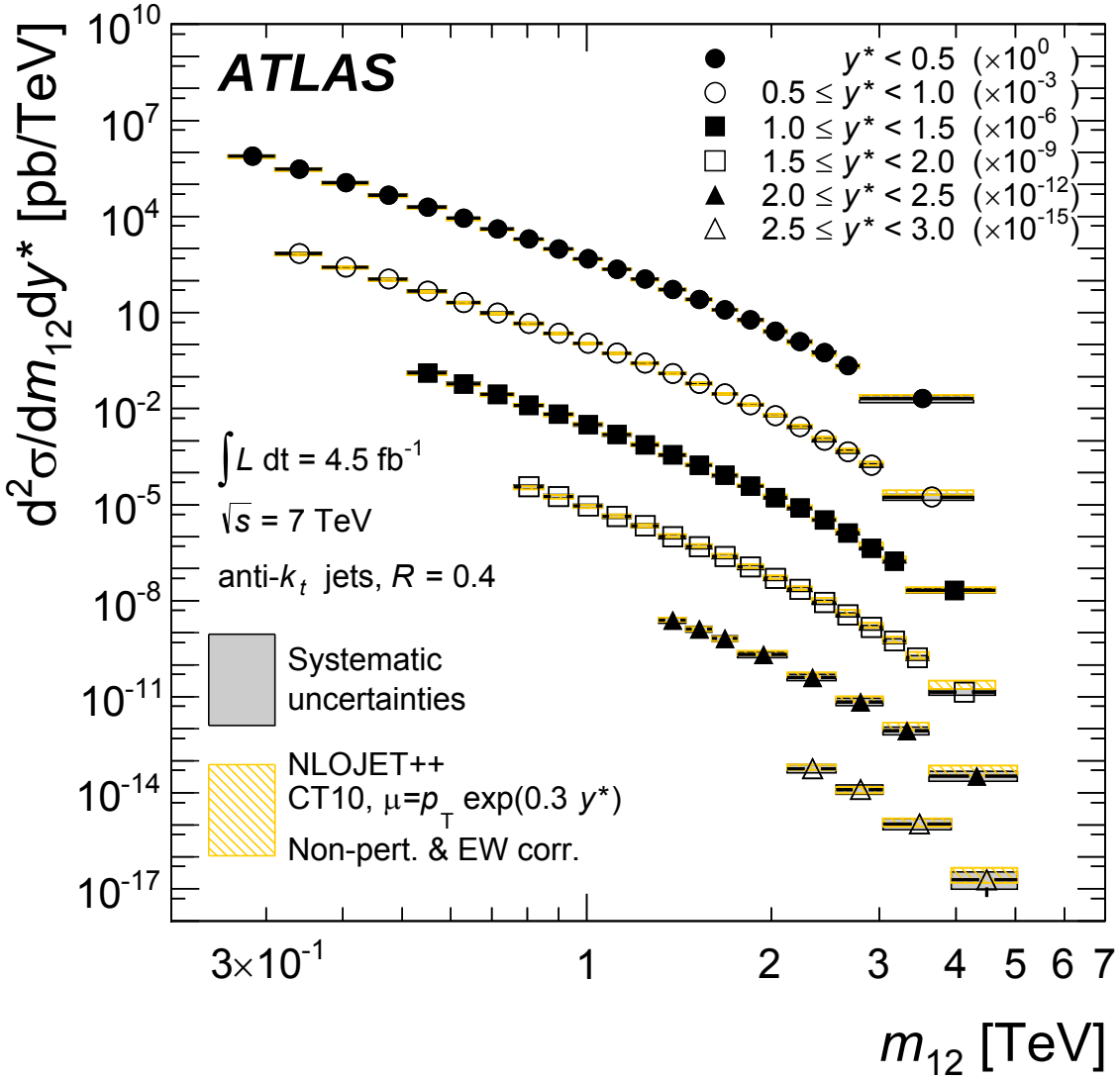

JHEP 05 (2014) 059

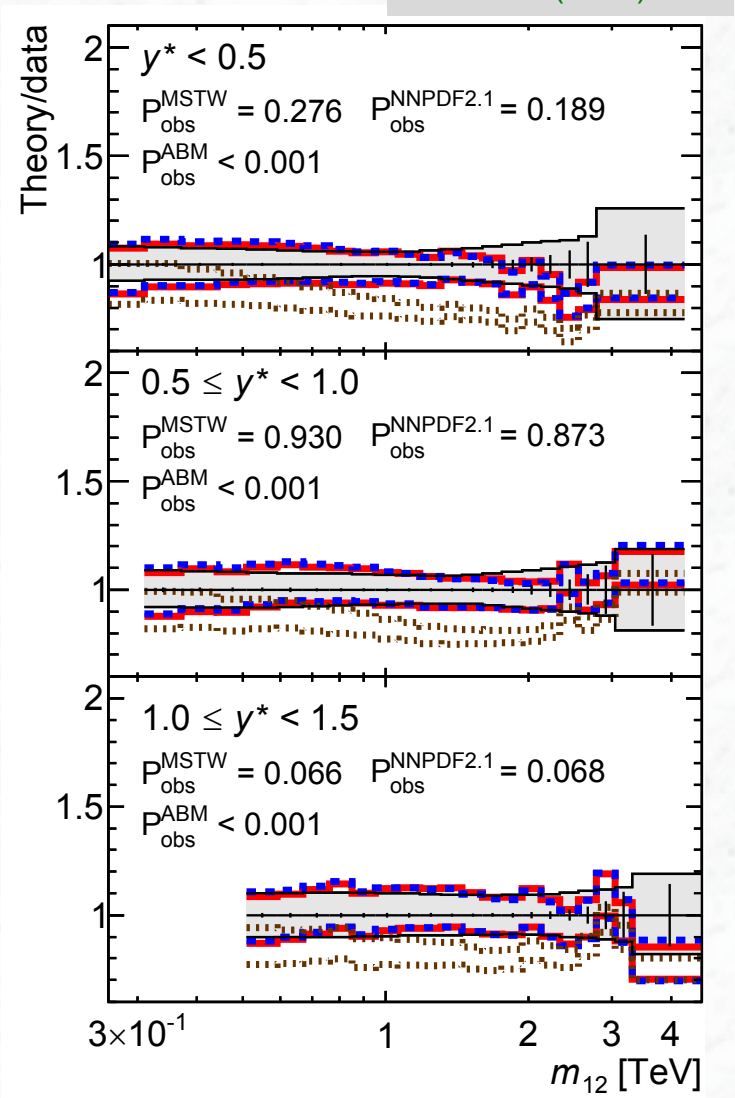

Important for:
- Test of QCD
- Search for new resonances decaying into two jets (see later)

Invariant di-jet mass spectra, ratio data/theory:

JHEP 05 (2014) 059

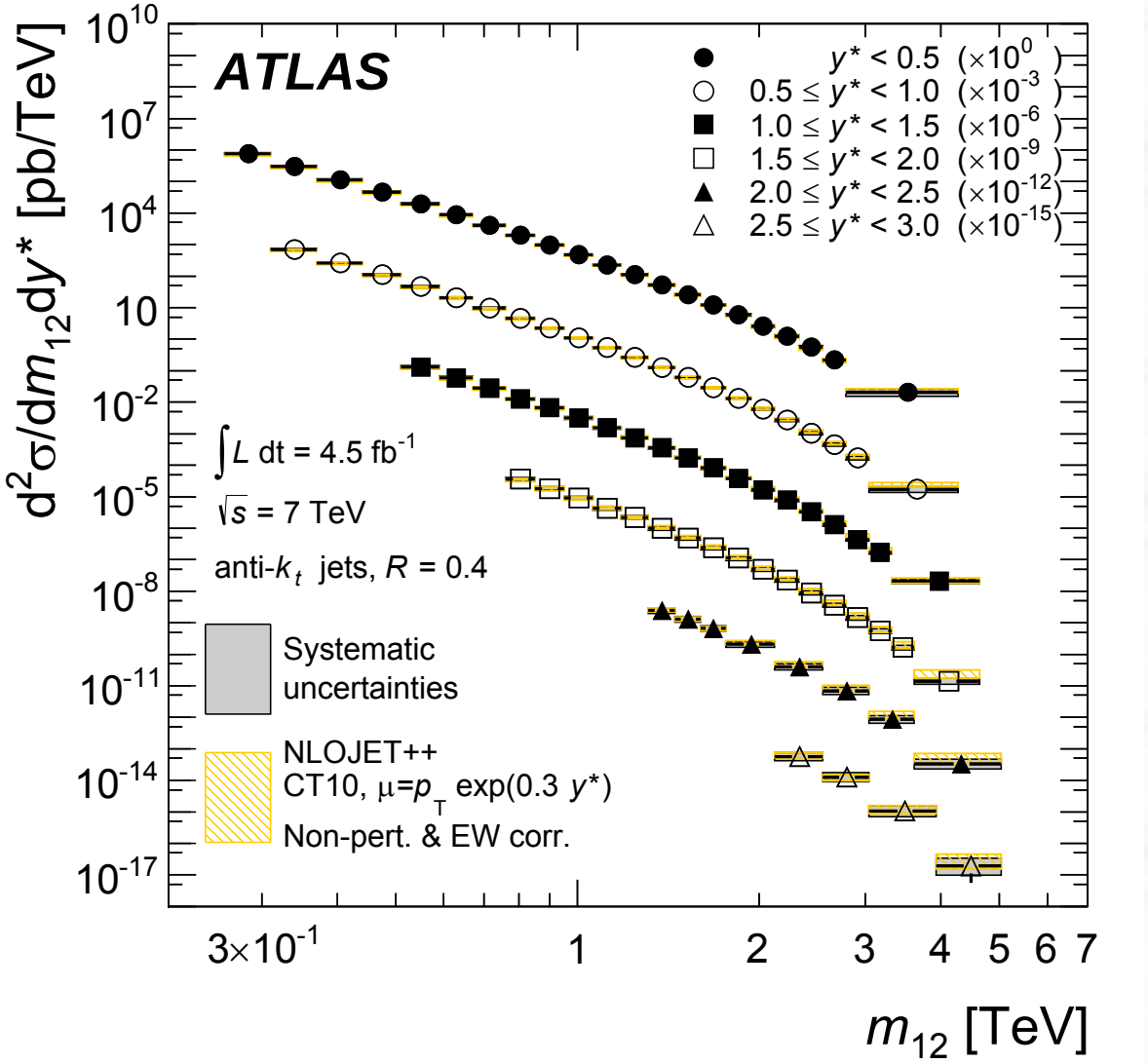

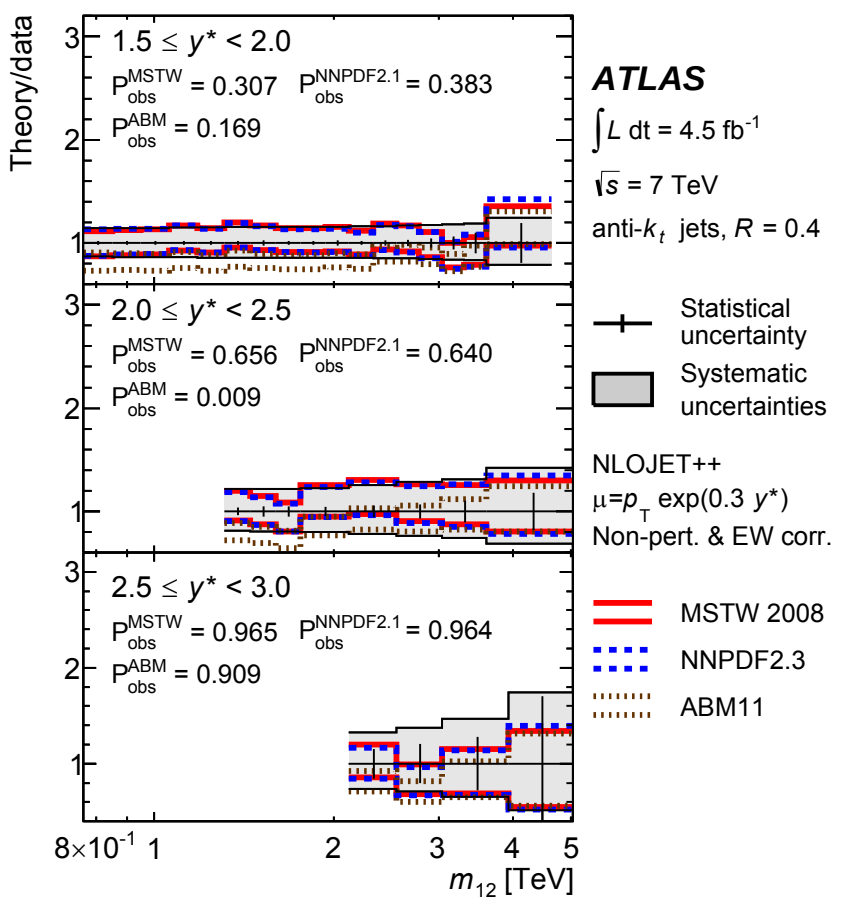

Important for:
- Test of QCD
- Search for new resonances decaying into two jets (see later)

Study of Compatibility

JHEP 05 (2014) 059

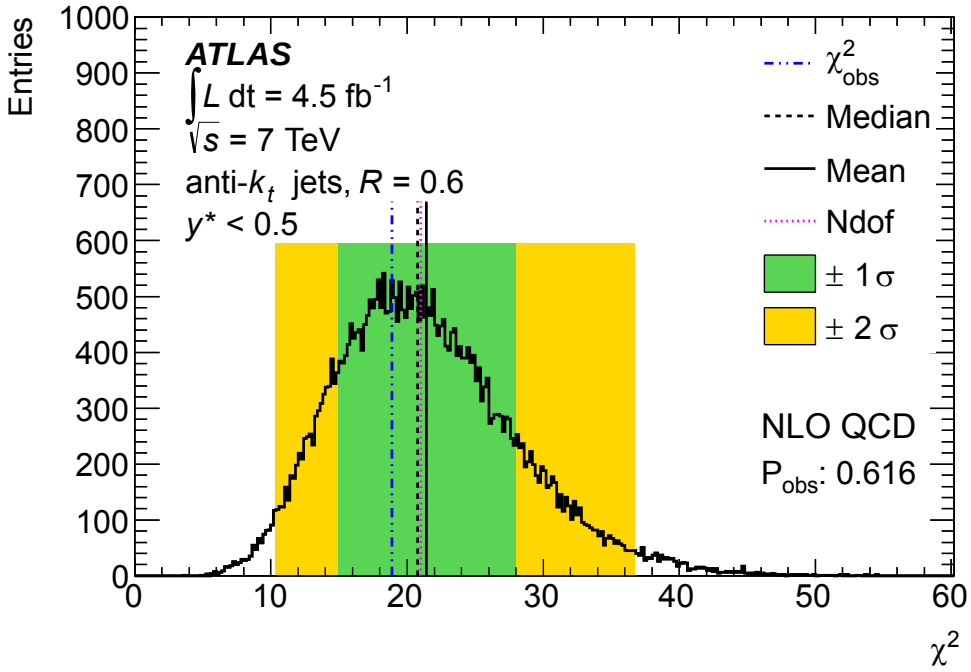

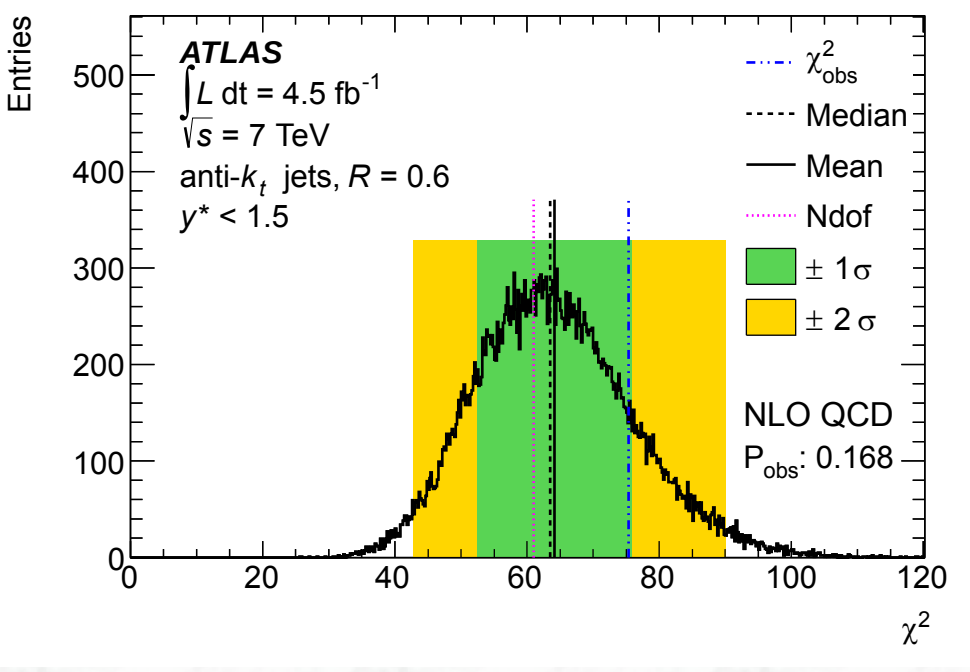

The χ^2 distribution of pseudo-experiments (black histogram) for NLO QCD using the CT10 PDF set. The full information on the uncertainties, including their asymmetries and correlations, is used. The black vertical dashed (solid) line indicates the median (mean) of the distribution, while the green (yellow) band indicates the ± 1σ (± 2σ) region. The blue dot-dashed vertical lines indicate the observed χ^2, with the corresponding observed p-value given in the legend. The pink dotted lines show the number of degrees of freedom, 21 for (a) and 61 for (b). The plots correspond to (a) the range y^* < 0.5, and (b) the first three ranges of y^* < 1.5 combined, for jets reconstructed with radius parameter R = 0.6.

In addition to QCD test: Sensitivity to New Physics

- Di-jet mass spectrum provides large sensitivity to new physics

  e.g. Resonances decaying into qq, excited quarks q*, ….

- Search for resonant structures in the di-jet invariant mass spectrum

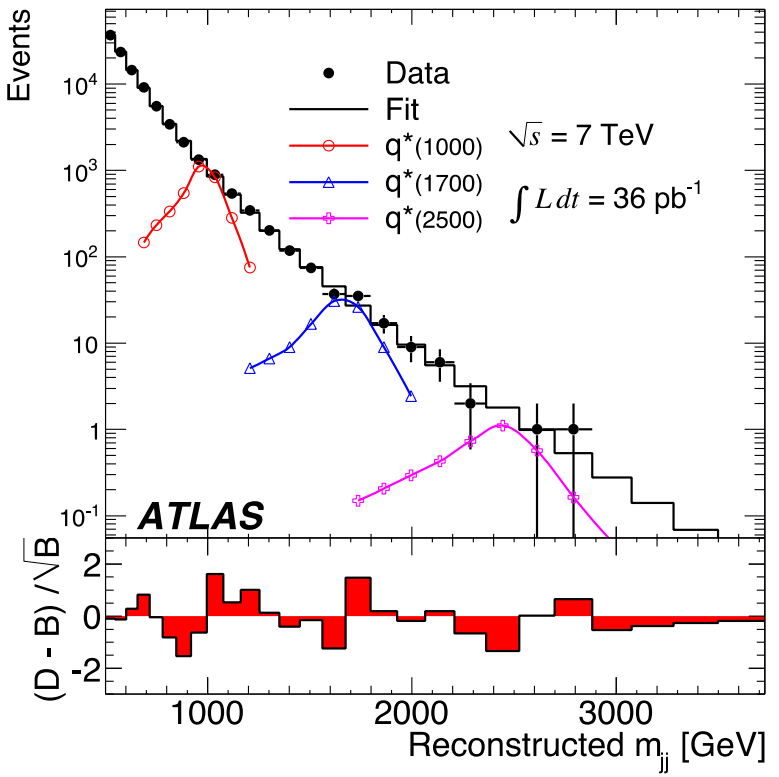

CDF (Tevatron), L =1.13 fb^{-1}: 0.26 < m_{q^*} < 0.87 TeV

ATLAS (LHC), L = 0.000315 fb^{-1} exclude (95% C.L) q* mass interval
0.30 < m_{q^*} < 1.26 TeV

L = 0.036 fb^{-1}: 0.60 < m_{q^*} < 2.64 TeV

Latest results (2014), including full LHC Run-1 dataset

PI JHEP 05 (2014) 059

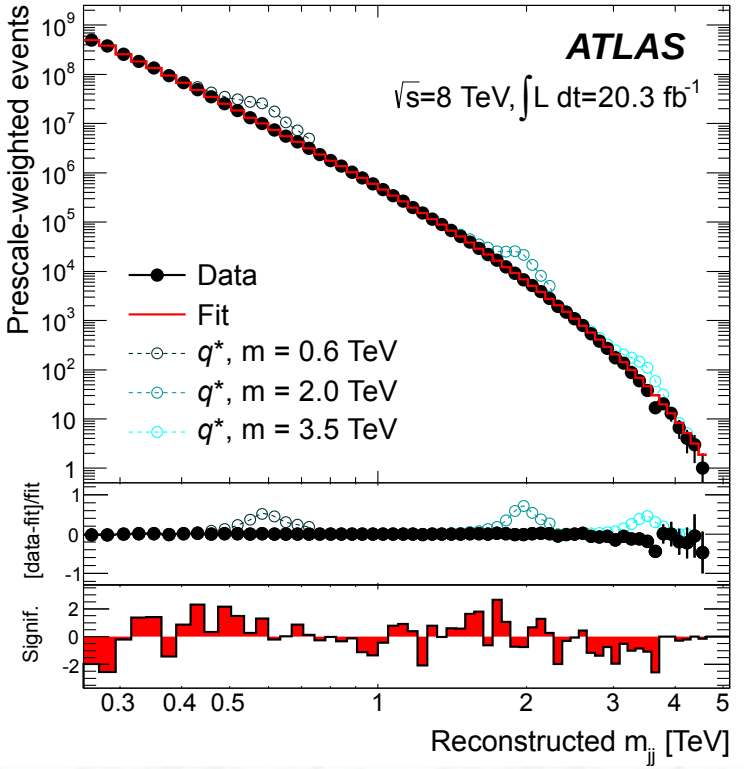

- Di-jet mass spectrum provides large sensitivity to new physics

  e.g. Resonances decaying into qq, excited quarks q*, ….

- Search for resonant structures in the di-jet invariant mass spectrum

CDF (Tevatron), $\sqrt{s}$ = 1.96 TeV	L =1.13 fb^{-1}:	0.26 < m_{q^*} < 0.87 TeV
ATLAS (LHC), $\sqrt{s}$ = 7 TeV	L = 0.000315 fb^{-1}	exclude (95% C.L) q* mass interval 0.30 < m_{q^*} < 1.26 TeV
ATLAS (LHC),	L = 20.3 fb^{-1}, 8 TeV:	exclude (95% C.L.) m_{q^*} < 4.09 TeV

5.4 Impact on the parton density distributions

- As discussed before: there is a sizeable gluon contribution in the QCD jet cross sections; even larger at the LHC than at the Tevatron

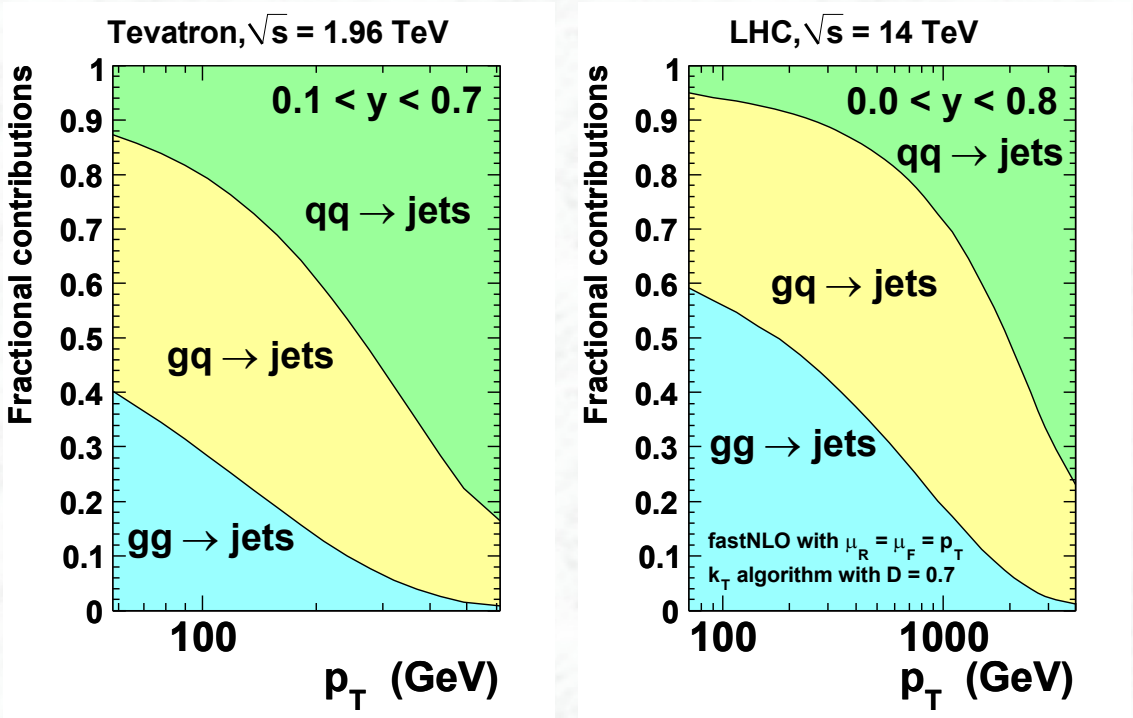

- The gluon distribution, at particular at large x-values (high P_T jets) is not well constrained from deep inelastic scattering or other experiments

  → large uncertainties

ATLAS data at 7 TeV:

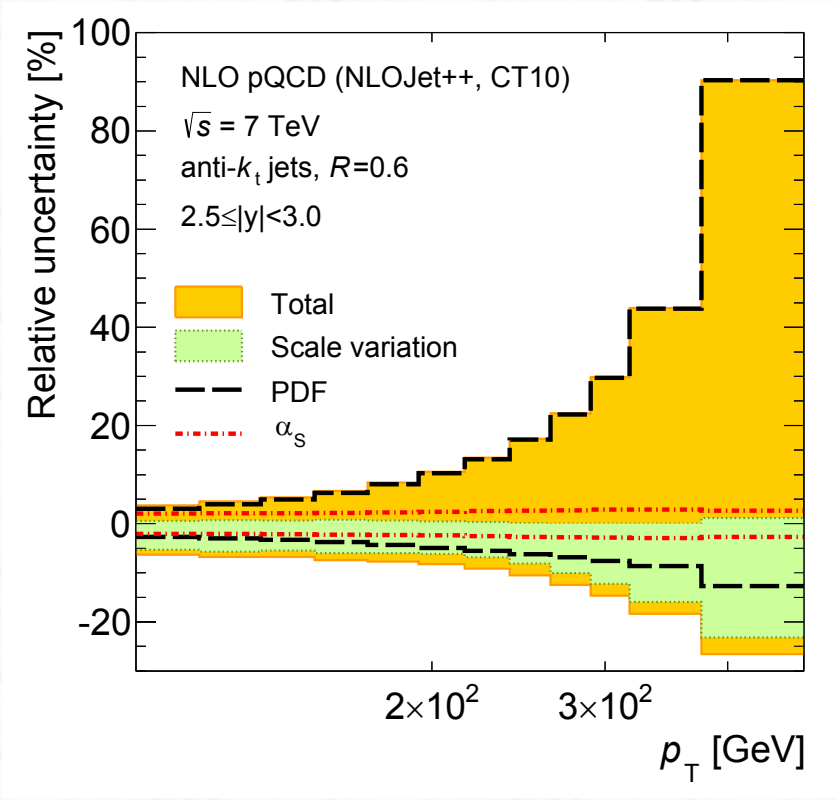

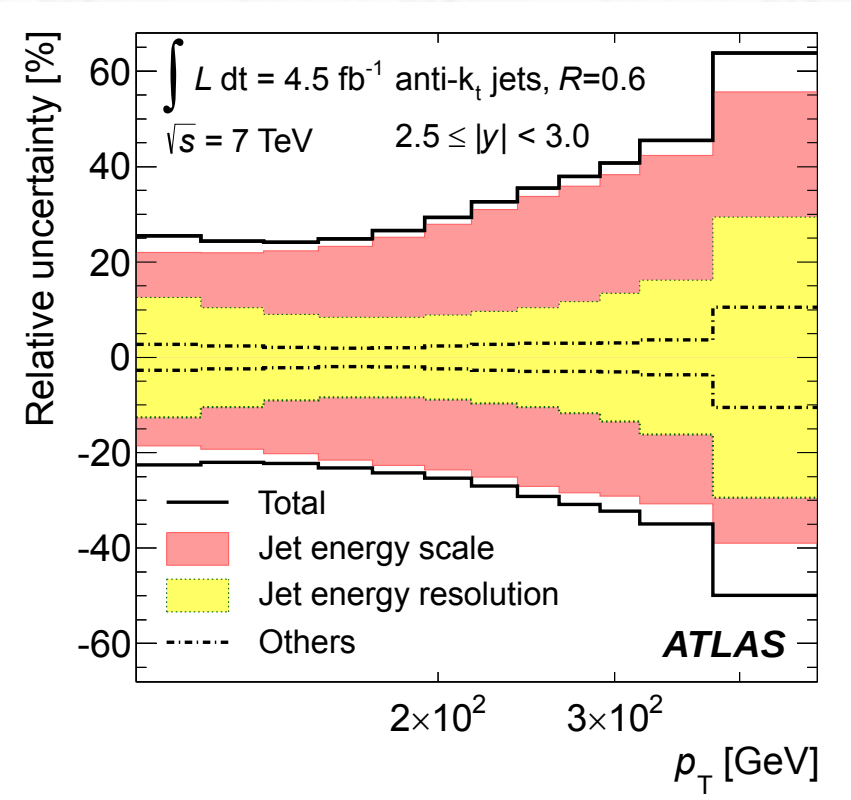

Since the experimental uncertainties are smaller than the pdf uncertainties, the latter can be reduced / pdfs can be more constrained

Tevatron jet data are included in recent pdf fits:

- Reduced pdf uncertainty
  (already included and used in recent cross-section calculations at the Tevatron and at the LHC)

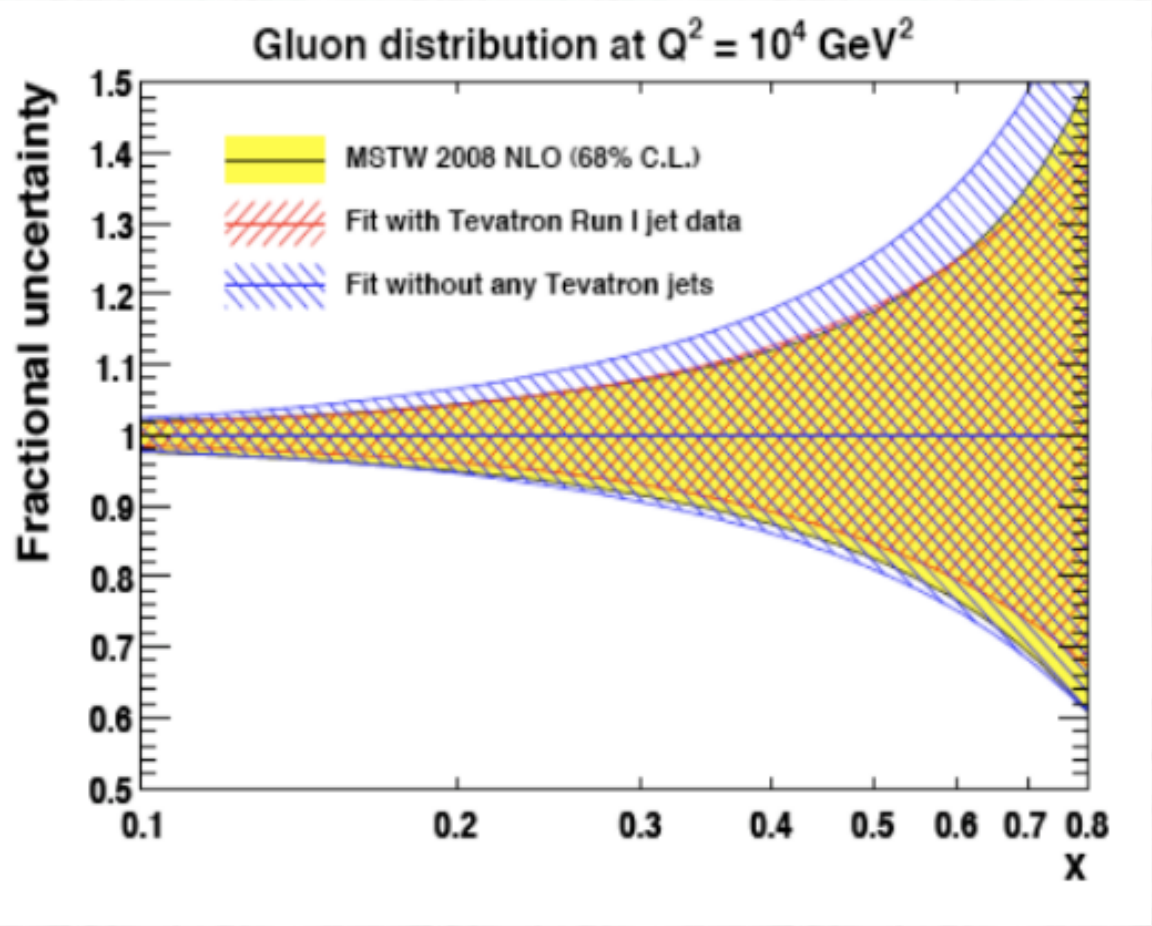

It is expected that LHC data will be added as well very soon → further constraints

Relevance for Searches for new physics:

- Several models for new physics, e.g. quark substructure, predict deviations from the QCD behaviour at large PT

  Effects from pdfs and “new physics” must be separated

- Famous “historical example”: evidence for quark substructure in the CDF experiment in 1997

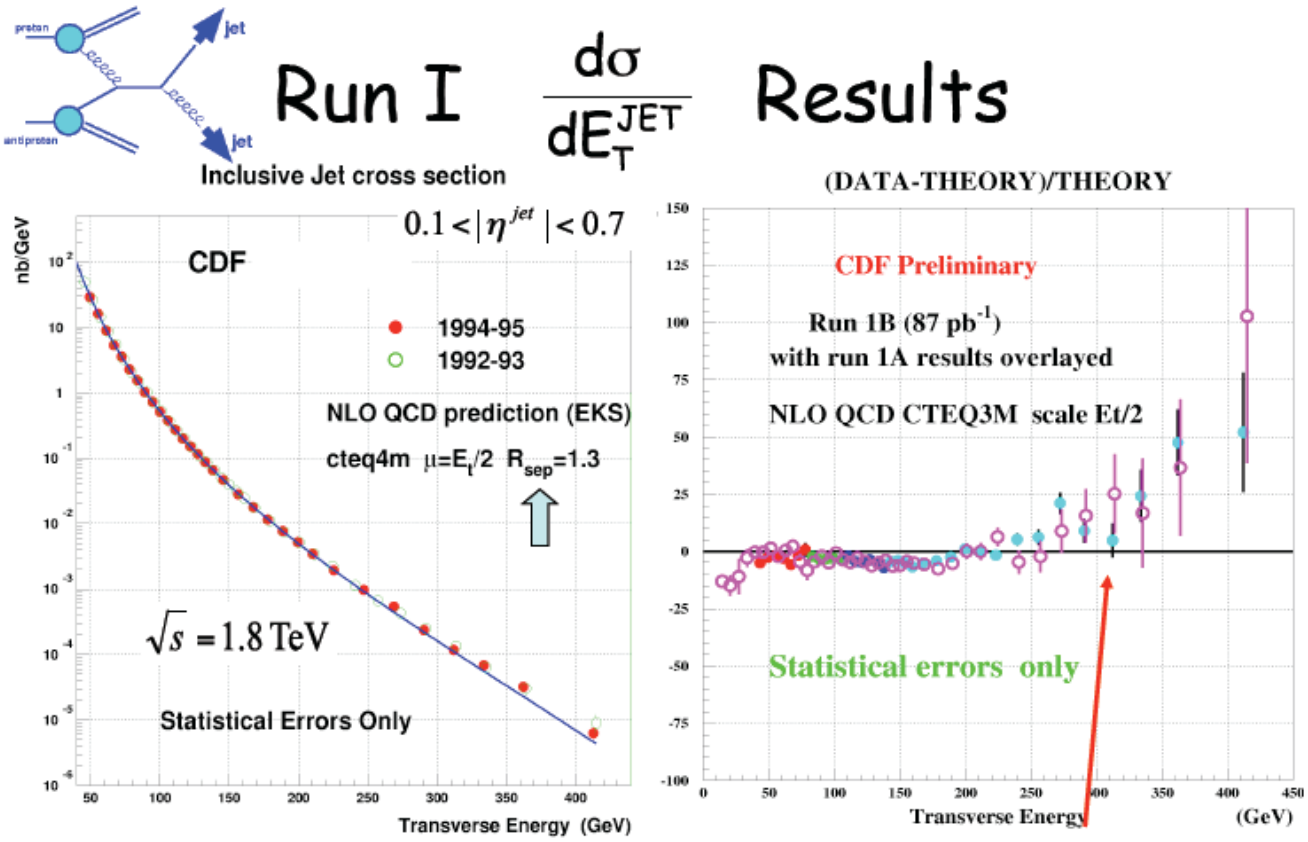

Run I data compared to pQCD NLO

Observed deviation in tail ..... was this a sign of new physics ?

Some important comments:

- Disentangling the effects of pdfs and “new physics” is not easy

- All data entering the pdf fits must be described in the global fits by the pdf fitting groups…. it is important to have uncorrelated data sets (different physics processes, accelerators, as little common systematic uncertainties as possible)

- pdf uncertainties must be evaluated and interpretation of new physics must take these uncertainties into account

  Evaluation of pdf uncertainties:

  (i) Uncertainties on the fitted parameters, within one parametrization (these uncertainties are provided by the pdf-fitting groups)

  (ii) As an additional check → systematic uncertainties a comparison between different pdf fits (groups) must be performed

  (iii) Uncertainties on the strong coupling constant α_s (enters via pdf evolution)

Error bands of individual parametrizations and consistency among them:

- MSTW (2008) is always used as a reference
- uncertainties depend on the x-values or the c.m.s energy of the parton-parton-system

gg luminosity at the LHC:

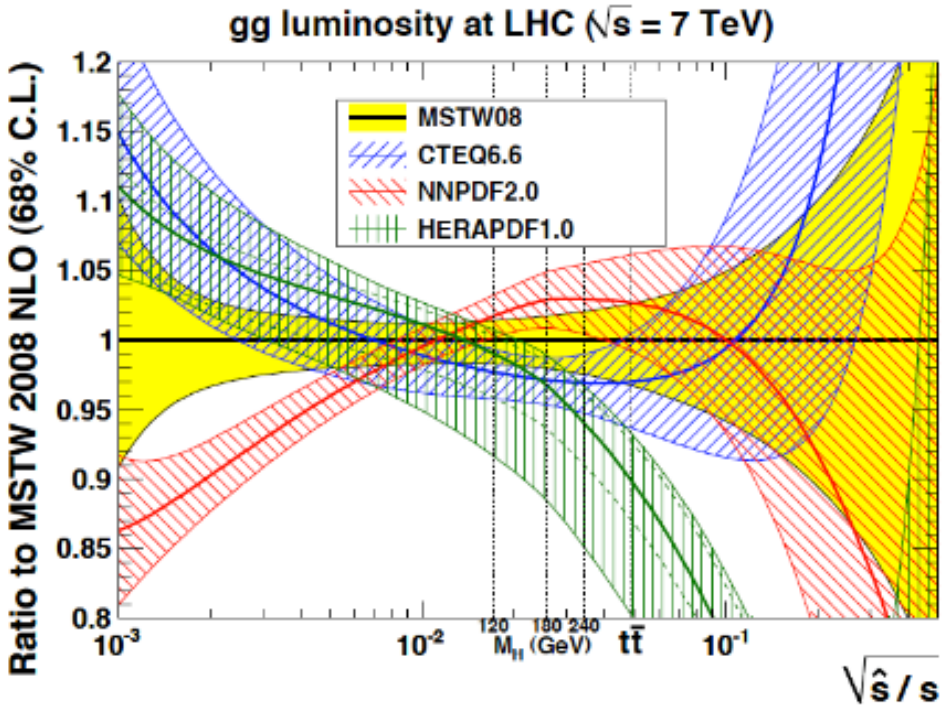

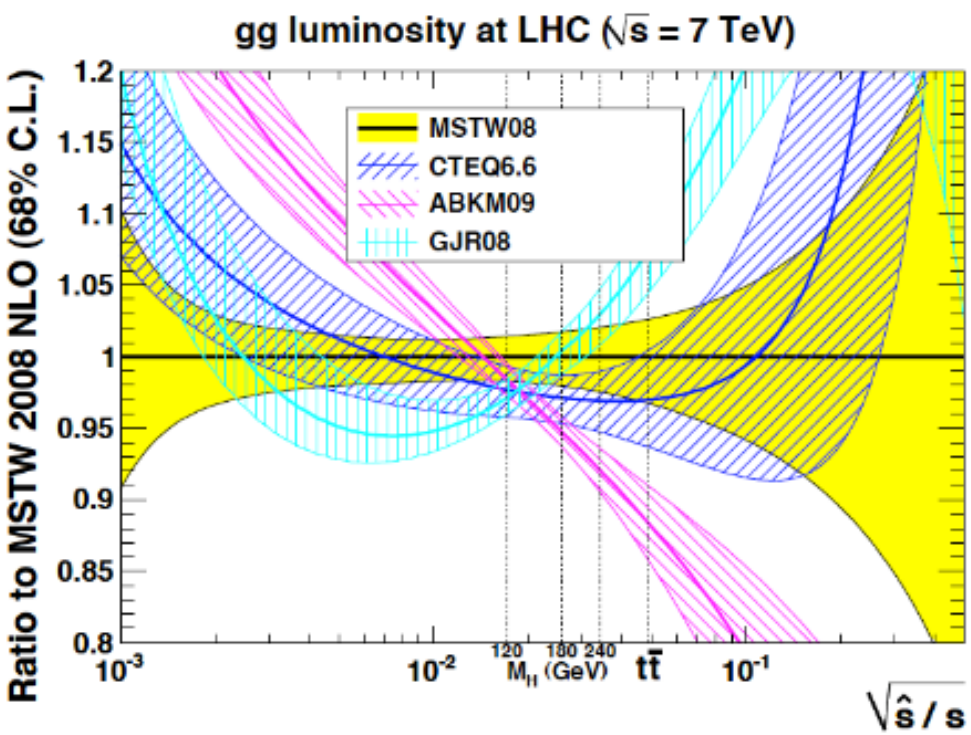

Error bands of individual parametrizations and consistency among them:

- MSTW (2008) is always used as a reference
- uncertainties depend on the x-values or the c.m.s energy of the parton-parton-system

Σ qq luminosity at the LHC:

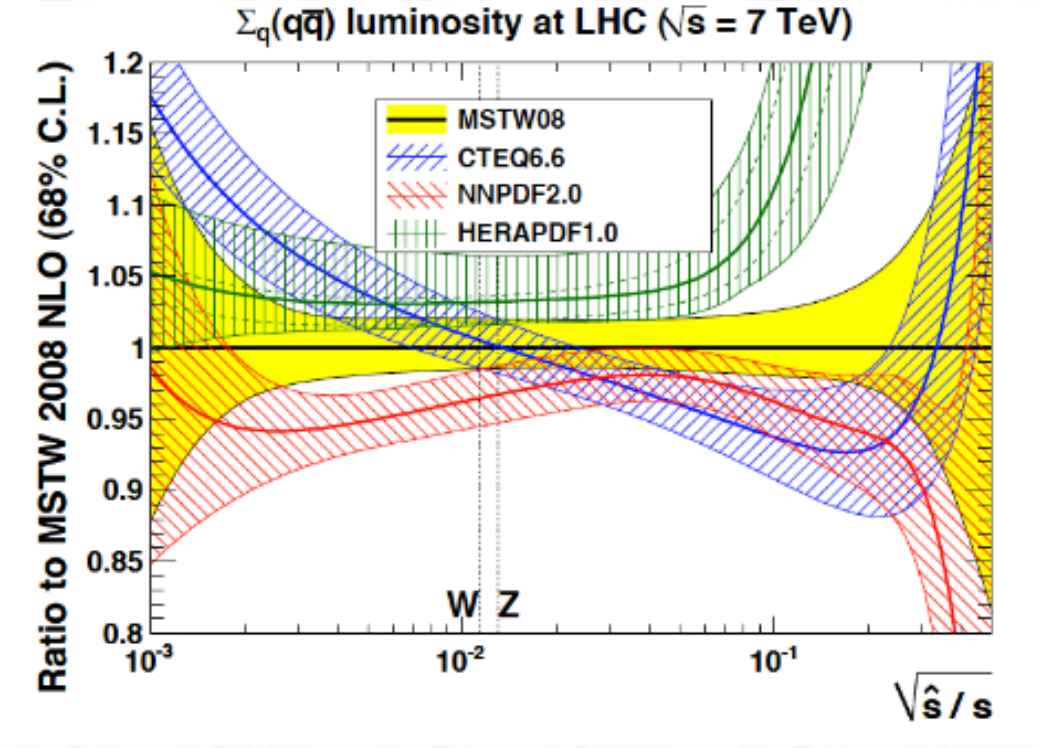

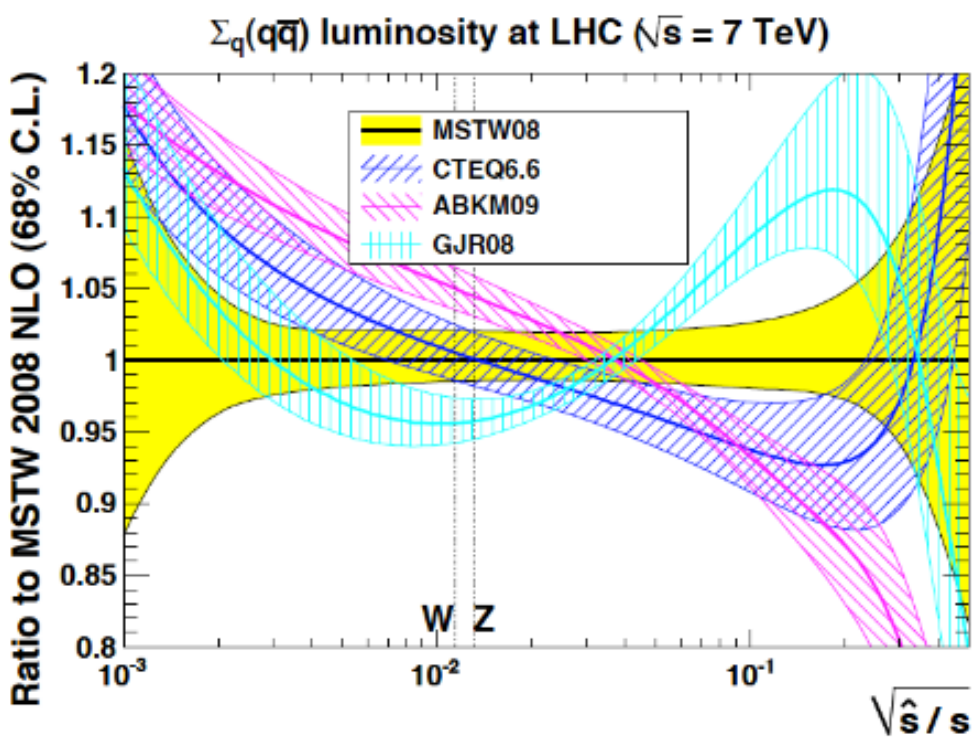

This has direct implications on the cross-section calculation at the LHC:

Example: Higgs boson production (via gluon fusion)

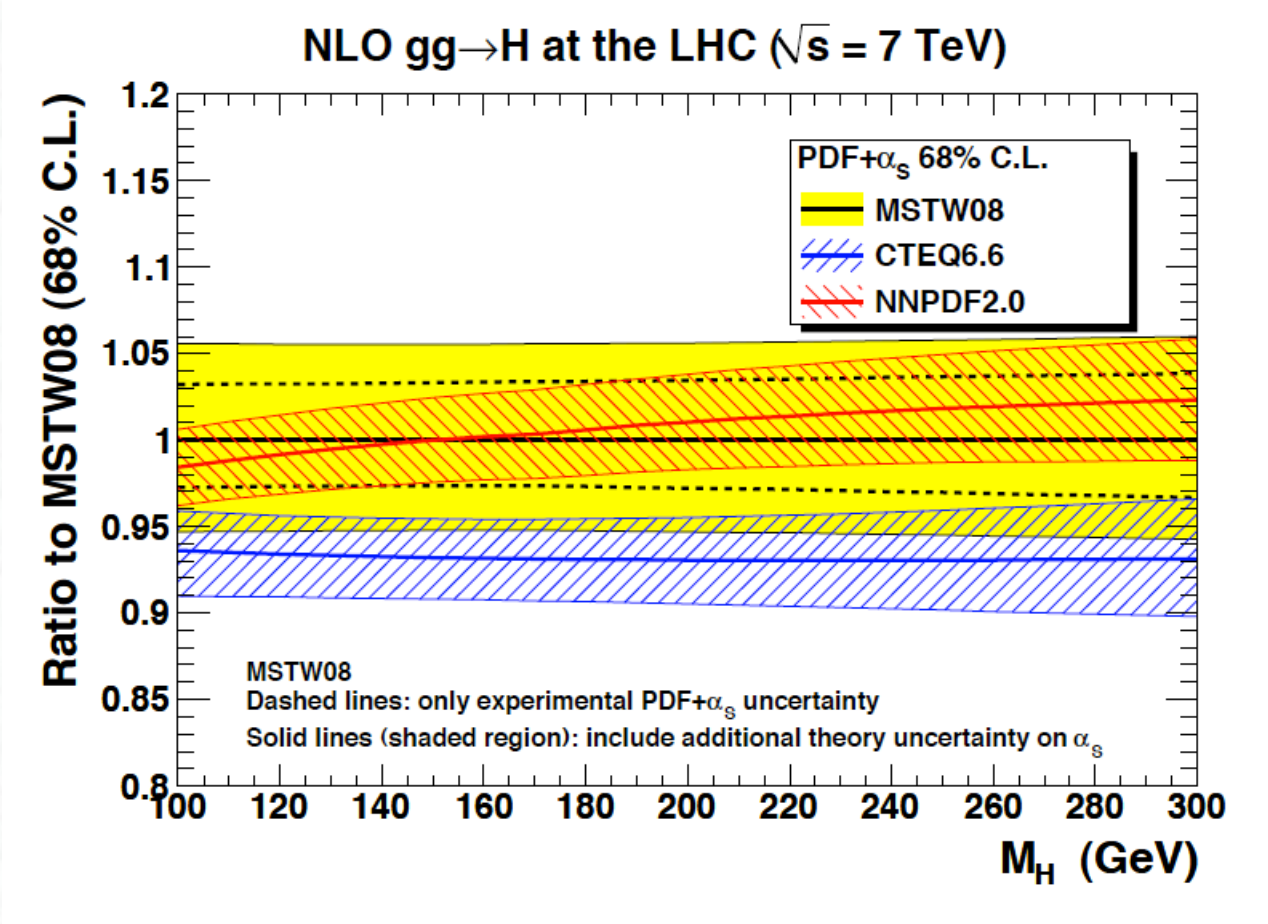

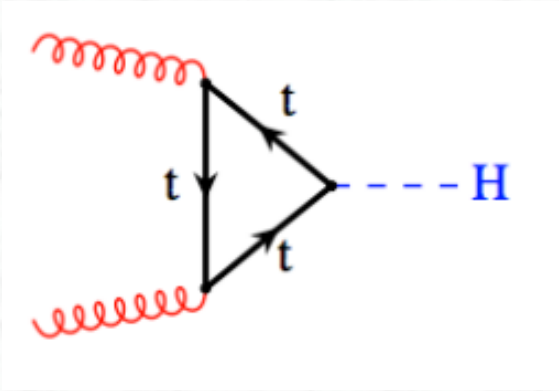

Correlation between pdfs and α_s (most affected is the gluon distribution):

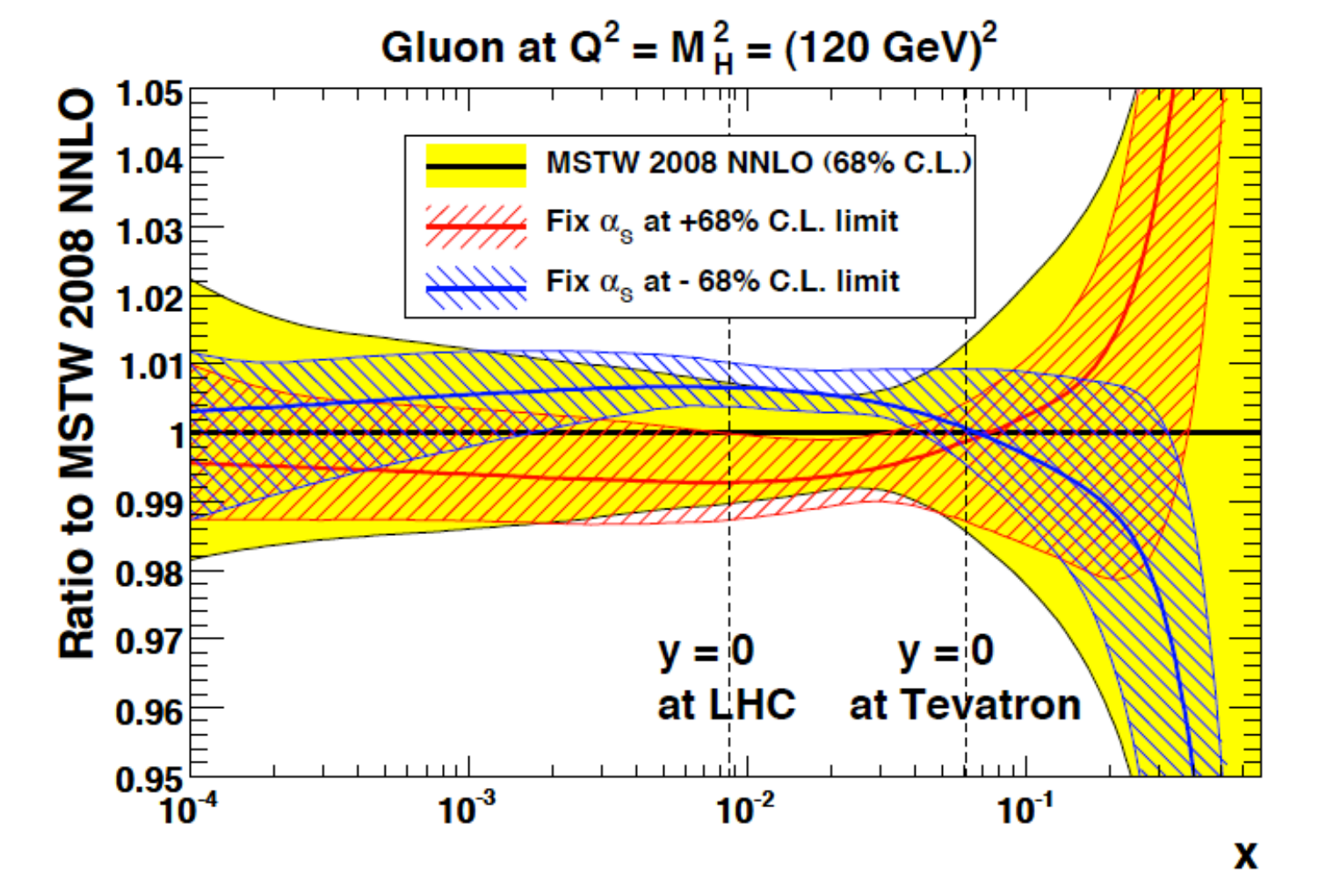

… less dramatic for quark distributions:

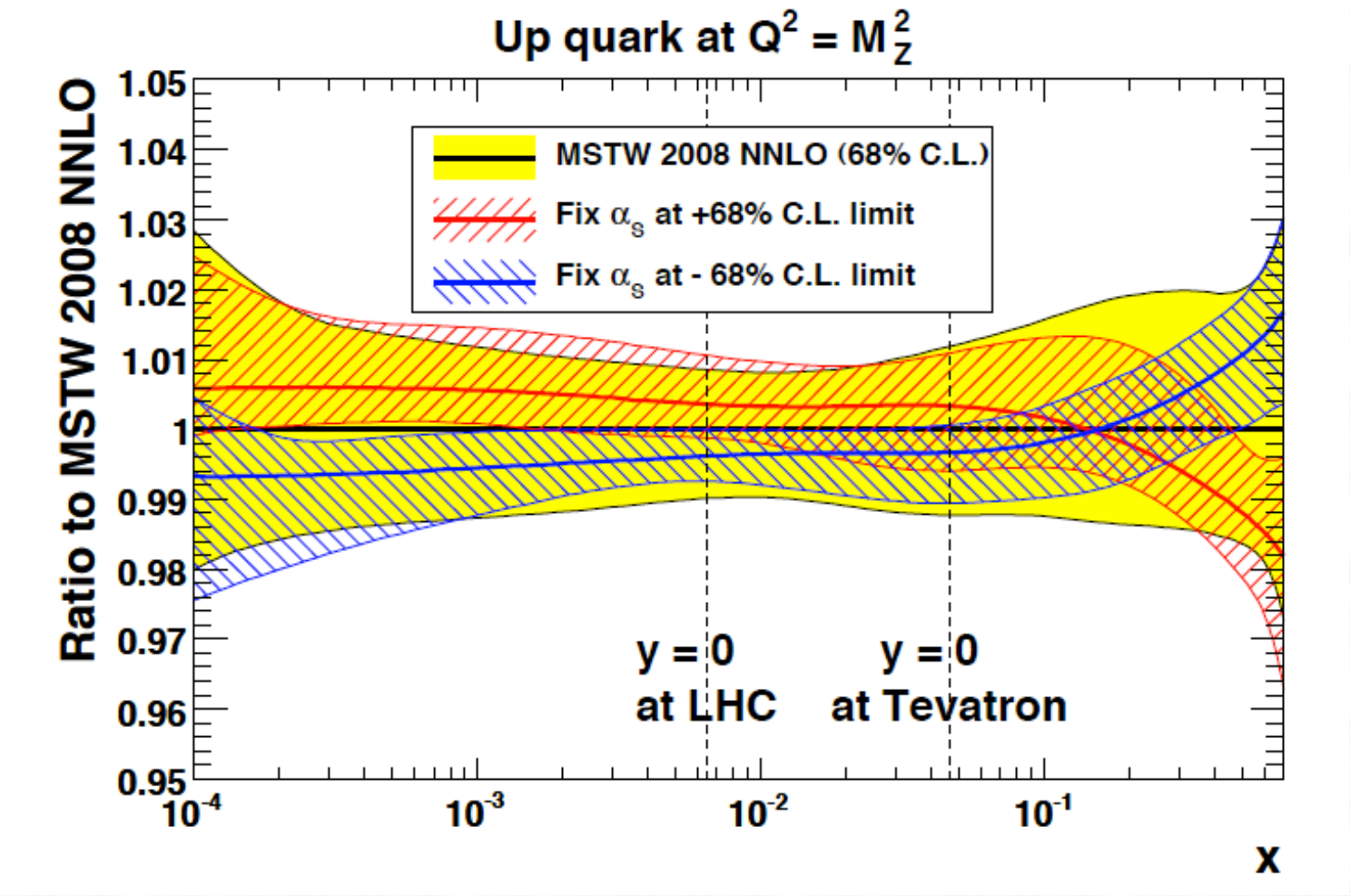

Implications on the cross-section calculation at the LHC:

Example: Higgs boson production via gluon fusion, m_H = 120 GeV

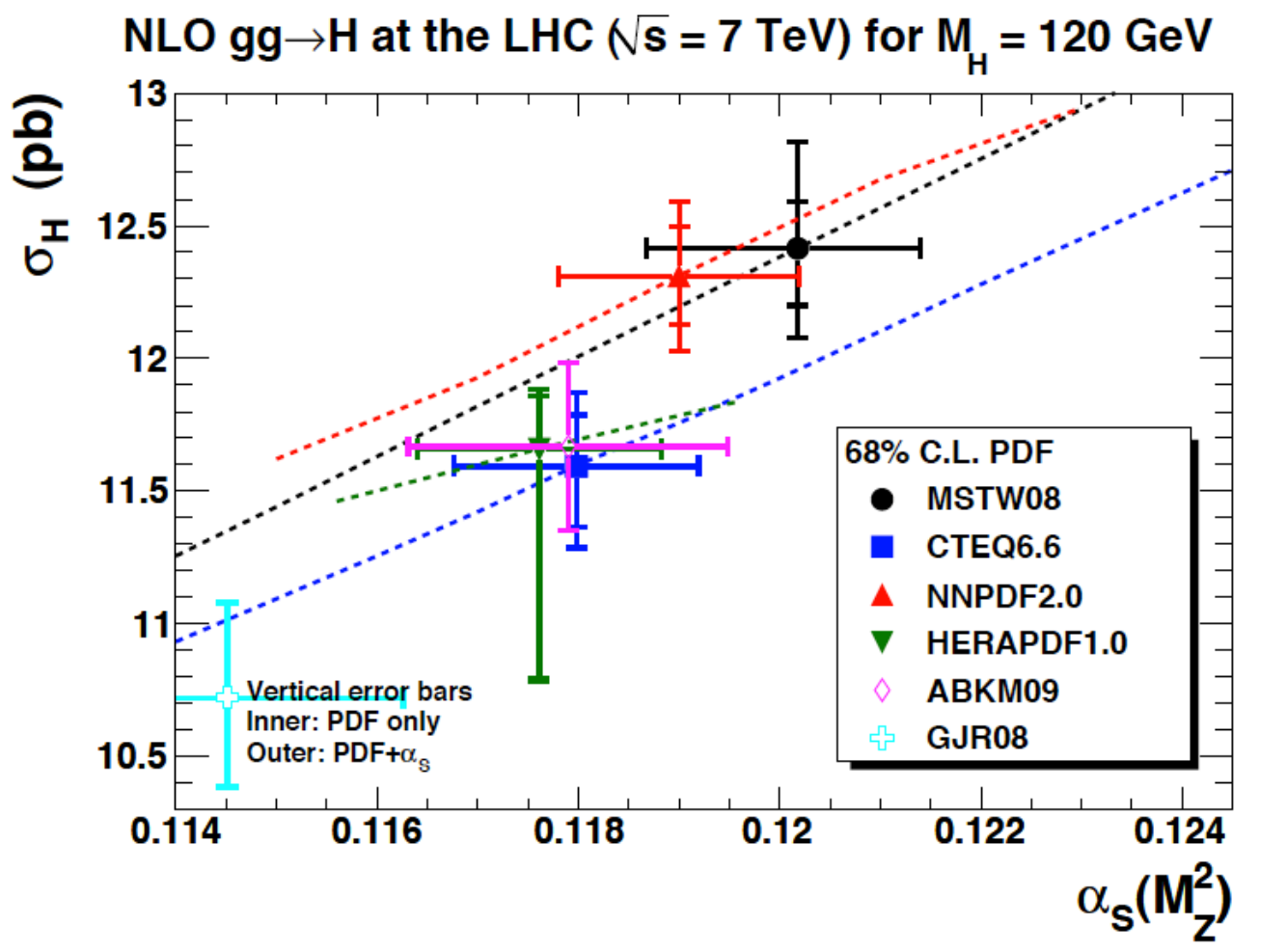

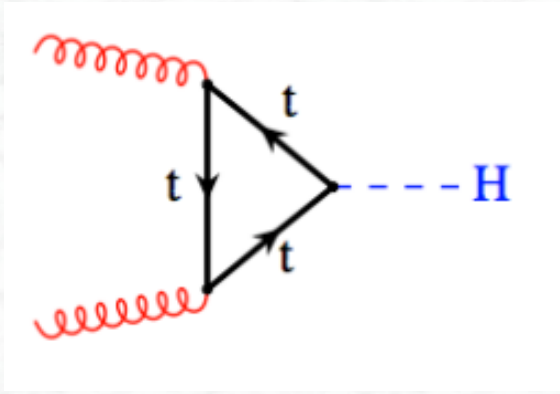

Implications on the cross-section calculation at the LHC:

Example: top pair production via gluon fusion

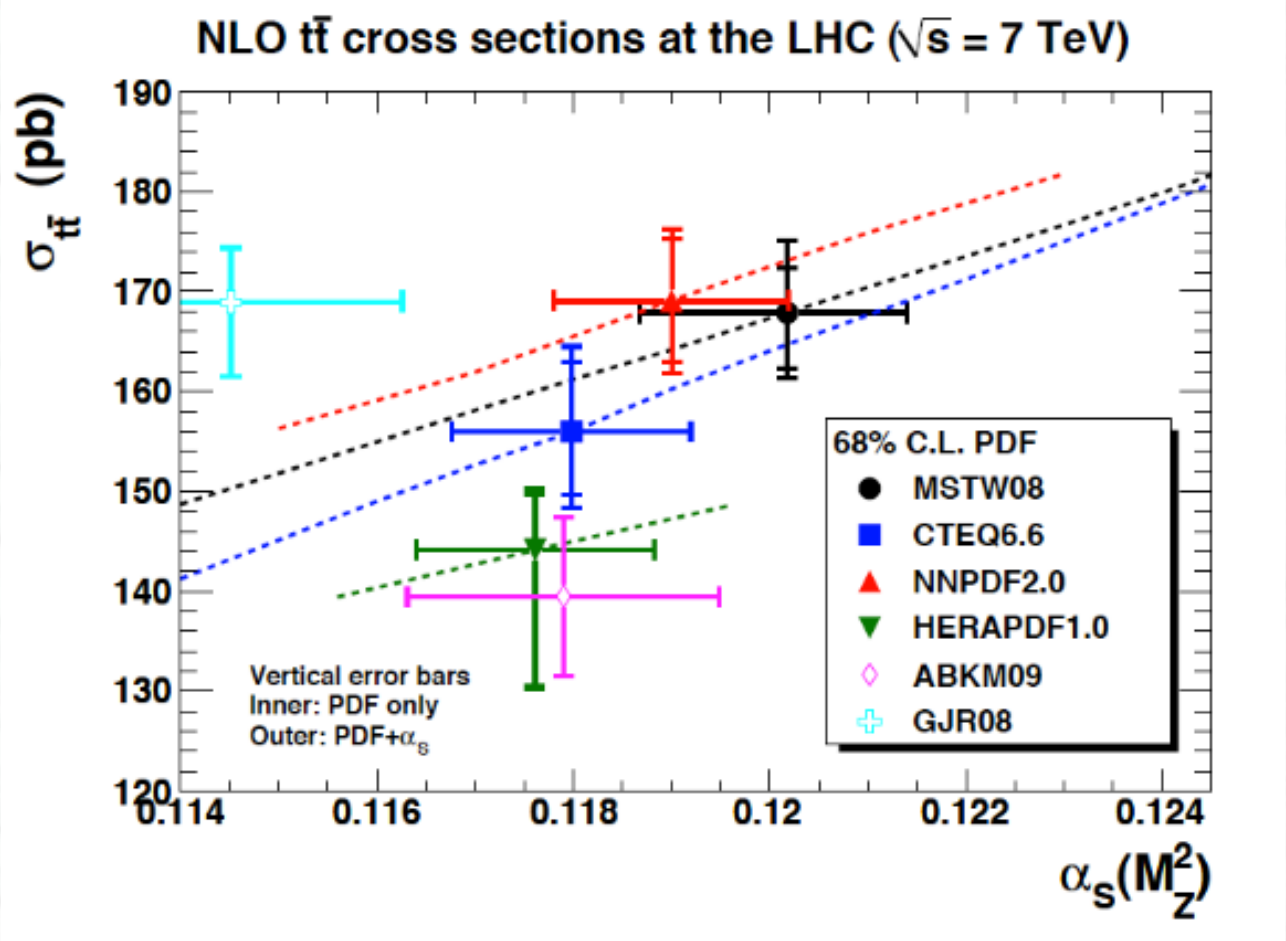

Example: Production of W and Z bosons at the LHC

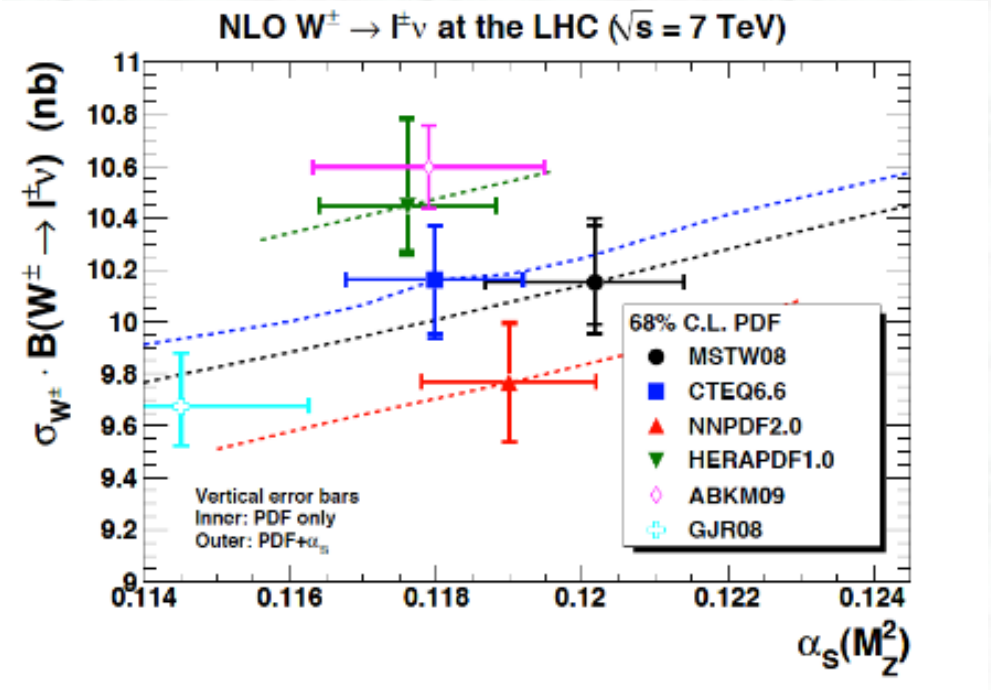

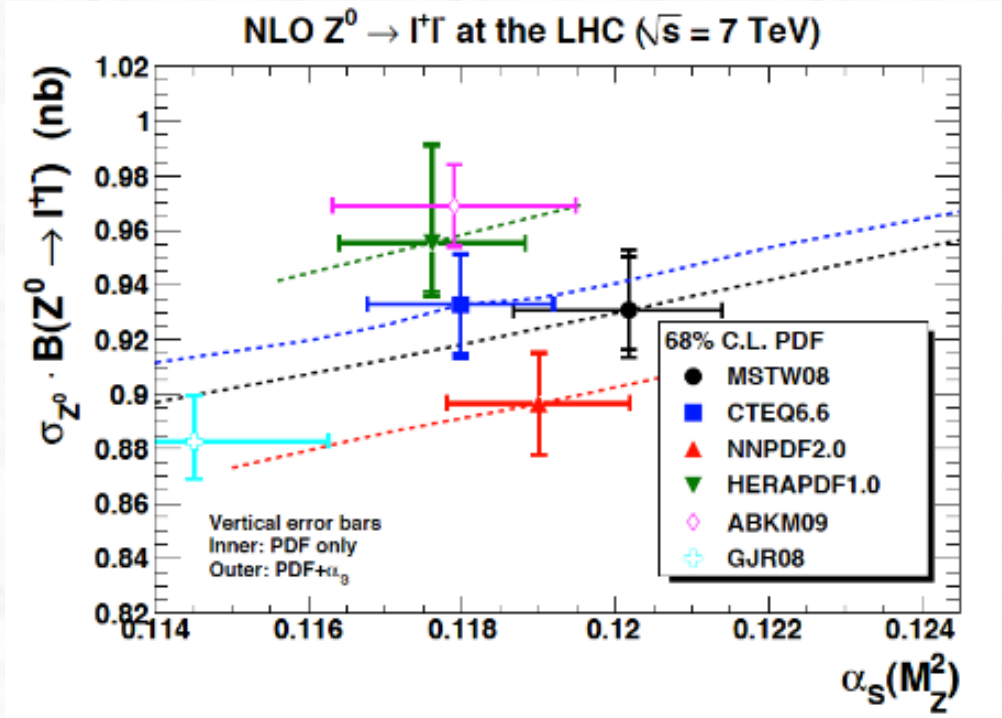

All these processes have been measured in detail at the LHC (see next lectures), differential measurements will provide significant constraints on pdfs

5.5 Direct photon production

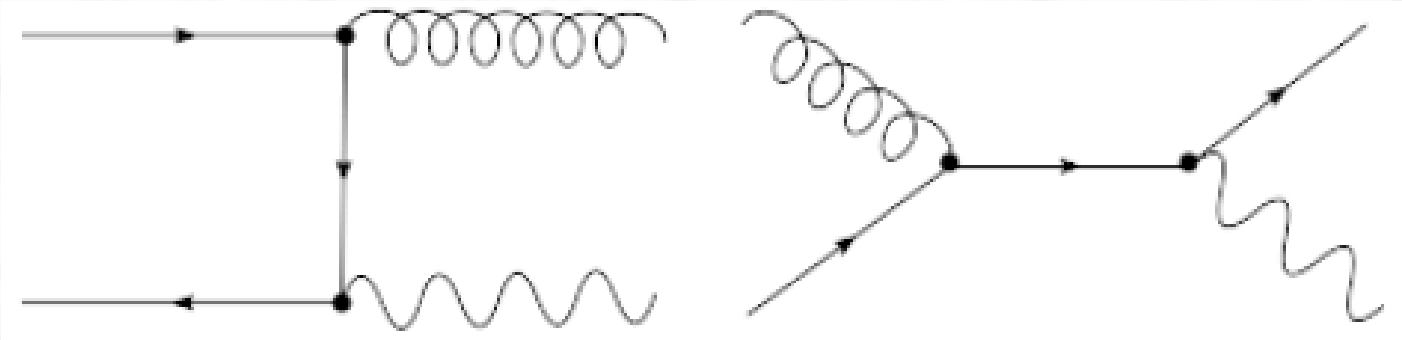

Motivation:

- Test of perturbative QCD
- The gluon-initiated process dominates up to ~150 GeV
  → the high statistics Tevatron and LHC datasets can further constrain the gluon pdf

- Better energy resolution of photons, as compared to jets
  (no decay, fragmentation, no jet algorithm, better el.magn calorimeter resolution)

  → process plays a key role in jet calibration

Direct photon production has been measured in many fixed target and collider experiments:

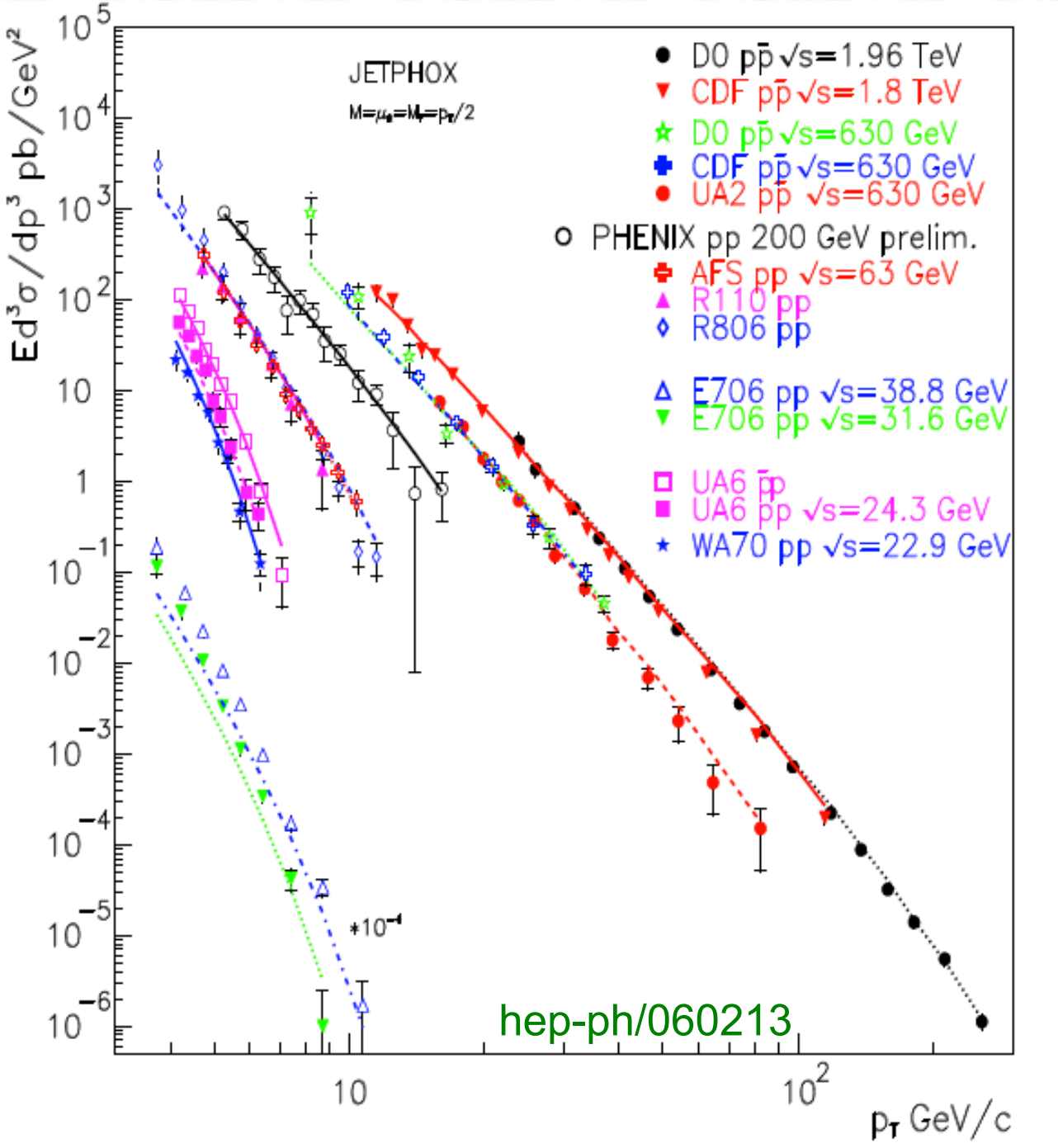

- Highest p_T values from Tevatron experiments so far
- In general, data are well described by NLO pQCD predictions

Some details on the experimental measurement:

- Main backgrounds: photons from final state radiation off quarks
  → di-jet production is a background

  decays of high p_T π^0 mesons inside jets
  → di-jet production is a background

- To suppress backgrounds: require isolated photons
  (cut on energy deposited in a cone of R=0.4 around the photon)

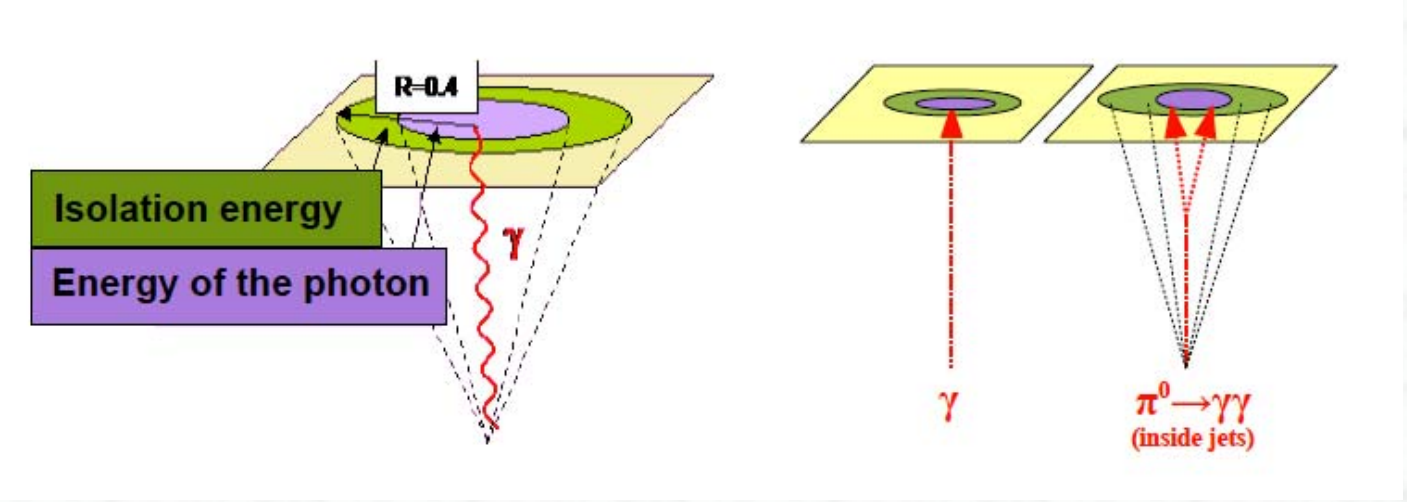

Example: Isolation variable, as measured in the CDF experiment

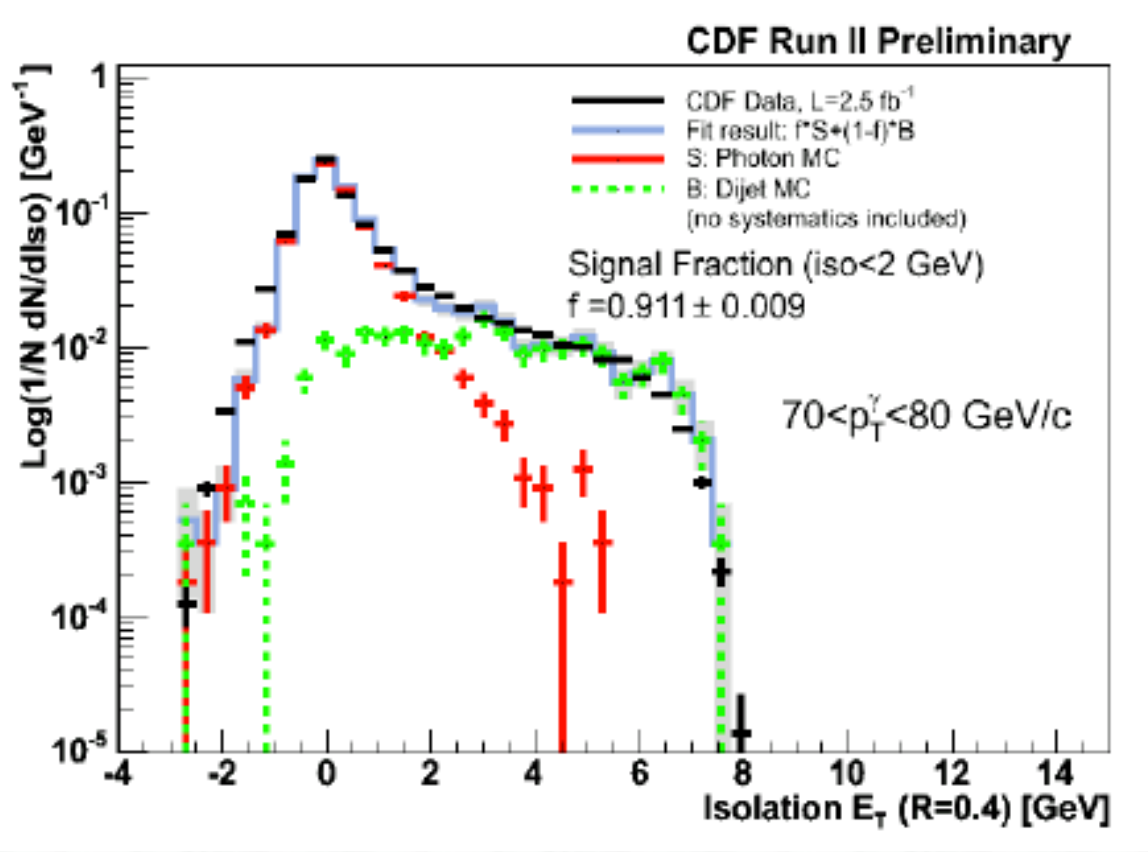

- Photon fraction is determined from a fit to the experimental data (templates, i.e. shapes of photons from Monte Carlo simulation, cross-checked with electron shapes from Z → ee data)

The photon fraction as a function of p_T:

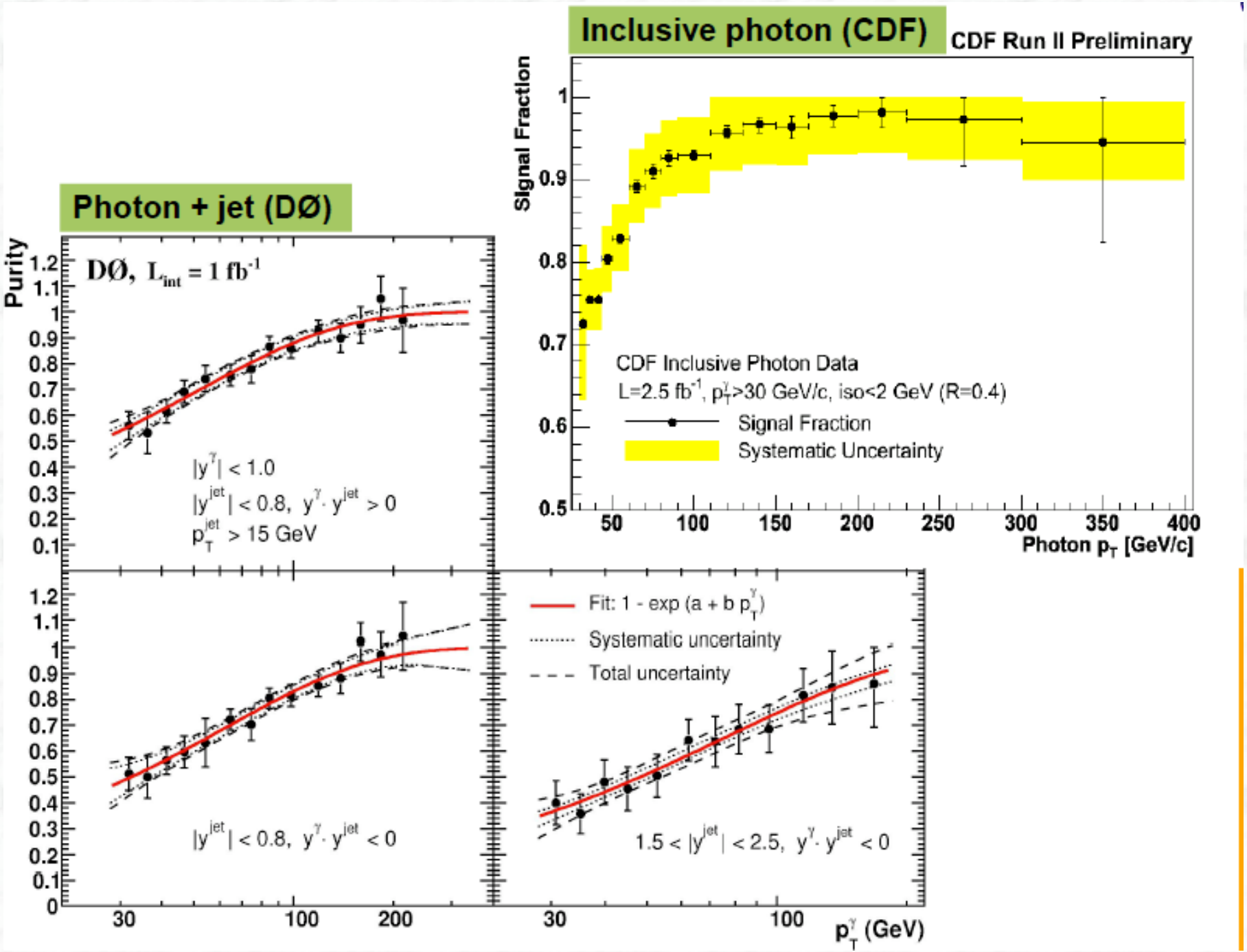

Measured photon p_T spectra at the Tevatron:

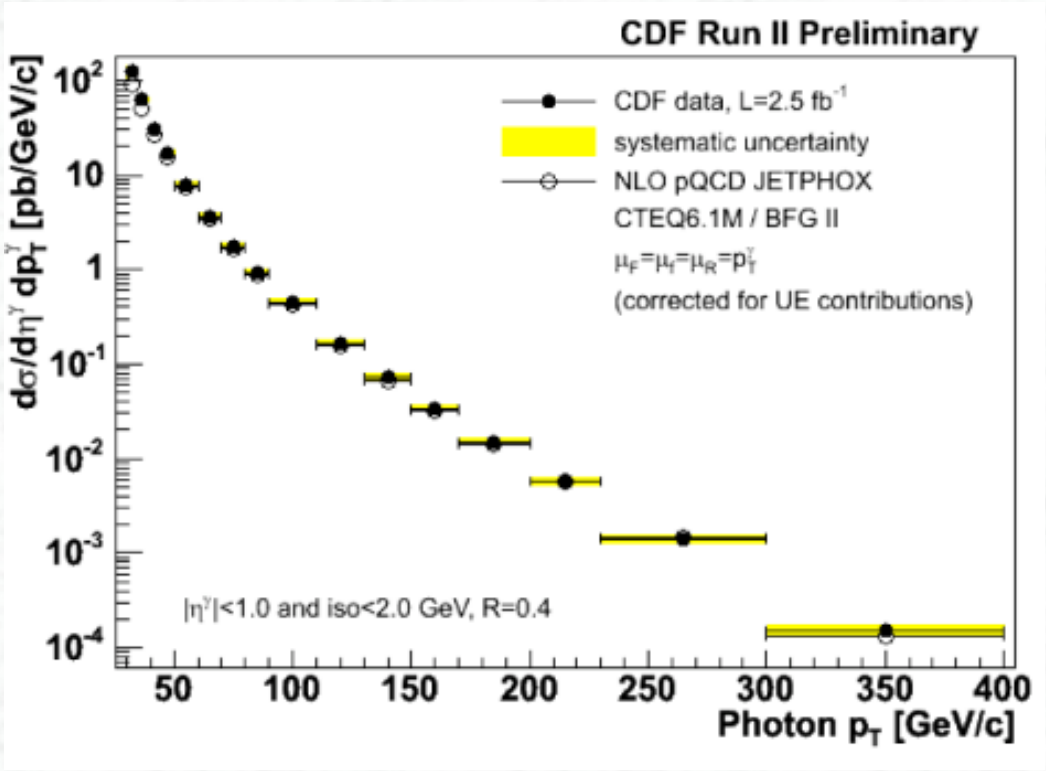

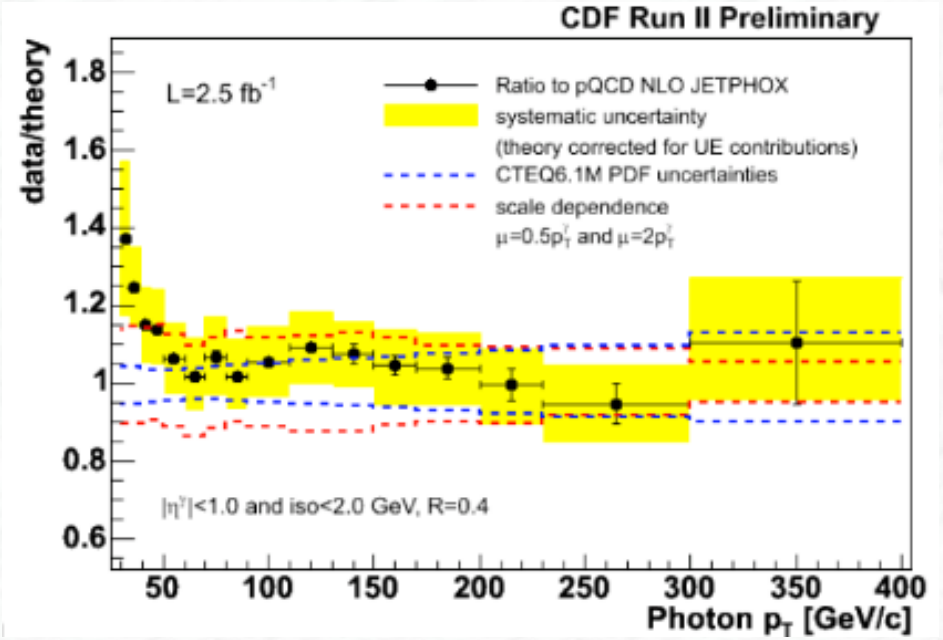

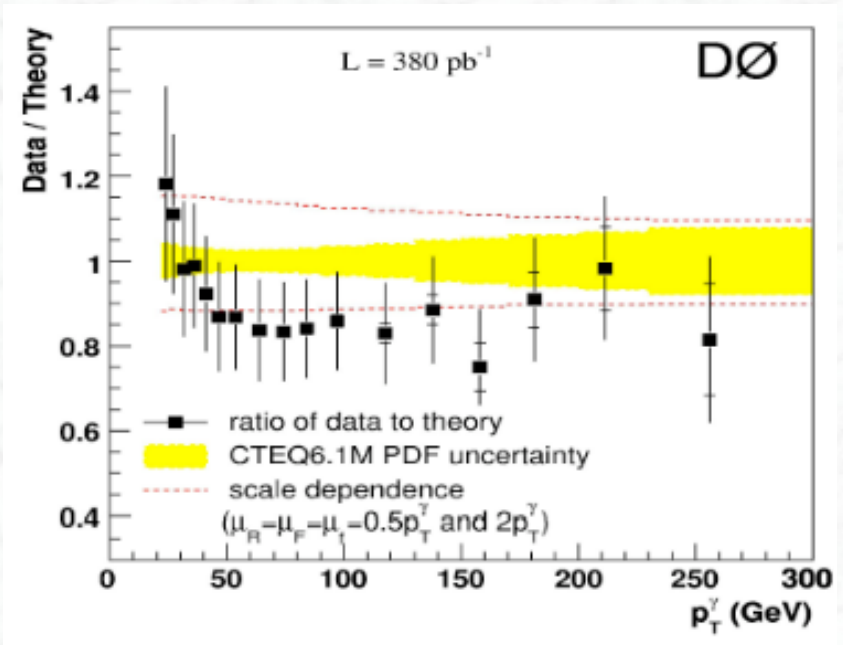

- In general good agreement within the experimental and theoretical uncertainties
- However, both experiments measure an excess (data/theory) in the low p_T region;

  origin: unclear !!

Photons at the LHC

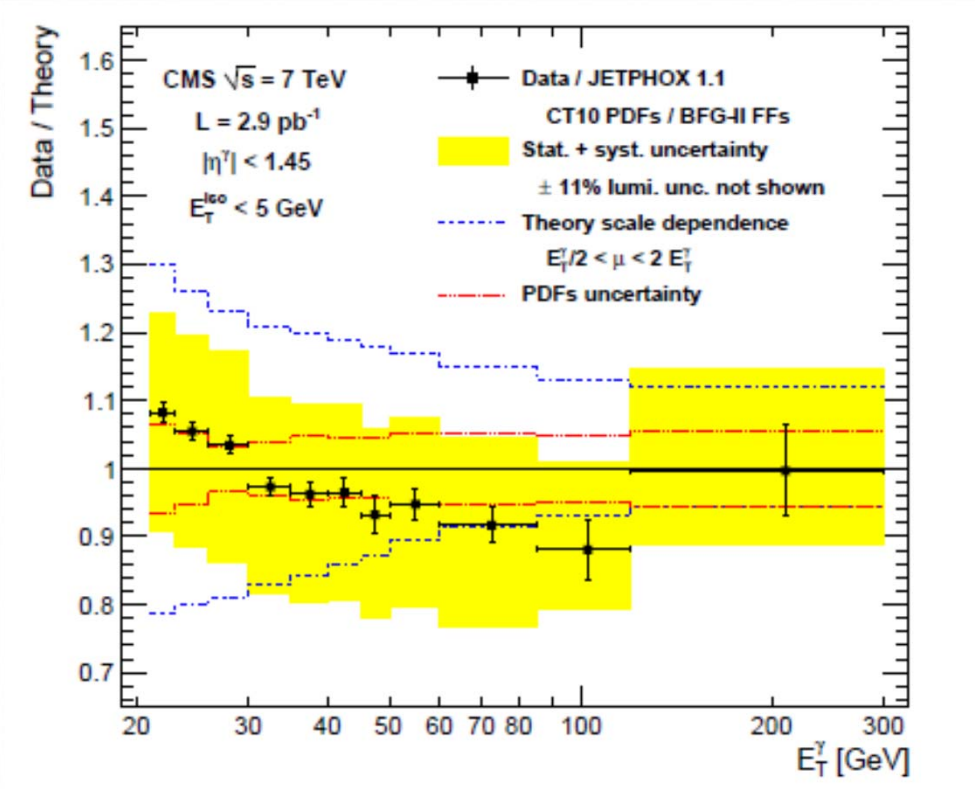

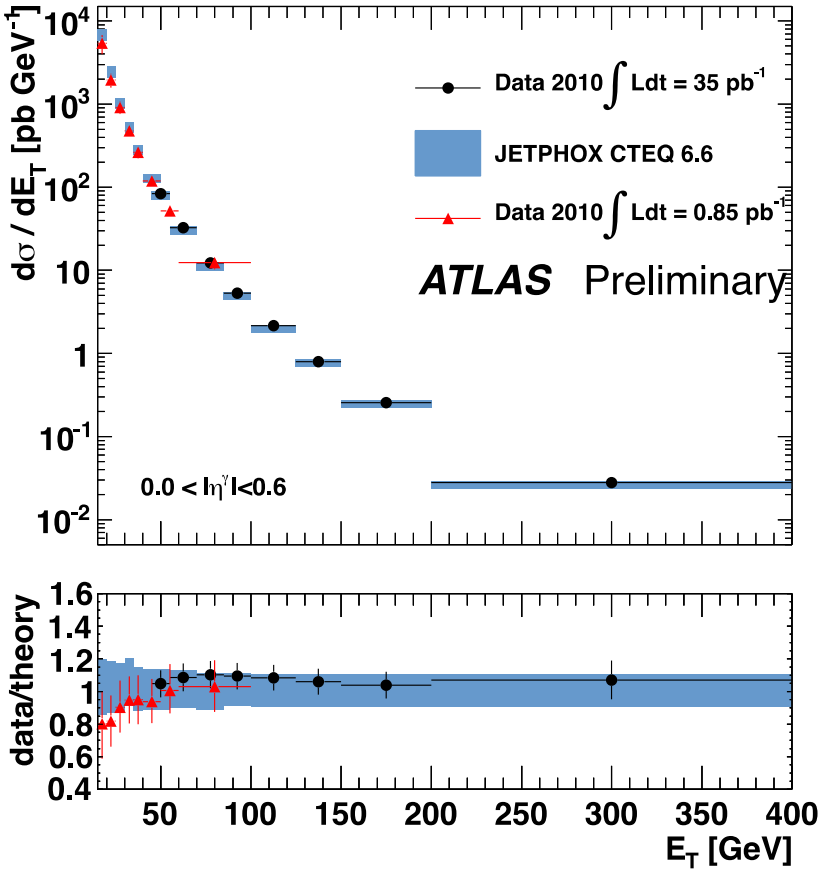

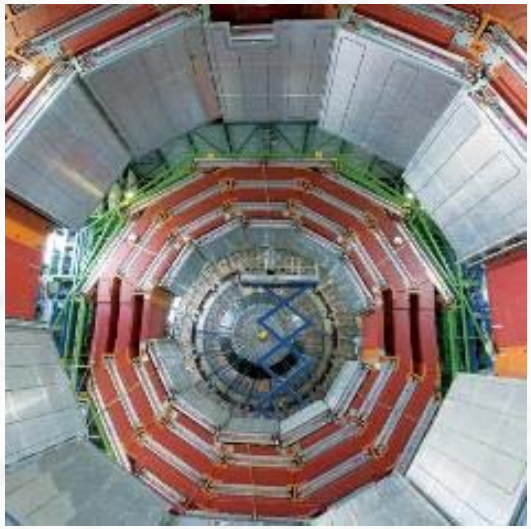

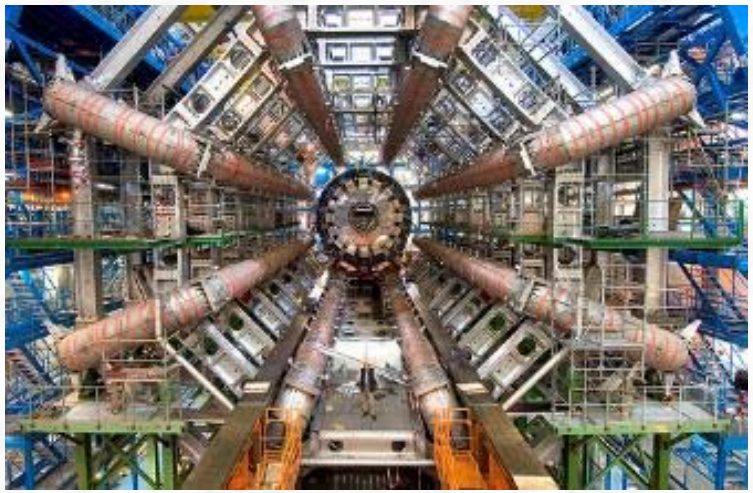

Photons at the LHC

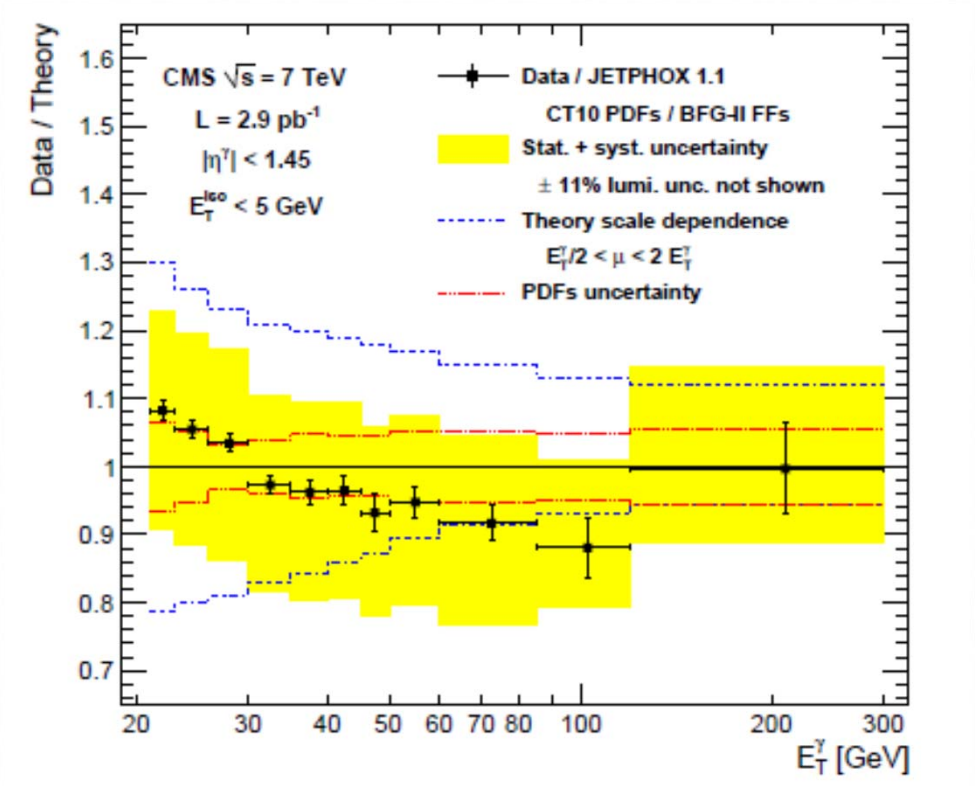

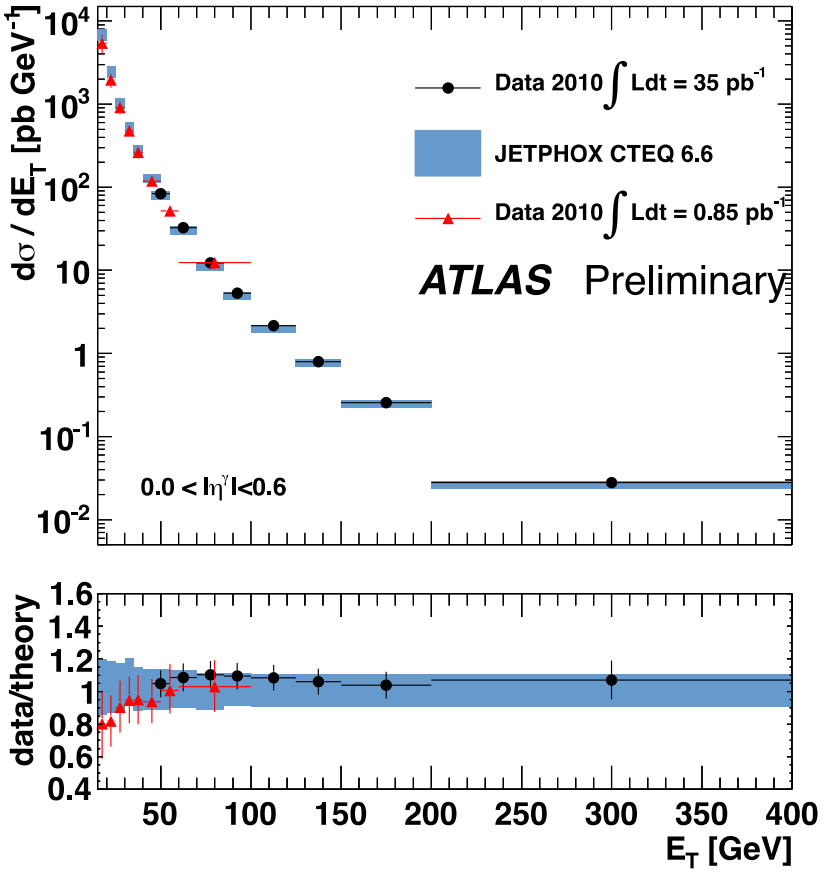

- There is still something not understood going on below 50 GeV
  - However, due to different energies, effects from pdf and matrix elements can be separated (LHC probes a different x-range for the same p_T value)
- The additional kinematic reach of the LHC is apparent
  - For the same x_T, the LHC goes out 3.5x further in E_T.
  - With only 1% of the data, the kinematic reach is the same as the Tevatron's
  - This represents 1-10% of the data the LHC has already collected

Recent Results from the LHC

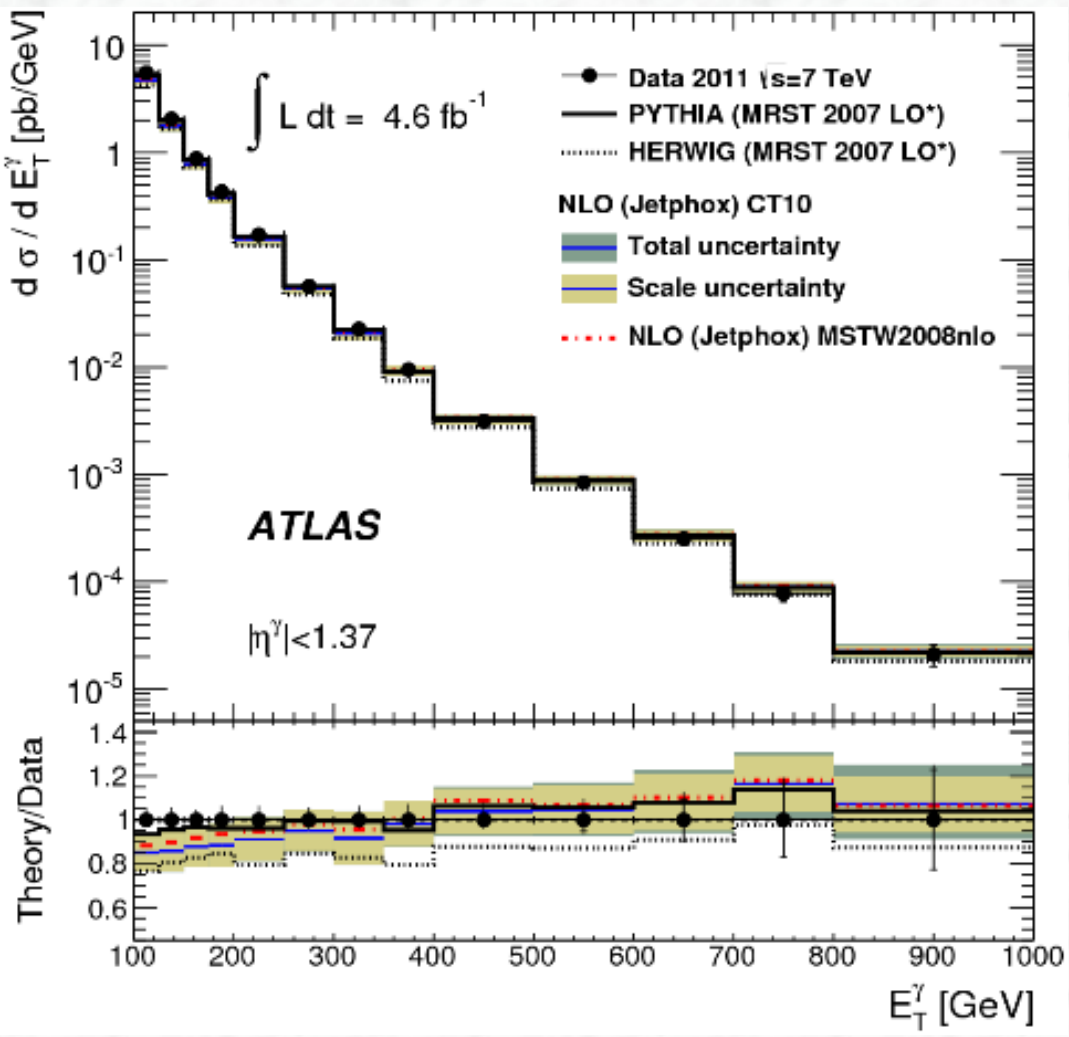

Good agreement between data and theory in the high-p_T region at the LHC

The next step: Di-photon production

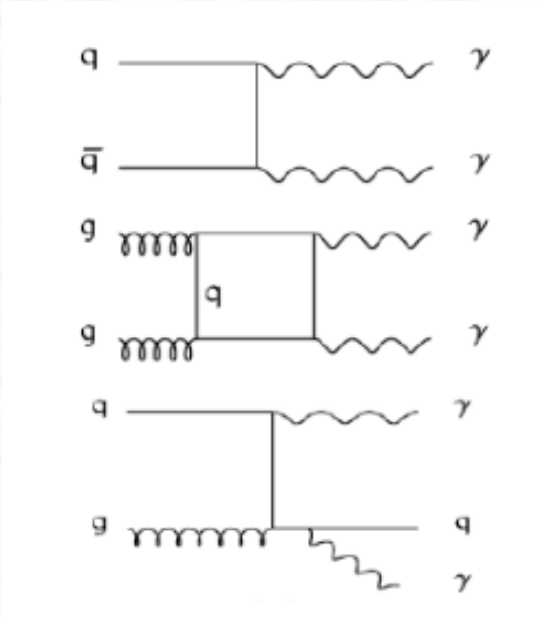

- Direct probe of qq → γγ process (QED)
- Sizeable gg-box contribution

- Irreducible background in searches for new physics

  - Higgs bosons
  - SUSY searches with light gravitinos,….
  - …..

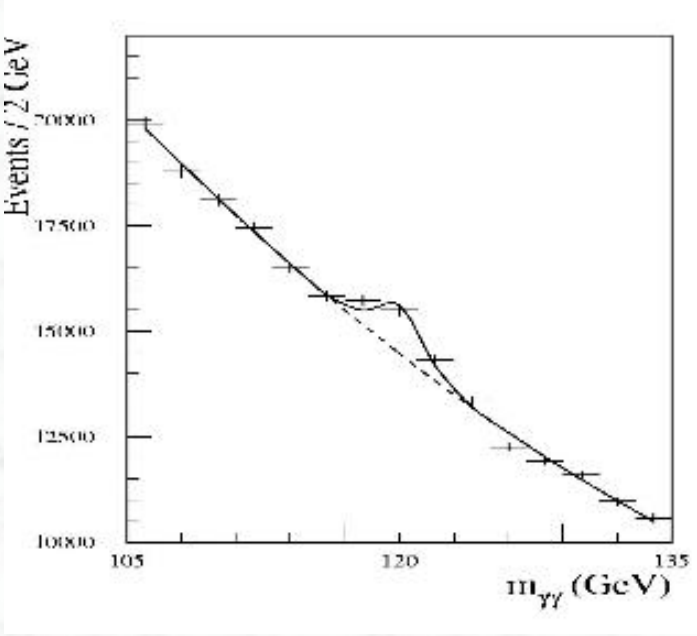

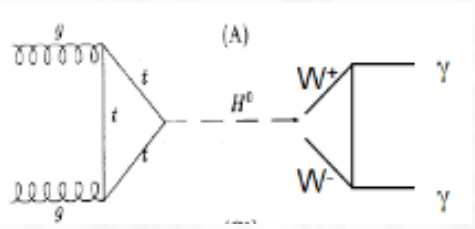

$H \rightarrow \gamma\gamma$

Main backgrounds:

$\gamma\gamma$ irreducible background

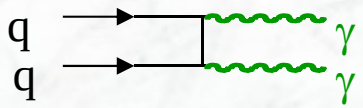

γ-jet and jet-jet (reducible)

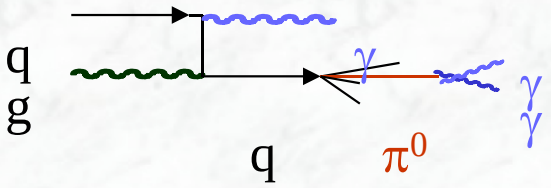

$\sigma_{\gamma j+jj} \sim 10^6 \, \sigma_{\gamma\gamma}$ with large uncertainties

$\rightarrow$ need $R_j > 10^3$ for $\varepsilon_\gamma \approx 80\%$ to get

$\sigma_{\gamma j+jj} \ll \sigma_{\gamma\gamma}$

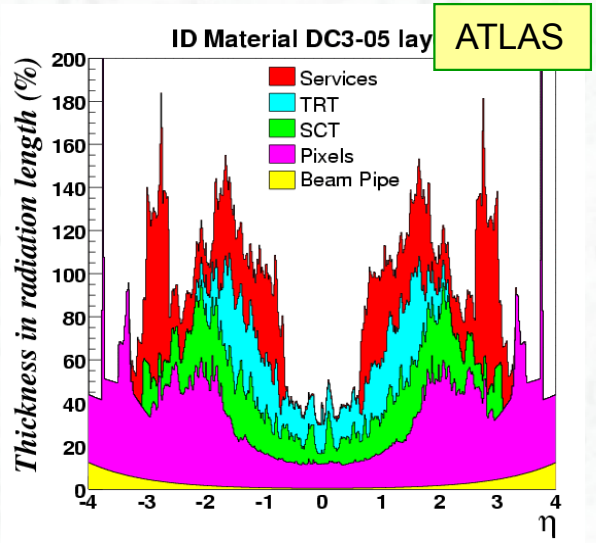

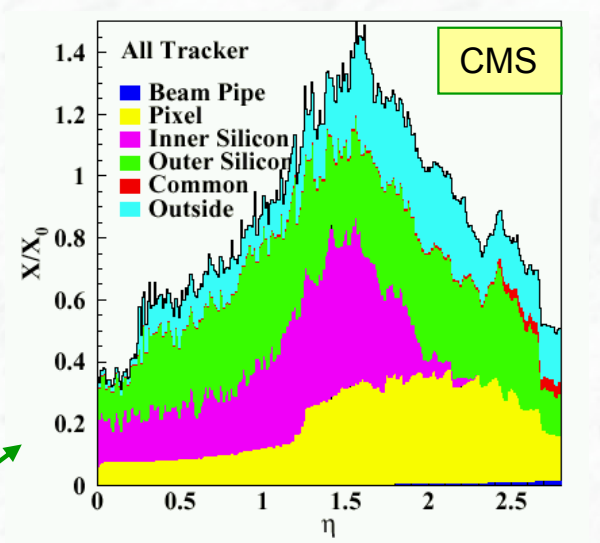

- Main exp. tools for background suppression:
  - photon identification
  - γ / jet separation (calorimeter + tracker)

  - note: also converted photons need to be reconstructed
    (large material in LHC silicon trackers)

CMS: fraction of converted γs

Barrel region: 42.0 %

Endcap region: 59.5 %

Result of the ATLAS search for H → γγ

Phys. Lett. B726 (2013) 88

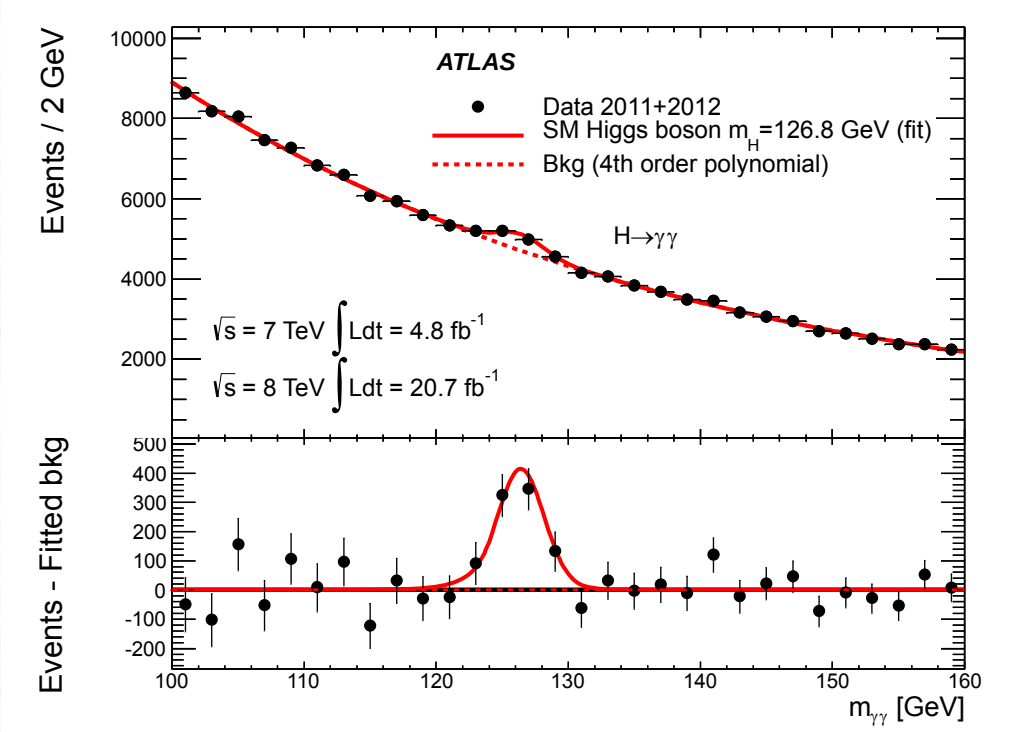

p-value for consistency of data with background-only: ~ 10^{-13}
(7.4σ observed)

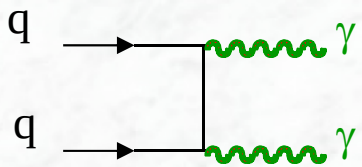

Background

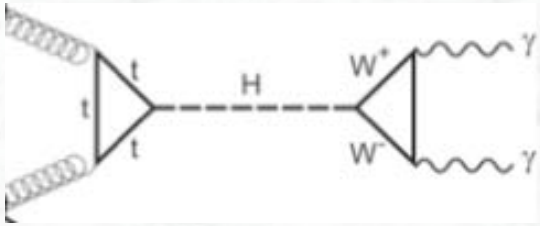

Higgs signal (main production process via gluon fusion)
(mass can be reconstructed from γγ)

Results on di-photon background

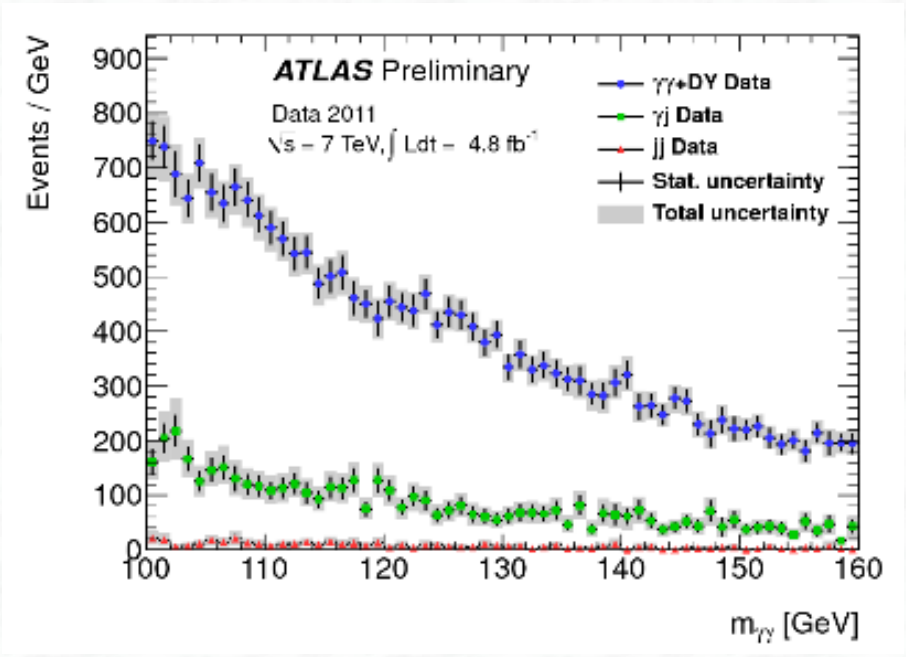

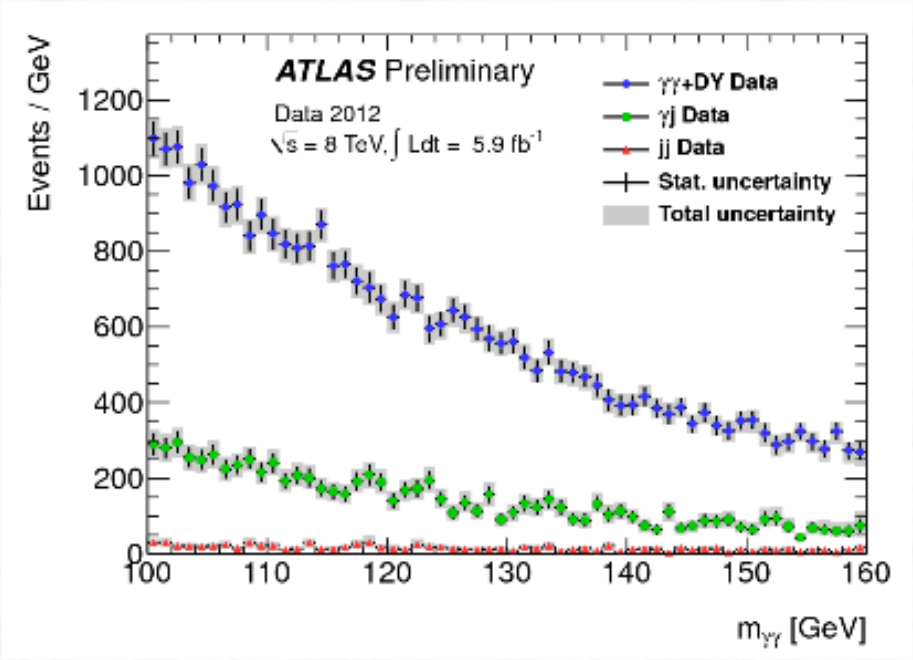

- The background is dominated by real di-photons (γj fraction ~25%, jj fraction ~7%)
- The 7 TeV and 8 TeV data look similar, but not identical
  (have to be handled separately in the combination)
- And finally: good agreement between Monte Carlo simulation and data

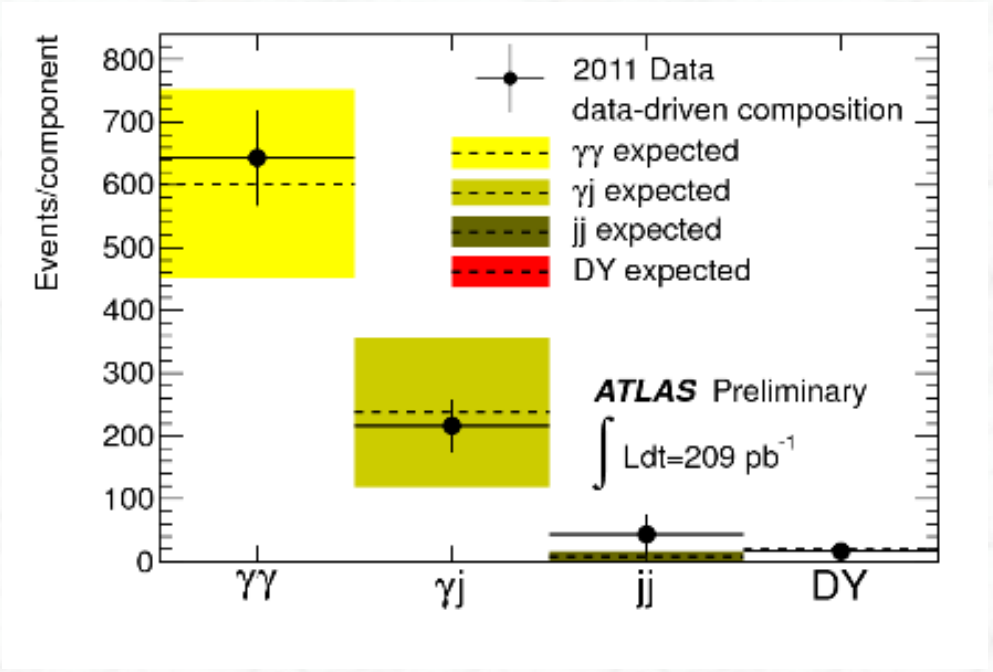

note: no absolute MC prediction necessary for Higgs analysis, but useful to extract functional form of the background

Results on di-photon production at the LHC:

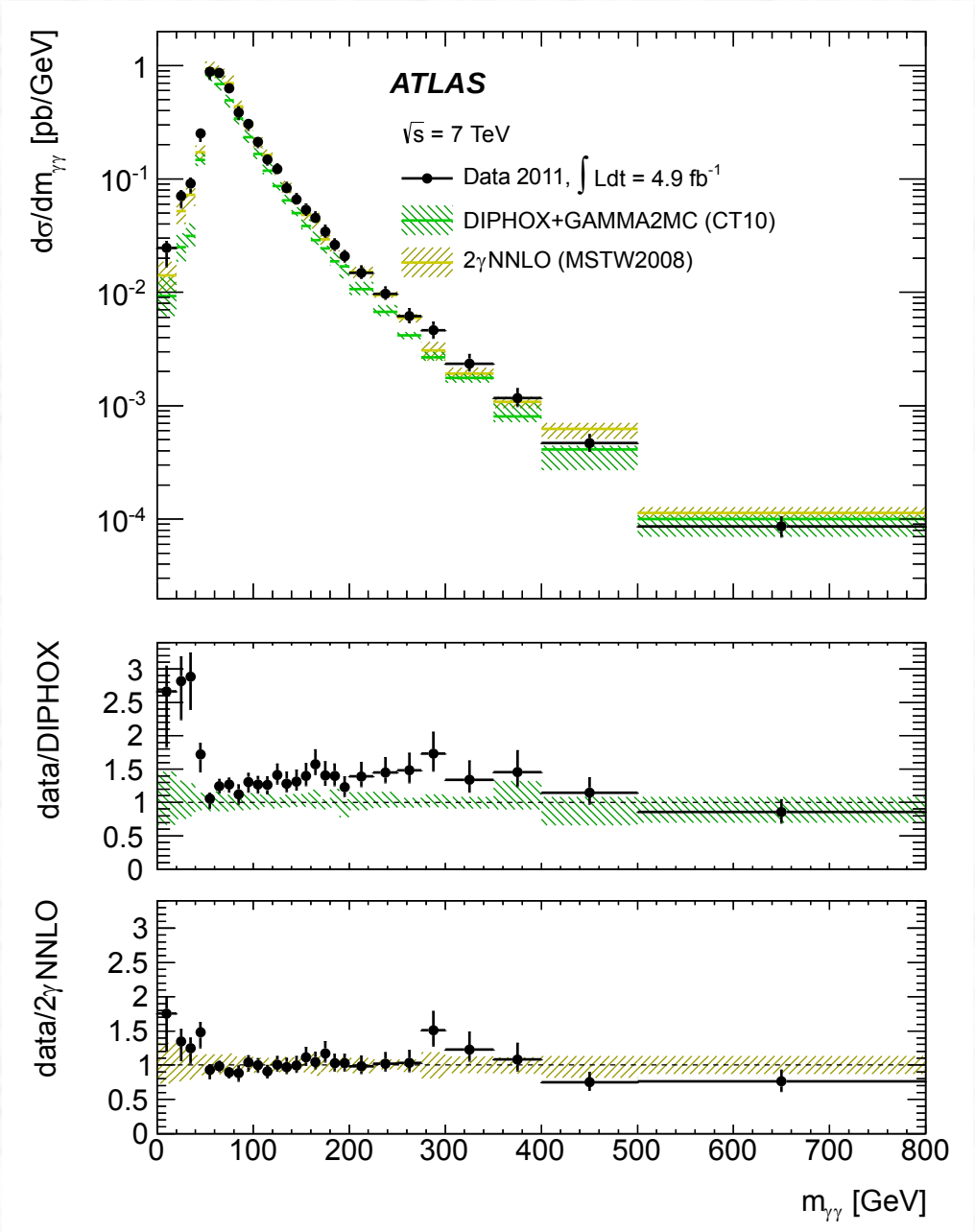

Reasonable agreement with recent NNLO calculations

5.6 Measurements of the strong coupling constant α_s

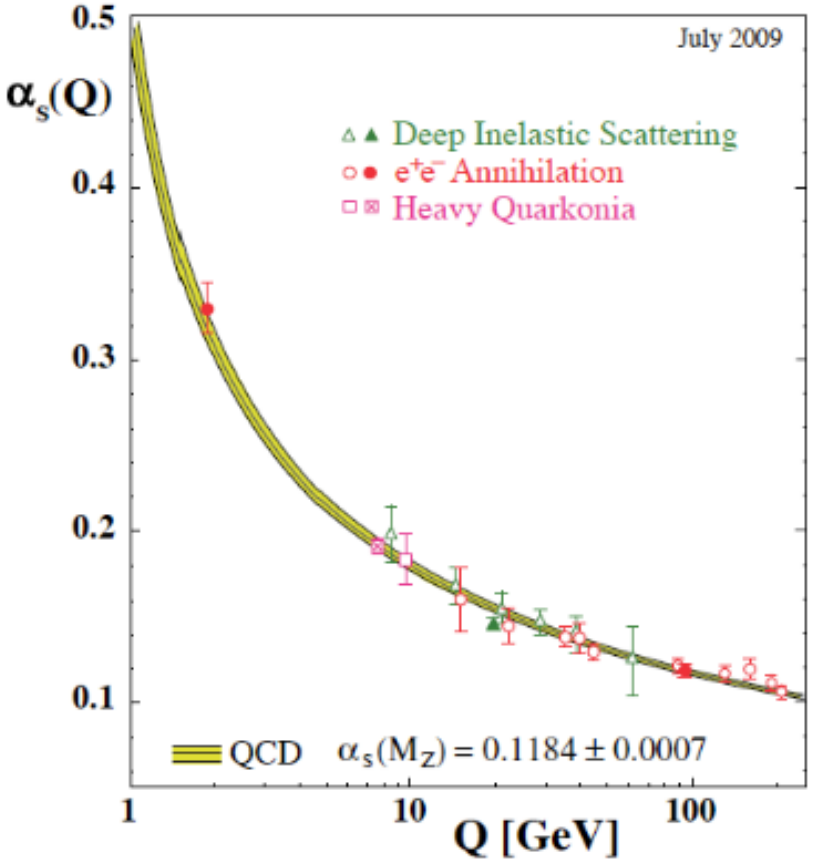

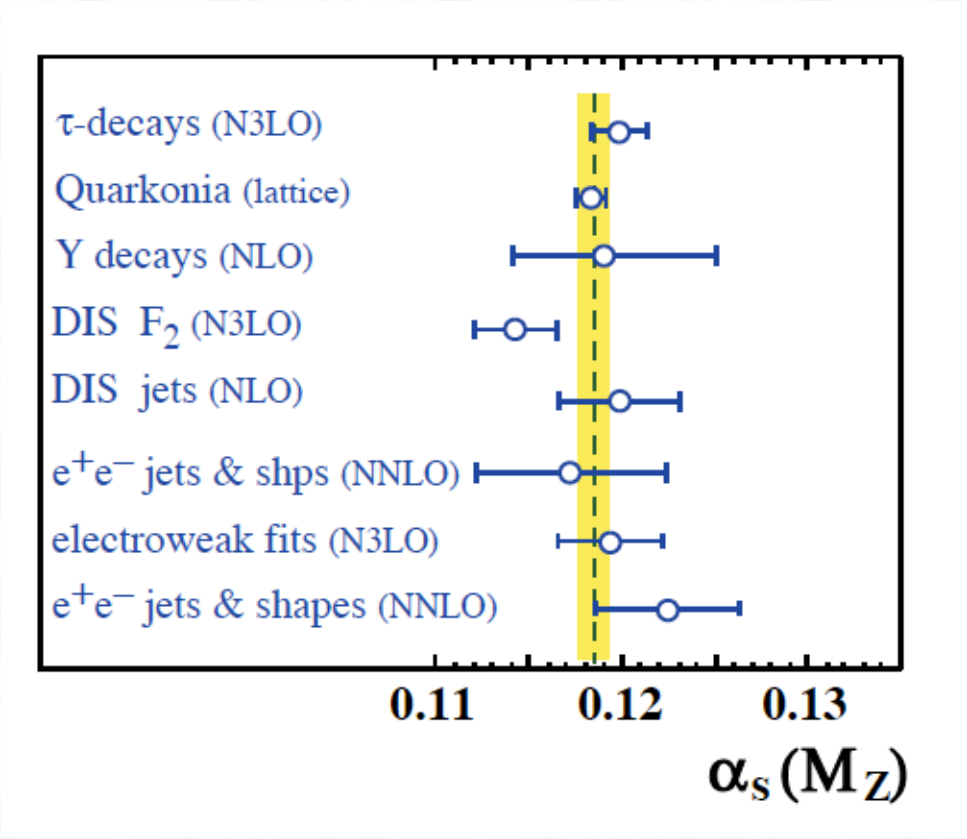

- Running of α_s well established, in agreement with predictions from QCD

World average (2010): $\alpha_s = 0.1184 \pm 0.0007$

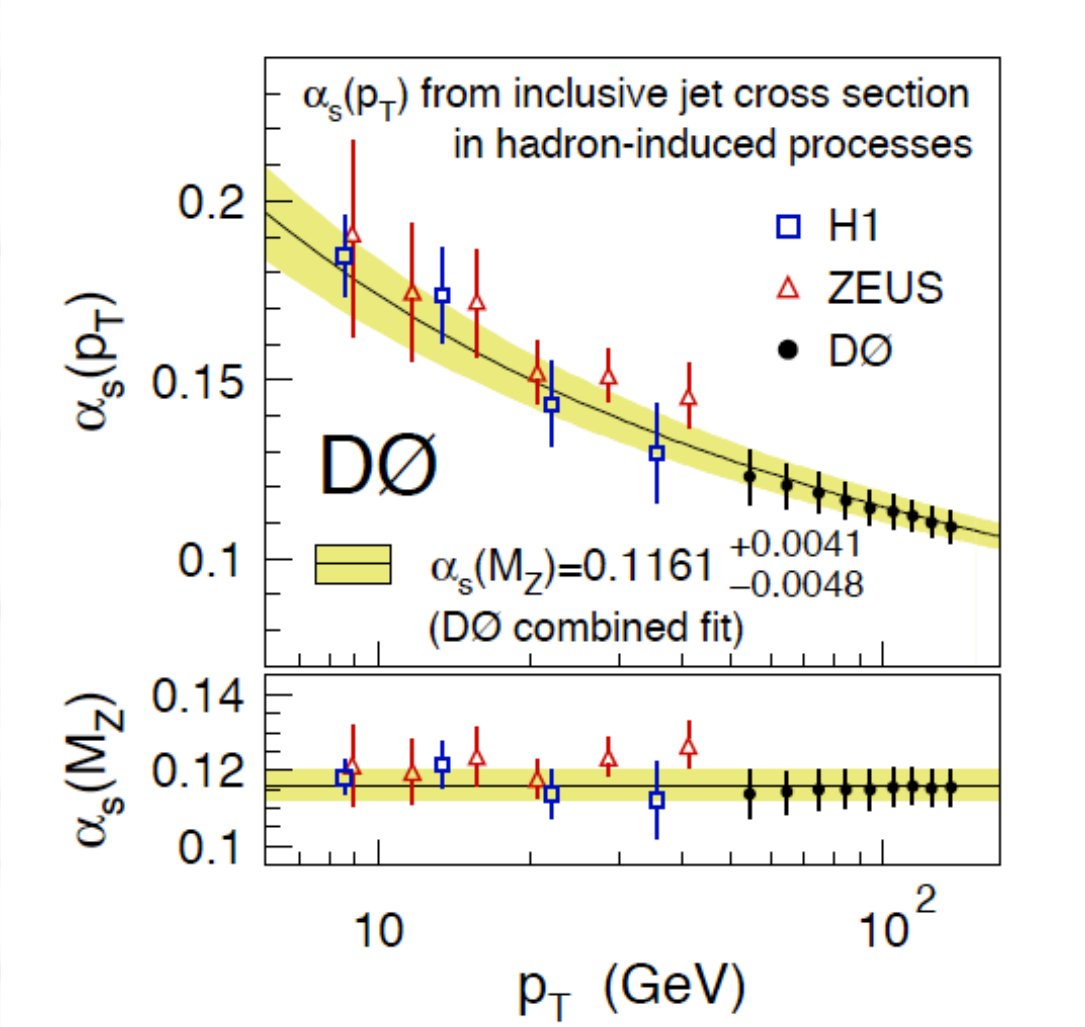

The results for α_s (p_T) top and α_s (m_Z) (bottom). The results are based on 22 selected data points. For comparison, results from HERA DIS jet data have been included. The running of a s for the value measured in D0 is superimposed as yellow band. All data points are shown with their total uncertainties, the D0 values are correlated.

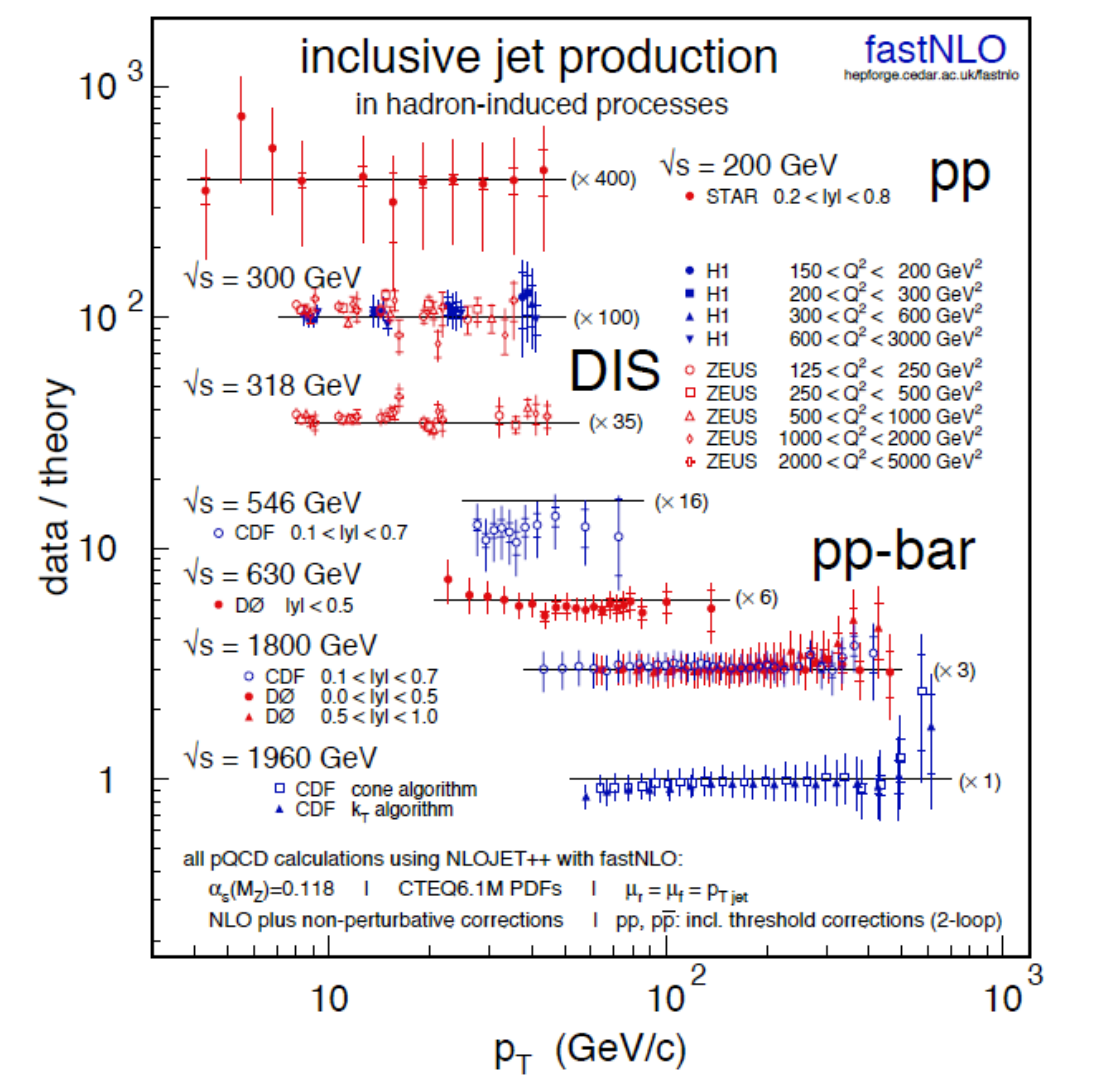

Jet cross sections over large energy range and for many hadron collider experiments consistent
with $\alpha_s = 0.118$

A compilation of data-over-theory ratios for inclusive jet cross sections as a function of the jet transverse momentum (pT), measured in different hadron-induced processes at different centre-of-mass energies (Particle Data Group, 2010).
The various ratios are scaled by arbitrary numbers (indicated between parentheses) for better readability of the plot. The theoretical predictions have been obtained at NLO accuracy, for parameter choices and structure functions as indicated at the bottom of the figure.

Towards precision tests of QCD at the LHC

arXiv:1410.6765

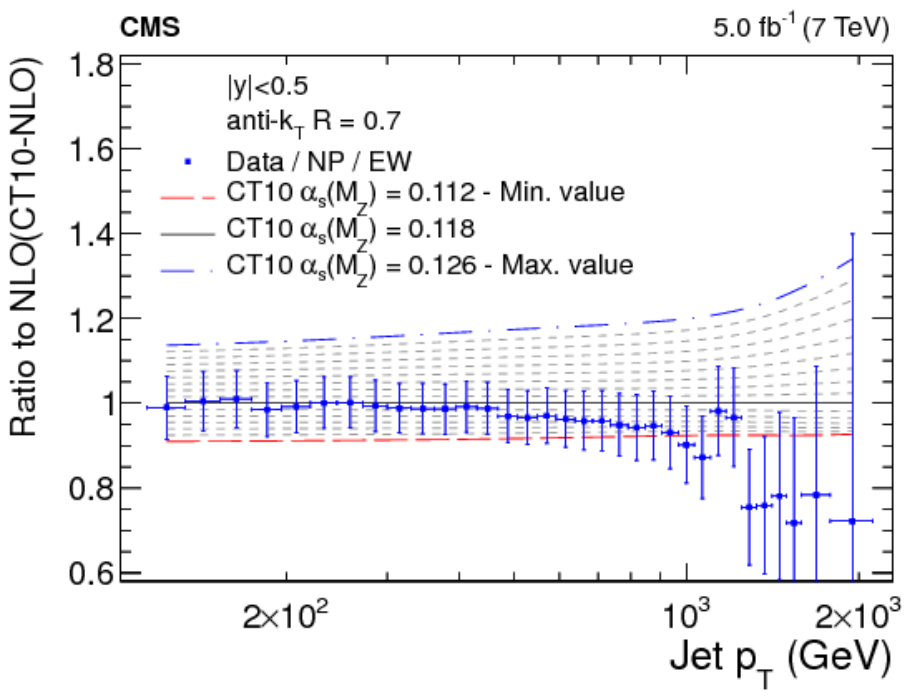

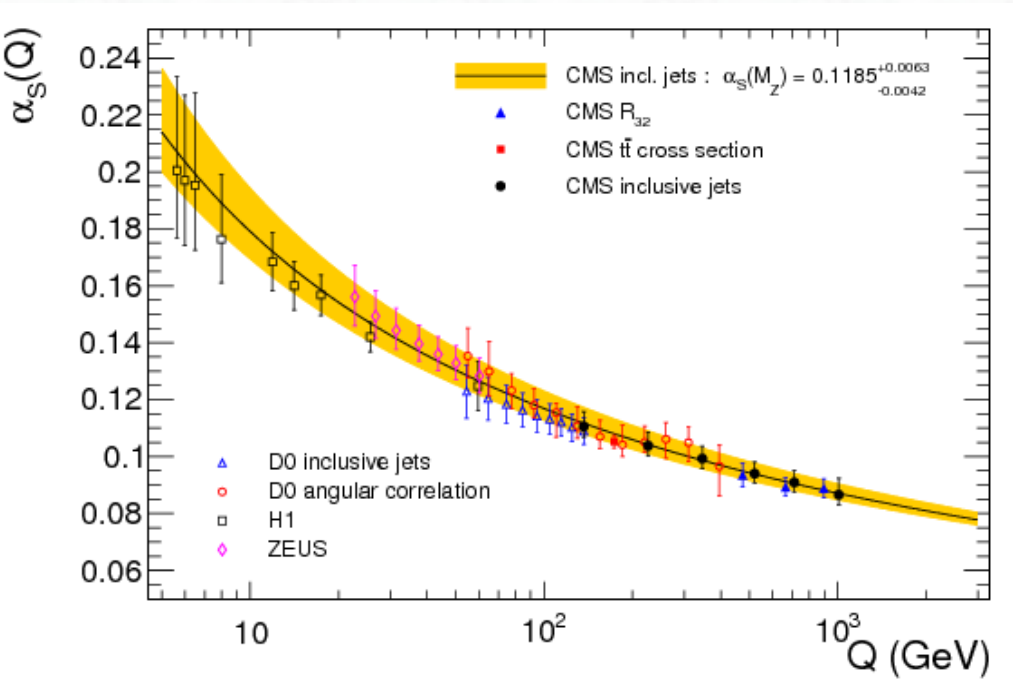

$\alpha_s\,(m_Z) = 0.1185 \pm 0.0019\,(\mathrm{exp})\ ^{+0.0060}_{-0.0037}\,(\mathrm{theo})$